# CHARACTERIZATION OF THE MEMBRANE ASSOCIATION OF TOMATO RINGSPOT VIRUS PROTEINS CONTAINING THE NTP BINDING DOMAIN

By

SUMIN HAN

B.Sc., Hebei Agricultural College, Changli, China, 1989
M.Sc., Shenyang Agricultural University, Shenyang, China, 1992

A THESIS SUBMITTED IN PARTIAL FULFILMENT OF
THE REQUIREMENTS FOR THE DEGREE OF
DOCTOR OF PHILOSOPHY

in

THE FACULTY OF GRADUATE STUDIES

(Department of Botany)

We accept this thesis as conforming
to the required standard

THE UNIVERSITY OF BRITISH COLUMBIA

January, 2003

Department of Botany

The University of British Columbia
Vancouver, Canada

Date April 22 2003

## ABSTRACT

Replication of all known positive-strand RNA viruses occurs in replication complexes associated with intracellular membranes. The putative Nucleoside Triphosphate Binding (NTB) protein of *Tomato ringspot virus* (ToRSV) contains a stretch of hydrophobic residues at its C-terminus suggesting that it may act as a membrane anchor for the replication complex. Anti-NTB antibodies detected two predominant proteins in membrane-enriched fractions (the 66 kDa NTB and the 69 kDa NTB-VPg) along with other larger proteins. The proteins containing NTB co-fractionated with markers of the endoplasmic reticulum (ER) and with ToRSV specific RNA-dependent RNA polymerase activity in sucrose gradients. ToRSV infection induced severe changes in the morphology of the ER in plants expressing an ER-targeted green fluorescent protein (ER-GFP), and proteins containing NTB co-localized with the ER-GFP in indirect immunofluorescence assays. The proteins containing NTB have properties of integral membrane proteins. Proteinase K protection assays using purified membranes from infected plants revealed that although the central portion of NTB is exposed to the cytoplasmic face of the membranes, an 8 kDa fragment, recognized by anti-VPg antibodies, is protected by the membranes. This fragment probably consists of the 3 kDa VPg and the 5 kDa stretch of hydrophobic residues at the C-terminus of NTB, suggesting a lumenal location for the VPg in at least a portion of the molecules.

To study whether NTB-VPg could associate with membranes, an *in vitro* membrane association assay was used. A truncated NTB-VPg protein containing the transmembrane domain could associate with canine microsomal membranes. The NTB-VPg and cNTB-VPg were glycosylated in the VPg domain in *vitro* suggesting a topology similar to that observed in infected plants. The cNTB-VPg protein was also processed by a membrane-associated proteinase *in vitro* at a site immediately upstream of the VPg domain. Expression of the cNTB-VPg protein in

protoplasts revealed that this processing might also take place *in vivo*. Taken together, our results provide evidence that proteins containing the NTB domain are transmembrane proteins associated with ER-derived membranes and support the hypothesis that one or several of the proteins containing NTB anchor the replication complex to the ER.

# TABLE OF CONTENTS

## LIST OF FIGURES

# LISTS OF ABBREVIATION

| | |
|---|---|
| 3' | three prime |
| 5' | five prime |
| A | alanine in the context of amino acid sequence |
| AUG | triplet codon as a start codon |
| 1A | *Poliovirus* 1A coat protein |
| 2A | *Poliovirus* 2A protease |
| 3A | *Poliovirus* 3A protein that contains a trans-membrane domain |
| 3AB | *Poliovirus* 3AB, precursor of 3A and 3B |
| BMV | *Brome mosaic virus* |
| BiP | binding protein |
| 2B | *Poliovirus* 2B protein |
| 2BC | *Poliovirus* 2BC protein |
| 3B | *Poliovirus* viral genome-linked protein (VPg) |
| cDNA | complementary DNA |
| C | cytidine in the context of nucleotide sequence |
| C | cysteine in the amino acid sequence |
| CP | coat protein |
| CPMV | *Cowpea mosaic virus* |
| C-terminal | carboxy-terminal |
| C-termini | carboxy-termini |
| C-terminus | carboxy-terminus |
| Cys | cysteine |
| 2C | *Poliovirus* 2C protein (helicase-or NTB-like protein) |
| 3C | *Poliovirus* 3C protease |
| 3CD | *Poliovirus* 3C protease and 3D polymerase precursor |
| DNA | deoxyribonucleic acid |
| D | aspartic acid |
| 3D | *Poliovirus* 3D RNA dependent RNA polymerase |
| DTT | dithiothreitol |
| E | glutamine |
| EDTA | ethylenediamintetraacetic acid |
| eIF4G | Eukarotic initiation factor 4G |
| ER | endoplasmic reticulum |
| FMDV | *Foot-and-mouth disease virus* |
| Fig | Figure |
| G | glycine in the context of amino acid sequence |
| G | guanosine in the context of nucleotide sequence |
| GDD | Tripeptide sequence of G, D and D, a conserved amino acid sequence in |

| | |
|---|---|
| | RNA-dependent RNA polymerases |
| GFLV | *Grapevine fanleaf virus* |
| GFP | green fluorescence protein |
| Gly | glycine |
| Gln | glutamine |
| Glu | glutamic acid |
| HC-Pro | *Potyvirus* HC protease |
| H | histidine |
| His | histidine |
| IRES | internal ribosome entry sites |
| K | lysine in the context of amino acid sequence |
| kDa | kilodalton |
| 6k2 | *Potyvirus* 6k2 protein located between CI and NIa-VPg |
| L | leucine in the context of amino acid suquence |
| M | methionine in the context of amino acid sequence |
| M | molar in the context of concentration |
| M | microsomal membrane |
| MP | movement protein |
| mRNA | messenger RNA |
| N | asparagine |
| Nepo- | *Nepovirus* |
| NIa | *Potyvirus* VPg and 3C-like protease domains |
| $NIa^{pro}$ | *Potyvirus* 3C-like domain |
| $NIa^{VPg}$ | *Potyvirus* VPg domain |
| NIb | *Potyvirus* RNA-dependent RNA polymerase domain |
| NS3 | *Flavivirus* NS3 serine protease |
| NS4A | *Flavivirus* NS4A serine protease cofactor |
| NS5B | *Flavivirus* RNA-dependent RNA polymerase |
| N-terminal | amino-terminal or $NH_2$-terminal |
| N-terminus | amino-terminus or $NH_2$-terminus |
| NSPs | non-structural proteins |
| NTB | nucleotide triphosphate-binding motif |
| NTB-VPg | precursor protein of NTB and VPg |
| NTP | nucleotide triphosphate |
| NXT/S | conserved amino acid sequence of glycosylation (N: asparagine, X: any amino acid, T/S: threonine or serine |
| ORF | open reading frame |
| OST | oligosaccharyltransferase |
| (+) ss RNA virus | positive single stranded RNA virus |
| P1 | Polyprotein encoded by como- and nepovirus RNA-1 |
| P1 | P1 protease in the context of proteins encoded by potyviruses |

| | |
|---|---|
| P1 | P1 region encoding 1ABCD protein in the context of picornaviruses |
| P2 | Polyprotein encoded by como- and nepovirus RNA-2 |
| PAGE | polyacrylamide gel electrophoresis |
| PEG | polyethylene glycol |
| picorna-like | picorna-like viruse supergroup |
| Pol | polymerase |
| Poly (A) | polyadenylate or polyadenylic acid |
| Pro | protease |
| Pro-Pol | precursor of protease and polymerase |
| PV | *Poliovirus* |
| Q | glutamine |
| R | Arginine |
| RdRp | RNA dependent RNA polymerase |
| SDS | sodium dodecyl sulfate |
| Ser | serine |
| SRP | signal recognition particles (SRP) |
| SPC | signal peptidase complex |
| SS | single strand |
| T | threonine in the context of amino acid |
| TBRV | *Tomato black ring virus* |
| TEV | *Tobacco etch virus* |
| TMD | transmembrane domain |
| U | uridine |
| UTR | untranslated region |
| VPg | viral protein genome-linked |

# ACKNOWLEDGMENTS

I would like to express my deepest appreciation to my major supervisor, Dr. Helene Sanfacon for incredible guidance, sound advice and financial support. Her encouragement, sense of humor and enthusiastic attitude toward research and life in general have been inspiring and refreshing. I truly enjoy the friendly, but still professional atmosphere in her lab. She treated me as though what I thought was important. Yet she showed me how I can improve at every opportunity. It is the kind of attitude that I appreciate and enjoy the most. I would also like to thank my supervisory committee members, Drs. Janet Chantler, Ljerka Kunst, and Beverley Green for providing sound advice and helpful discussions as well as critical reading of this thesis.

I wish to express my warmest thanks to Mrs. Joan Chisholm for expert technical assistance and valuable discussions, Dr. Aiming Wang for preliminary immunoblotting experiments with the anti-NTB and anti-VPg antibodies and valuable discussions in the early stages of this project, Dr. Yu Xiang for preliminary extraction experiments of membrane-associated proteins with various biochemical treatments, technical assistance and helpful discussions, Dr. Shuocheng Zhang for valuable discussions. I would like to extend my appreciation to many people in the Pacific Agriculture Research Center for their help and generous permission to use facilities and supplies.

I would like to thank Mr. M. Weis and Mrs. E. Humphrey (Dept. of Botany, University of British Columbia) for help with confocal microscopy, Dr. M. Chrispeels (University of California, San Diego) for the anti-Bip antibodies, Dr. A.Sturm (Friedrich Miescher Institute) for the anti-$\beta$-xylosyl antibodies, Dr. D. Baulcombe (John Innes Centre) for the ER-GFP

transgenic plants. Drs. D. A. Theilmann and J. Wellink and Mrs. J. Chisholm are gratefully acknowledged for critical reading of the manuscript (published in Journal of virology) contained in my thesis. This study was supported by a grant from the Natural Sciences and Engineering Research Council of Canada to Dr. Helene Sanfacon.

I want to express my heartfelt gratitude to my friend Bell Kendrick for her generosity, encouragement and support. I have been extraordinarily lucky to have lived in her house for the last three years. She has helped me in hundreds of ways and she has made my life much easier during my struggle to complete my Ph.D.

I am truly indebted to my husband Weiquan Wu for his patience, sense of responsibility, and unconditional support during hard times. I owe my deepest thanks to my daughter Jan Wu for being good in the last four years. She is the sunshine of my life. I promise to try to make up for some of her sacrifices after I complete my Ph.D.

# CHAPTER 1

# LITERATURE REVIEW: REPLICATION AND MEMBRANE ASSOCIATION OF POSITIVE SINGLE STRANDED RNA VIRUSES

## 1.1 Introduction

A virus is a parasite composed mainly of nucleic acid within a protein coat. The nucleic acid can be either DNA or RNA, double stranded or single stranded of positive or negative polarity. A virus must enter a host cell and use the host-cell macromolecular machinery and energy supplies to replicate. The genome of positive single stranded RNA [(+) ssRNA] functions as mRNA and is translated into viral proteins. The viral proteins then use the viral RNA as a template to generate multiple copies of this RNA. Because (+) ss RNA viruses have small genomes and contain only limited genetic information, they must rely on existing or modified cellular factors for viral protein translation and replication (Lai, 1998; Andino *et al.*, 1999). Replication of the genome of all characterized positive-stranded RNA viruses occurs in large complexes, which are associated with intracellular membranes (Buck, 1996). The identification of viral targeting proteins has provided valuable insights into the mechanisms of formation of the viral replication complex.

*Tomato ringspot virus* (ToRSV, genus *Nepovirus* subgroup C, family *Comoviridae*) is a plant (+) ss RNA virus. ToRSV is a major pathogen of small fruits and fruit trees in North America. When this study was initiated, little was known about the formation of nepovirus replication complexes. As will be discussed below, one of the ToRSV viral proteins thought to be involved in replication contains a putative transmembrane domain. The purpose of this thesis was to characterize association of this viral protein with membranes, possibly leading to the formation of the replication complex. A better understanding of the association of replication complexes with intracellular membranes may allow us to design new strategies to engineer resistance.

In this review, I will discuss the various mechanisms of interactions between viral proteins and intracellular membranes and strategies employed by (+) ss RNA viruses for their genome expression and replication. Because ToRSV is a member of the picorna-like viruses, we will put particular emphasis on the description of these viruses.

## 1.2 The intracellular membrane system and membrane proteins

### 1.2.1 The intracellular membrane system and special plant cell organelles

One universal feature of all cells is an outer limiting membrane called the plasma membrane. In addition, all eucaryotic cells contain elaborate systems of internal membranes which set up various membrane-enclosed compartments within the cell, such as the Golgi apparatus, the endoplasmic reticulum (ER), the nucleus and various specialized vesicles such as lysosomes (animal cells) or vacuoles (plant cells) which are involved in intracellular digestion (Fulton, 1982). Each compartment has its own characteristic contents and complex distribution system that transports specific products from one compartment to another. Biological membranes are composed of a continuous double layer of lipid molecules with various embedded membrane proteins (Jennings, 1989). Many vital biochemical processes take place in the membrane or on the membrane surfaces. In addition to the major intracellular compartments common to eucaryotic cells, a plant cell usually contains special organelles: chloroplasts, vacuole and cell wall. The vacuole is a very large single-membrane-bounded vesicles taking up more than 90% of the cell volume in epidermal cells. The ER is confined to a small layer between the vacuole and the cell wall. The plant cell wall is a thick, rigid and cellulose-based cell wall, which separates individual cells. Live plant cells are interconnected by plasmodesmata which stem from tubular ER strands. The plasmodesmata are gated intercellular channels that do not admit particles as large as virions

(Epel, 1994). Plant viruses have evolved specific movement functions mediated by movement proteins to modify or enlarge the plasmodesmata opening transiently to allow for the passage of viral nucleoprotein complexes and virus-like particles (Goldbach *et al.*, 1994).

### 1.2.2 The general properties of the ER

The ER is a dynamic organelle composed of a large number of discrete functional domains (Staehelin, 1997). It is composed of a network of branching tubules and flattened sacs extending throughout the cytosol. The ER underlying the plasma membrane is known as cortical ER, and is frequently distinguished from the ER that traverses the cytoplasm. However, the different ER domains are all thought to be connected with one another and with the continuous membrane of the nuclear envelope. These membranes form a continuous sheet enclosing a single internal space called ER lumen. The binding protein (BiP), one of the ER lumenal chaperone proteins, is distributed throughout the ER network. This distribution pattern makes BiP a general marker of the ER (Staehelin, 1997). The ER membrane system is flexible. The membrane can be expanded, contracted or spatially differentiated and reorganized. The large membrane surface area is available for incorporating membrane proteins.

The ER membrane system has multiple functions that are confined to distinct ER domains. Rough ER and smooth ER are classical types of ER subdomains. Rough ER has ribosomes on the membrane surface. The Rough ER membrane is the site of production and processing of transmembrane proteins and secretory proteins for the ER itself, the Golgi apparatus, vacuole and the plasma membranes (Pryme, 1986). Smooth ER has no ribosomes bound on the membrane surface. One of the principal functions of the smooth ER domain appears to be the synthesis of lipids (Nickel *et al.*, 1998).

### 1.2.3 Protein-membrane interactions

Proteins associate with membranes in several ways (Jennings, 1989 and references therein). All biological membranes are made up of a lipid bilayer and protein molecules, held together mainly by noncovalent interactions. Membrane lipids are amphipathic molecules. Many membrane proteins extend through the lipid bilayer. Their hydrophobic regions pass through the membrane and their hydrophilic regions are exposed to the outside of the membranes. Some proteins associate with membranes by an amphipathic helix which is an α-helix with opposing polar and non-polar faces oriented along the axis of the helix (Segrest *et al.*, 1992). Some membrane proteins are located entirely in the cytosol and associate with membranes by covalent linkage via lipid chains. Other membrane proteins do not extend into the hydrophobic interior of the lipid bilayer, but associate with membranes by noncovalent interactions with other membrane proteins. Treatments that interfere with protein-protein interaction, such as exposure to solutions of extreme pH, can release these loosely bound proteins which are called peripheral membrane proteins. By contrast, other membrane proteins that cannot be released with these treatments are called integral membrane proteins.

### 1.2.4 Protein sorting

Most proteins are initially synthesized in the cytoplasm. Their final destinations depend on their sorting signals that are regions with defined amino acid motifs. Proteins move between compartments in three fundamentally different ways (Bradshaw, 1989): (i) the protein traffic between the cytosol and nucleus occurs through the nuclear pore complex and is called gated transport; (ii) the initial transport of selected proteins from the cytosol into the ER lumen or into

the mitochondria or chloroplast occurs through transmembrane transport. The membrane-bound protein translocators directly transport specific proteins across a membrane; (iii) the transfer of soluble proteins in the secretory pathway, such as from the ER to the Golgi apparatus, occurs through vesicular transport. The transport vesicles pinch off from the membrane and become loaded with a cargo of molecules derived from the lumen from one compartment such as the ER. The transport vesicles deliver the cargo into a second compartment by fusing with its membrane. Each way of protein transfer is selectively guided by sorting signals in the transported proteins. Secretory proteins and membrane proteins destined for the ER itself, the Golgi apparatus, endosomes, lysosomes and the plasma membrane are directed to the ER first (Rapoport, 1992). Some of the proteins will remain in the ER, but most of the proteins will pass from ER to the Golgi apparatus (Teasdale and Jackson, 1996). Many soluble ER proteins, such as BiP, carry a C-terminal tetrapeptide H/KDEL motif for retention in the ER (Pelham, 1990).

In eucaryotic cells, transport of secreted and integral membrane proteins into ER is generally mediated by a signal sequence which is 16 to 30 hydrophobic amino acids in length, and is located at the N-terminus of the protein or in the internal region of the protein (Von Heijne, 1990). The signal sequence is recognized by the signal recognition particles (SRP) and directs the translation complex into the ER membrane during translation. The SRP-mediated ER transport occurs only cotranslationally. In contrast, a class of tail-anchored proteins does not seem to follow this general rule. This class of integral membrane proteins is anchored in the membrane by a hydrophobic C-terminal sequence called "insertion sequence". The insertion sequence is too close to the C-terminus of the protein (within the last 50 residues) to have emerged from the ribosome before termination of translation, precluding the co-translational SRP-dependent membrane insertion.

As a consequence, membrane association of tail-anchored proteins occurs posttranslationally (Kutay *et al.*, 1993).

Little is known about the mechanisms that regulate membrane selectivity of tail-anchored proteins. A membrane-spanning domain is thought to anchor the protein in the membrane. However, a high degree of conservation of the primary structures of transmembrane domains (TMDs) of various proteins among different species makes it likely that the membrane-spanning domain contains important information to confer targeting to specific intracellular address. The following observations support this hypothesis: (i) TMDs of Golgi residuent proteins suffice to localize reporter molecules to the Golgi apparatus, suggesting TMDs play a role in protein sorting (Machamer, 1993); (ii) the presence of one or several hydrophilic residues within the hydrophobic TMD sequence has been reported to be involved in ER retention (Cocquerel *et al.*, 2000 and references therein); (iii) the length of TMDs may be involved in protein sorting (Yang *et al.*, 1997). For example, UBC6 is a C-terminal membrane-anchored ER protein. The transmembrane domain (TMD) consists of 17 hydrophobic amino acids. Lengthening of the TMD to 21 hydrophobic amino acids allows UBC6 to localize in the Golgi and further lengthening the TMD to 26 hydrophobic amino acids allows UBC6 to localize to the plasma membrane.

In summary, proteins contain sorting signals for their final destinations. These signals have been used to design molecular markers of different cellular compartment. For example, transgenic N. *Benthamiana* plants have been engineered that express the green fluorescence protein (GFP) only in the ER. The GFP fusion protein contains an N-terminal cleavable signal peptide and a C-terminal HDEL retention signal and therefore is targeted to the lumen of the ER (Haseloff *et al.*, 1997).

### 1.2.5 Protein modifications in the ER

After targeting to the ER membranes, two early events may occur in the transport process: the cleavage of signal peptides by the signal peptidase complex (SPC) and the addition of core oligosaccharides to Asn-X-Ser/Thr (N-X-S/T) acceptor tripeptides by the oligosaccharyltransferase (OST) (Dalbey *et al.*, 1997). The signal peptidase is an ER integral membrane protein. The active site of SPC faces the ER lumen. The cleavage of signal peptide by SPC occurs after a stretch of hydrophobic residues. The cleavable signal sequences have a common structure: a short, positively charged amino-terminal region; a central hydrophobic region; and a more polar carboxy-terminal region characterized by the presence of residues conforming to the (-1, -3) rule (i.e., cleaved sequences consist of a small residue in the -1 and a non-polar, small amino acid in position -3 upstream of the cleavage site (Von Heijne, 1990; Nilsson *et al.*, 2002). OST is an ER integral membrane protein and the active site faces the ER lumen. N-linked glycosylation generally indicates a lumenal location of at least the glycan attachment site (Doms *et al*, 1993). Therefore, the introduction of a consensus glycosylation site (NXT) in a specific region of a membrane protein has been extensively used to map the topology of the protein in the membranes (Hasler *et al.*, 2000).

## 1.3 Positive single stranded (+) ss RNA virus replication

Many important animal and plant viruses have genome of (+) ss RNA. (+) ss RNA viruses. These include many virus families such as *Picornaviridae* (e.g., *Hepatitis A virus*, *Poliovirus* and *Foot-mouth disease virus*), *Flaviviridae* (e.g., *Yellow fever virus* and *West nile virus*), *Coronaviridae* (e.g., *Hepatitis C virus* and *Mouse hepatitis virus*), *Potyviridae* (e.g., *Plum pox virus*, *Tobacco etch virus* and *Potato virus Y*) and *Comoviridae* (e.g., *Cowpea mosaic virus*,

*Grapevine fanleaf virus* and ToRSV). They are important pathogens of humans, animals and plants.

The viral RNAs of positive stranded RNA viruses serve as mRNAs once the viruses enter cells and need to synthesize viral proteins required for replication. During infection, the genomic RNAs of positive-stranded RNA viruses must first be translated into viral proteins and then must serve as a template for negative-stranded RNA synthesis. The minus strand is then used as a template to synthesize positive stranded RNA. The (+) ss RNA genome functions sequentially as an mRNA for viral protein synthesis and then as a template for viral negative RNA synthesis. Therefore, positive stranded RNA viruses must have evolved mechanisms to regulate the alternate functions of the genomic RNA. These RNA viruses contain only limited genetic information and yet are able to replicate efficiently, rapidly and with high fidelity. In fact, they have evolved a remarkable variety of strategies to employ host factors. In this review, I will examine strategies for (+) ss RNA gene expression and genome replication.

### 1.3.1 Strategies for gene expression of (+) ss RNA viruses

In most case, cellular mRNAs contain a single open reading frame; the 80 S ribosomes are adapted to translate only the ORF immediately downstream from the 5' region of an mRNA. ORFs beyond this point in a cellular mRNA normally remain untranslated. Viral RNAs encode several genes on a single RNA. As viruses do not harbor a functional translation apparatus in their virions, successful replication of the viral genomes requires that viral mRNAs compete with cellular mRNAs for the host cell' translation apparatus. (+) ss RNA viruses must have adapted to the host translation apparatus and to the special needs of their particular genome structure. In

this section, I will review the strategies used by viruses for competing for the translation apparatus with cellular mRNAs and strategies for viral gene expression.

### 1.3.1.1 Competing for the translation apparatus

Cellular mRNAs have a cap structure at their 5' end ($m^7$GpppN, where N is any nucleotide). The ubiquitous $m^7$G cap and the associated cap binding protein(s) are required for translation initiation of cellular mRNA. Eucaryotic ribosomes scan the mRNA from the cap and efficiently recognize AUG initiation codons that are 5' proximal. A cellular mRNA also contains a poly (A) tail, which binds the poly (A) binding protein (PABP). Recently, eIF4G, a component of cap-binding protein complex has been found to interact with PABP. Therefore, in the current model of translation initiation of cellular mRNAs, the 3' and 5' ends of the mRNA are held in a proximal conformation in a closed-loop via interactions between proteins that bind to the 3' poly A and the 5' cap structure (Michel *et al.*, 2000). mRNAs in this configuration show a significant increase in the efficiency with which they recruit and recycle ribosomes (Sachs *et al.*, 1997). Some viral RNAs do not have the cap structure at their 5' end and some viral RNA do not have a poly (A) tail. Viruses may take these opportunities to recruit the host translation machinery in favor of viral protein synthesis.

#### 1.3.1.1.1 Internal ribosome entry sites (IRES) directed initiation of translation of viral proteins

Many viruses including picornaviruses, *Tobacco etch virus* (TEV), *Hepatitis C virus* and other members of family *Flaviviridae* do not have a cap structure at the 5' end of their genome, instead, they contain highly structured segments at 5' nontranslated RNAs which form internal

ribosome entry sites (IRES) (Xiang *et al.*, 1997; Gallie, 2001; Carrington and Freed, 1990; Rosenberg, 2001). Picornaviruses IRES elements are large *cis*-acting RNA regions that guide ribosomes to an internal site of the viral RNA. The IRES elements consist of highly conserved RNA secondary structure domains and have a characteristic oligopyrimidine tract followed by a conserved AUG triplet at their 3' border. In addition to the standard initiation factors, picornaviruses IRES elements recruit other cellular binding proteins that include polypyrimidine tract-binding protein, the La protein and the poly (rC) binding protein (PCBP). These proteins enhance translation or modulate the balance of translation and replication (Gamarnik and Adino, 1998; Andino *et al.*, 1999). In addition to these proteins, numerous other proteins have been shown to bind specifically to several picornaviruses IRES (Belsham and Sonenberg, 1996), but little is known about their potential role in internal initiation of translation. Comparison of the IRES elements of picornaviruses indicates that the nucleotide sequences are not conserved except for a short polypyrimidine tract. When the comparison is extended to other distantly related viruses, it is clear that not only the sequence but also the length are different among different IRES elements (Sasaki and Nakashima, 2000). The large variation indicates differences in structural organization, suggesting that different strategies are used to interact with the translational machinery.

The cap-independent IRES directed initiation gives these viruses opportunities to recruit host translation machinery in favor of viral protein synthesis. Picornaviruses have evolved mechanisms to modify eukaryotic initiation factors (eIF factors) to favor viral translation over cellular mRNA translation. *Poliovirus* (PV) proteinase $2A^{pro}$ cleaves eIF4G (a component of the cap-binding complex) that functions as an adapter and recruits many of the factors involved in stimulating 40S ribosomal subunit binding to an mRNA (Krausslich *et al.*, 1987). The C-terminal cleavage product of eIF4G, in complex with canonical translation factors, stimulates internal binding of ribosomes

to the viral 5' noncoding region directly (Ziegler *et al.*, 1995). PV proteinase $3C^{Pro}$cleaves PABP(Joachims *et al.*, 1999). The cleavage removes the COOH-terminal fragment of PABP, which contains binding sites for other PABP molecules and for the 60S ribosomal subunit (Bushell and Sarnow, 2002). Therefore, PV has employed a strategy to destroy both the cap-binding complex and end-to-end interaction of cellular mRNAs. The virus presumably inhibits cellular translation to increase the translation rate of the viral genome and, possibly, to prevent any host defense that requires new protein synthesis.

**1.3.1.1.2 Substitution of PABP and eIF4G**

(+) ss viral RNAs function as mRNAs before they function as a template replication. Therefore, it is reasonable to believe that viral RNAs act like cellular mRNAs to form closed-loop complexes. (+) ss RNA viruses show a wide variation in their terminal structures. Unlike cellular mRNAs that depend on PABP (binding the polyA tail) and eIF4G (a component of cap-binding complex) to form closed -loop complexes, some viral m RNAs utilize alternate ways to circularize the viral RNA. For example, the genome of *Brome mosaic virus* (BMV) has a cap at 5' end, but does not possess a poly (A) tail at its 3' end. The 3' end of viral RNA binds to the cell protein Lsm1p that facilitates the formation of closed-loop complexes (Diez *et al.*, 2000). The genome of PV has a poly (A) tail, but does not have 5' cap structure. The proteinase-polymerase precursor 3CD is known to bind to the 5' and 3' untranslated region (UTR). Therefore, a homodimer of 3CD bound to both ends of the viral RNA might support the formation of a circular RNA-protein complex (RNP) (Andino *et al.*, 1993). Also, the PCBP and PABP are known to bind to the 5' end and 3' end of PV RNA, respectively. These two proteins have been shown to bind to each other in an RNA-dependent fashion (Wang and Kiledjian, 2000). The interactions between the two

proteins may also facilitate the formation of closed-loop complexes. In *West nile virus* (a member of *Flavivirdae*), RNA-RNA interaction between the 3' and 5' complementary sequences has been proposed to facilitate viral genome circularization (Brinton, 2002). Many other examples have been reviewed recently (Bushell and Sarnow, 2002). These examples illustrate how a virus circularizes viral RNA by encoding a protein or recruiting host proteins to facilitate translation of viral RNAs (Sachs *et al.*, 1997).

#### 1.3.1.2.1 Polyprotein processing

To ensure that all the genes are accessible to the eukaryotic protein-synthesizing system, viral RNA genomes employ a few strategies. One of the strategies is the production of a single polyprotein from a viral RNA that is processed into mature proteins and intermediate precursors. RNA viruses in many families including *Picornaviridae* (e.g., PV), *Flaviviridae,* (e.g., *Hepatitis C virus*), *Potyviridae* (e.g.,TEV) and *Comoviridae* (e.g., CPMV) express their genomes using polyprotein strategies. The genome expression strategy of these families has been reviewed extensively in recent years (Ryan and Flint, 1997; Ryan *et al.*, 1998; Goldbach and Wellink, 1996; Spall *et al.*, 1997). Proteinases may cleave in an intramolecular manner (*in cis*), or in an intermolecular manner (*in trans*). When the proteinase is present on the molecule containing the cleavage site, the cleavage reaction is called *in cis*. *Cis*-cleavage is rapid and insensitive to dilution. When proteinase present on one molecule cleaves a second molecule containing the cleavage site, the cleavage reaction is called *in trans*. Cleavage *in trans* is slower, dependent on the concentration of proteinase and generally shows a greater sensitivity to sequence variation flanking the scissile amino acid pair (Carrier, *et al.*, 1999; Ryan and Flint, 1997).

#### 1.3.1.2.1.1 Proteinases

##### 1.3.1.2.1.1.1 Viral proteinases

Viral proteinases are involved in the specific proteolytic processing of virus proteins. The proteinases have a catalytic site and a substrate-binding pocket. The three-dimensional structure of the amino acids that make up the active site is conserved and provides the basis for proteinase classification. There are four different classes of proteinases including the serine proteinases, the cysteine proteinases, the aspartic acid proteinases and the metallo proteinases (Ryan *et.al*, 1998). Positive stranded RNA viruses generally encode cysteine and/or serine proteinases. Cysteine proteinases have a catalytic dyad consisting of Cys and His residues. The catalytic triad of serine proteinases consists of His, Glu (or Asp) and Ser. In addition, another type of viral proteinase (e.g., the 3C proteinase of picornaviruses) has a cysteine instead of serine at the active site, but its three-dimensional structure resembles that of a serine proteinase. These are serine-like proteinases (Ryan and Flint, 1997; Ryan *et al.*, 1998). In some cases, an RNA virus encodes several proteinases of different types to process the viral polyproteins. For example, potyviruses encode three types of proteinases: P1 (a serine proteinase), helper component proteinase HC-Pro (a cysteine proteinase) and NIa proteinase (a serine-like proteinase)(Carrington *et al.*, 1990).

The substrate-binding pocket is used to recognize the amino acids at the cleavage site and place the cleavage site in proper alignment for hydrolysis of the peptide bond by the active site of the proteinase. The cleavage site specificity of each proteinase is determined by its unique substrate binding-pocket. The substrate -binding pocket may have a preferences for only a single amino acid or may recognize cleavage sites that contain up to seven amino acids. Although the amino acids that make up the catalytic triad are conserved within one class of proteinases, there is little conservation in the amino acids that make up the substrate-binding pocket of the proteinase.

An exception to this is a conserved His residue in the substrate-binding pocket of serine-like proteinases from a number of viruses (e.g., picornaviruses, potyviruses and comoviruses) (Ryan and Flint, 1997). These serine-like proteinases process exclusively at (Gln, Glu)/(Gly, Ser, Met) cleavage sites with Gln/Gly being the most common (Spall *et al.*, 1997; Ryan and Flint, 1997) and the His in the substrate-binding pocket has been shown to interact with the Gln at the –1 position at the cleavage site (Mathews *et al.*, 1994). In contrast, serine-like proteinases from nepoviruses of subgroup A/B recognize a wide range of dipeptide sequences on their polyproteins. The difference in substrate recognition may be the result of replacement of the conserved His with Leu in the proteinase of subgroup A/B nepoviruses (Margis *et al.*, 1992 and 1994). However, other factors may play a role in substrate recognition. Virus-encoded proteinases are responsible for highly specific and regulated proteolysis of other virus polyproteins and may control the production of different, alternative functional proteins from the same precursor.

Virus-encoded proteinases may cleave host-cell proteins thereby modifying or inhibiting host cell function. For example, transcription factors, including the TATA-binding protein, that are required for transcription by RNA polymerase I, II, and III are cleaved by PV 3C $^{pro}$ (Das and Dasgupta, 1993). The viral function of this cleavage can block host defenses that require new viral RNA synthesis and/or to increase intracellular concentration of ribonucleotides. We also discussed above the cleavage of translation factors by viral proteinases. In addition to proteolytic processing, the viral proteinases of some picorna-like viruses have an RNA binding activity (Daros and Carrington, 1997; Cornell and Semler, 2002). Viral proteinases may have other functions and will be discussed in chapter 1.3.2.1.3.

**1.3.1.2.1.1.2 Host proteinases**

In some cases, host proteinases are involved in processing of the polyprotein. So far, there are two kinds of cellular proteinases involved in viral proteolytic processing: furin and signal peptidase. Furin is a membrane-bound proteinase whose primary site of action is in the trans-Golgi network. In some virus families, surface glycoproteins are initially synthesized as inactive precursors and then are cleaved by furin for maturation and full functional activities (Zimmer *et al.*, 2002). The signal peptidase and the virus-encoded serine proteinase catalyze the cleavage of the polyprotein precursor in the ER lumen and in the cytoplasm, respectively (Rice, 1996; Lee *et al.*, 2000).

#### 1.3.1.2.1.2 Proteolytic processing in well-characterized viruses

##### 1.3.1.2.1.2.1 *Poliviorus* polyprotein processing

The genome expression strategy of PV (*Picornaviridae*) has been extensively studied (Spall *et al.*, 1997). The polyprotein is co-translationally processed *in cis* into three intermediate precursors (primary products) P1, P2 and P3. These three primary products are further processed either in *cis* or *trans* into mature proteins and intermediate precursors (Fig. 1.1). The 3CD form of the proteinase is required for complete processing of the P1 intermediate precursor (Ypma-Wong *et al.*, 1988). Both the 3C and 3CD forms of the enzyme are capable of secondary processing of the P2 and P3 polyproteins, which occurs *in trans* and *in cis*. Interaction between 3CD and 3AB facilitates the release of mature products 3A, 3B, $3D^{Pol}$, and $3C^{Pro}$ (Molla *et al.*, 1994).

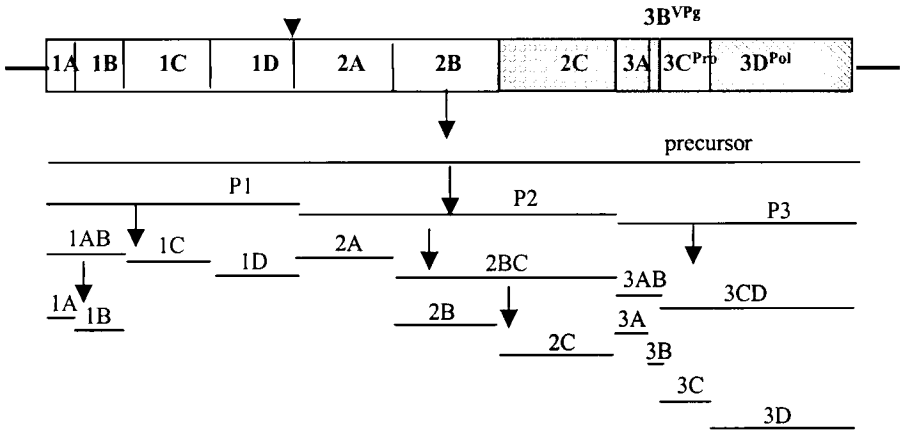


**Fig. 1.1. Processing strategy of the PV polyprotein.** The organization of the PV genome is shown at the top of the figure. The open reading frame is indicated by a box. Horizontal lines at the sides of the open reading frame represent non-coding regions. Vertical lines through the open reading frame indicate the cleavage sites. The domains for the different mature proteins (1A, 1B, 1C, 1D, 1A, 2B, 2C, 2D, 3A, 3B, 3C and 3D) are indicated in the open reading frame. The processing strategy of the polyprotein is shown at the bottom of the figure and includes a drawing of the precursor polyprotein, the intermediate gene products (P1, P2, P3, 1AB, 2BC, 3AB, 3CD) and the mature proteins. An arrow above the open reading frame indicates the cleavage site processed by the 2A proteinase. All other cleavage sites are processed by the 3C proteinase. 1A, 1B, 1C, 1D: capsid protein, 2A: proteinase, 2B: unknown function, 2C: membrane binding and putative helicase, 3AB: membrane-anchor protein, 3B: VPg (covalently linked to 5' end of each genomic RNA), 3CD and 3C: proteinase, 3D: polymerase.

#### 1.3.1.2.1.2 *Tobacco etch virus* polyprotein processing

The genome of TEV (family *Potyviridae*) encodes one open reading frame. The polyprotein is cleaved by three proteinases (Schaad *et al.*, 1996; Carrington *et al.*, 1993; Carrington and Dougherty, 1988; Carrington *et al.*, 1990). Two of the proteinases (P1 and HC-Pro) are responsible for their autocatalytic release from the amino terminus of the polyprotein. NIa $^{VPg\text{-}Pro}$, a proteinase related to the serine-like 3C proteinase of PV is involved in all the other cleavage events *in cis* and *in trans* (Fig. 1.2). Regulation of proteolytic processing of the NIa proteinase occurs at two levels. One level of regulation is at the primary amino acid sequence of the cleavage site (Schaad *et al.*, 1996). Another level of regulation involves the subcellular localization of the NIa proteinase (Carrington *et al.*, 1991 and 1993). The regulation of the NIa proteinase will be discussed in detail in chapter 1.3.1.2.1.4.

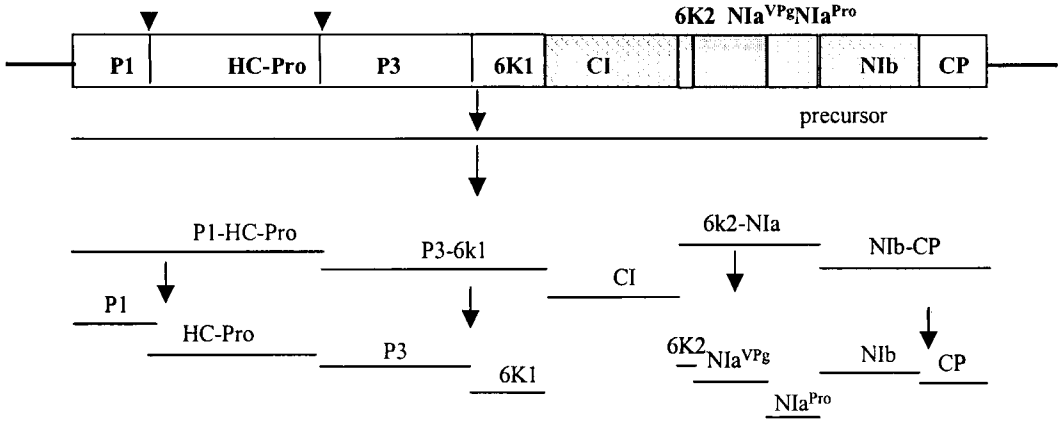


**Fig. 1.2. Processing strategy of the TEV polyprotein.** The organization of the *Tobacco etch virus* genome is shown at the top of the figure. The open reading frame is indicated by a box. Horizontal lines at the sides of the open reading frame represent non-coding regions. Vertical lines through the open reading frame indicate cleavage sites. The domains for the different mature proteins (P1, HC-Pro, P3, 6K1,CI, 6K2, VPg, NIa, NIb, CP) are indicated in the open reading frame. The processing strategy of the polyprotein is shown at the bottom of the figure and includes a drawing of the precursor polyprotein, the intermediate gene products and the mature proteins. The cleavage sites that are not processed by the NIa proteinase are indicated by arrows above the open reading frame. P1: proteinase, HC-Pro: proteinase, P3: unknown functions, CI: helicase, 6k2: membrane-anchor protein, $NIa^{VPg}$ : VPg, $NIa^{VPg\text{-}Pro}$ and $NIa^{Pro}$: proteinase, NIb: polymerase.

#### 1.3.1.2.1.3 *Cowpea mosaic virus* polyprotein processing

*Cowpea mosaic virus* (CPMV, genus *Comovirus*, family *Comoviridae*) contains a bipartite genome (Goldbach, 1987; Goldbach and Wellink, 1996). CPMV B-RNA and M-RNA are translated into P1 and P2, respectively. P1 and P2 are processed into intermediate and mature proteins by the P1 containing 3C-like proteinase (Goldbach and Wellink *et al.*, 1996; Van Bokhoven *et al.*, 1993) (Fig. 1.3). The P2 is cleaved *in trans* by the proteinase encoded in P1. *In vitro* proteolytic processing reveals the P1 (200 kDa) polyprotein is rapidly cleaved into the 32 kDa and 170 kDa protein (Peters *et al.*, 1992). The 32 kDa protein remains associated with the 170 kDa protein (NTB-VPg-Pro-Pol ) via an interaction between 32 kDa and NTB domain contained in the 170 kDa protein. The protein complex inhibits further cleavage of NTB-VPg-Pro-Pol. In contrast, this complex is required for the cleavage of P2. Therefore, the 32 kDa protein acts as a cofactor in the cleavage of P2 and a regulator in the cleavage of P1 (Peters *et al.*, 1992). In protoplasts, the rate of proteolytic processing is also strongly affected by the presence of the 32 kDa protein (Van Bokhoven, *et al.*, 1993). Unlike PV and TEV, processing of polyprotein P1 occurs efficiently only *in cis in vitro* (Peters *et al.*, 1992; Peters *et al.*, 1995). Furthermore, kinetic studies on the processing of the 170 kDa polyprotein (NTB-VPg-Pro-Pol) have shown that NTB-VPg and NTB proteins appear to be produced at the same time, indicating that it is unlikely that NTB-VPg is the direct precursor of VPg (or NTB). The VPg-Pro-Pol and Vpg-Pro may be the precursors for VPg (Peters *et al.*, 1995).

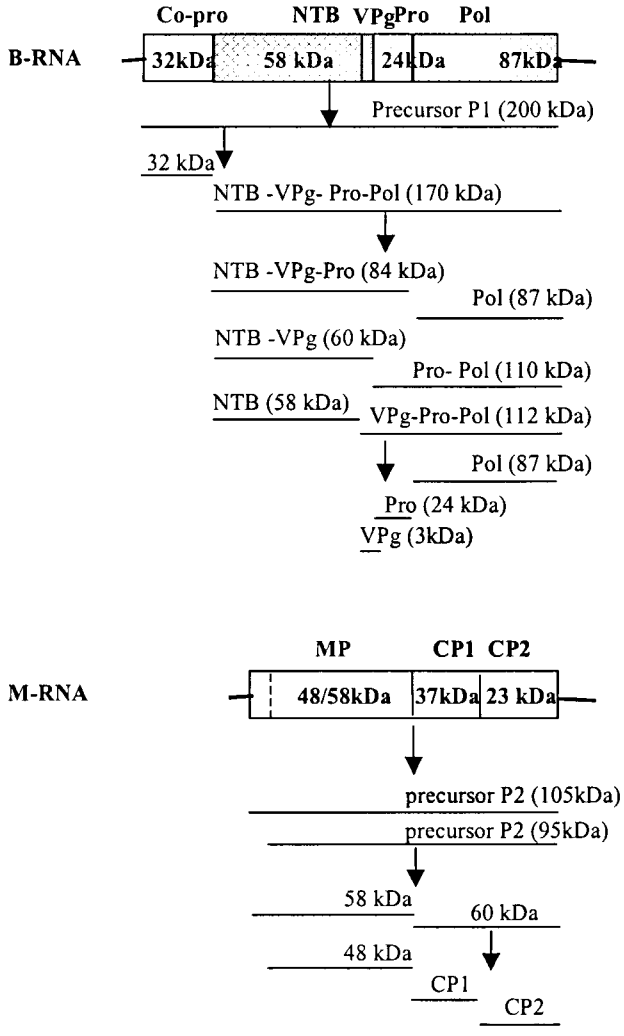


**Fig. 1.3. Processing strategy of the CPMV polyproteins.** The organization of the CPMVgenome is shown at the top of the figure. The open reading frames are indicated by boxes. Horizontal lines at the sides of the open reading frame represent non-coding regions. Vertical lines through the open reading frame indicate cleavage sites. The vertical dotted line through the RNA2 open reading frame indicates an alternative translation initiation. The domains for B-RNA and M-RNA are indicated in the open reading frame. The processing strategy of the polyprotein is shown at the bottom of the figure and includes a drawing of the precursor polyprotein P1 (200 kDa) and P2 (105/95 kDa), the intermediate products and the mature proteins. NTB: protein containing a NTP binding motif, VPg: viral genome linked protein, Pro: proteinase, Pol: RNA-dependent RNA polymerase, MP: movement protein, CP1: coat protein 1, CP2: coat protein 2.

#### 1.3.1.2.1.3 Advantages of polyprotein processing

(+) ss RNA viruses encode limited genetic information. Polyprotein processing has the advantage that several functional proteins can be produced from a minimum of genetic information. The proteins have distinct functions from their precursors. For example, PV encodes a single polyprotein that undergoes extensive proteolytic processing (Fig. 1.1). The proteinase-polymerase precursor 3CD is an intermediate precursor. The activities of PV $3CD^{pro-pol}$, $3C^{pro}$ and $3D^{pol}$ are strikingly different (Cornell and Semler, 2002). $3C^{pro}$ is a viral proteinase and also has been shown to possess RNA binding determinants. The 3D polymerase domain of 3CD modulates its RNA binding and protein processing activities. 3CD is a proteinase but does not possess polymerase activity (Harris *et al.*, 1992). Another example of this is *Rubella virus*. *Rubella virus* non-structural proteins (NSPs) are translated as a 200 kDa polyprotein that is fully functional in negative-stranded RNA synthesis, whereas cleavage products 150 kDa/90 kDa are required for positive stranded RNA synthesis (Liang and Gillam, 2001). This result suggests that temporal regulation of polyprotein processing results in different combinations of NSP components that regulate many steps of viral RNA synthesis.

#### 1.3.1.2.1.4 Regulation of viral proteinase activity

Polyprotein processing is tightly regulated, allowing proteins with different functions to be expressed at the required points during the virus life cycle. Viruses that use a polyprotein processing strategy encode one or more proteinases that are highly specific for their substrates. Viruses can use several strategies to regulate the efficiency of processing at different cleavage sites.

(i) The high degree of specificity between virus-encoded proteinases and their substrates regulates processing pathways. Proteinases cleave at specific peptide bonds. Variations in the amino acids sequence around the cleavage site of the substrate can modulate the cleavage rate (Carrier *et al.*, 1999; Schaad *et al.*, 1996). For example, TEV encodes a single polyprotein which undergoes extensive proteolytic processing (Fig.1.2). Conserved amino acids are found in the -6,-4 and -3 positions of TEV cleavage sites (Carrington and Dougherty, 1988). Mutations of the conserved amino acids have confirmed that these amino acid residues are important for proteolytic processing. One of the proteinases $NIa^{VPg\text{-}Pro}$ consists of a N-terminal VPg domain and a C-terminal proteinase domain. The domains are separated by an internal cleavage site. The cleavage site was shown to be a poor substrate for NIa proteolysis because of a suboptimal sequence context around the cleavage site. Despite the slow cleavage kinetics, a mutation that abolishes internal processing is lethal to virus replication, suggesting the cleavage site is essential to RNA replication. Mutants with accelerated internal proteolysis render the genome nonviable, supporting the hypothesis that slow internal processing provides a regulatory function (Schaad *et al.*, 1996). This differential regulation of processing at specific cleavage sites is also used during polyprotein processing of picornaviruses and flaviviruses (Rice, 1996; Lee *et al.*, 2000)

(ii) Proteinase activity may be regulated by the processing of the proteinase precursors. Viral proteinases function as discrete proteins and as proteolytic domains within larger polyprotein precursors. The proteinase and its precursors sometimes mediate different processing events (Ypma-Wong *et al.*, 1988; Failla *et al.*, 1994). For example, PV $3C^{Pro}$ is regulated by the presence of the 3D domain in the intermediate precursor 3CD. 3CD cleaves the capsid protein P1, but 3C cannot (Cornell and Semler, 2002). The 3C-like proteinase (Pro) from nepoviruses is responsible for the processing of the RNA1 encoded P1 and RNA2 encoded P2 polyproteins. Using an *in vitro*

system, it has been shown that the proteinase is more active than VPg-Pro intermediate precursor *in trans* processing of P2 (Margis *et al.*, 1994; Chisholm *et al.*, 2001).

(iii) Co-factors modulate the proteinase activity. For example, the proteinase function of *Flavivirus* NS3 is activated upon complex formation with the viral protein NS4A and is responsible for all the cleavage events occurring downstream of NS3 (Failla *et al.*, 1994). Another example is the CPMV 32 kDa protein which was discussed above.

(iv) The cellular compartment may regulate the concentration of active proteinase available for *trans* cleavage. For example, TEV $NIa^{VPg\text{-}Pro}$ proteinase is actually a polyprotein consisting of two domains separated by an inefficient cleavage site. The VPg domain of proteinase $NIa^{VPg\text{-}Pro}$ contains a nuclear localization signal. Thus, the $NIa^{VPg\text{-}Pro}$ is mainly targeted to the nucleus where it aggregates into an ordered crystal shape referred to as the nuclear inclusion body (Restrepo-Hartwig *et al.*, 1992). The small mature NIa proteinase is targeted to the cytosol where the TEV polyprotein processing occurs. However, when NIa is present in a polyprotein form containing the 6k2 protein which is an integral membrane protein, the membrane binding activity of the 6k2 protein dominates over the nuclear localization activity. Therefore, transport of this protein to the nucleus is suppressed and the proteinase localized in membranes in which polyprotein processing continue to proceed and the viral RNA replication takes place. This may be a method to regulate the concentration of active proteinase (Carrington *et al.*, 1991; Restropo-Hartwig and Carrington, 1991).

### 1.3.1.3 Other strategies for gene expression

Although a polyprotein-processing strategy has advantages, proteins produced from polyprotein processing are equimolar in amounts. To express differential amounts of various proteins and

make very efficient use of the limited amount of genomic nucleic acids they possess, many groups of RNA viruses employ additional strategies for gene expression. These strategies include (i) subgenomic RNAs and multipartite genomes; (ii) readthrough, frameshift and alternative initiation proteins. These strategies have been reviewed (Bustamante and Hull, 1998; Maia *et al.*, 1996) and will not be discussed here.

### 1.3.2 Strategies for viral genome replication

Viral RNA replication includes two steps: minus stranded RNA synthesis using viral RNA as a template and plus stranded RNA synthesis using the newly synthesized minus stranded RNA as a template. The selective amplification of a RNA molecule into thousands of RNA progeny involves *cis*-acting elements present in the viral genome, viral proteins and host factors (Sullivan and Ahlquist, 1997; Xiang *et al.*, 1997). These factors are assembled in membrane-associated replication complexes (Buck, 1996). In this section, we will discuss viral and host factors that are involved in virus replication.

#### 1.3.2.1 Viral factors involved in replication

##### 1.3.2.1.1 Viral proteins required for (+) ss RNA replication

The replication of viral RNA means polymerizing nucleoside triphosphate on an RNA template. As a genome of (+) ss RNA virus enters the host cells, it does not find enzymes specific for RNA-dependent RNA synthesis. RNA viruses must encode the RNA-dependent-RNA polymerase (RdRp) to catalyze the RNA synthesis. Helicase is also required for viral RNA replication. During the replication of (+) ss RNA viruses, viral genomes can be found in partially duplex form or double stranded RNA (ds RNA). However, the template must be repeatedly

available for a new round of replication. Therefore, a helicase may be required to resolve intramolecular base pairing in the template RNA and intermolecular base pairing between template RNA and the nascent complementary strand. Viruses also encode other proteins involved in replication. These viral proteins often have multiple functions.

#### 1.3.2.1.1 RNA dependent RNA polymerase

RNA viruses are divided into three major classes: ds RNA, positive stranded RNA or negative stranded RNA. To replicate viral RNA, all known RNA viruses encode an RNA dependent RNA polymerase (RdRp). These RdRps share multiple sequence motifs that are conserved across RNA viruses. Elucidation of the crystal structure of RdRps of RNA viruses has shown that RdRps share a structure similar to that of a right hand, with palm, thumb, and finger domains (Ahlquist, 2002). Sequence comparison studies on (+) ss RNA viruses have shown that the polymerases contain a consensus sequence motif Gly-Asp-Asp (GDD) flanked by hydrophobic amino acids (Buck, 1996). The conserved GDD motif is crucial for the RdRp activity. For example, substitution of the GDD in TEV NIb (RdRp) has been shown to be lethal. The NIb defective mutants can be rescued *in trans* by wild type NIb expressed in transgenic plants (Li and Carrington, 1995). Viral RdRps act in combination with other viral and host factors and function in membrane-bound specific complexes that target the polymerase to appropriate template and co-ordinate the various steps of RNA synthesis (Diez *et al.*, 2000; Chen *et al.*, 2001).

#### 1.3.2.1.2 Helicase

Helicases are NTP-driven motors that are capable of enzymatically unwinding duplex RNA structures by disrupting the hydrogen bonds that maintain the duplex form. The most conserved

motif among helicases is the NTP binding motif (NTBM) that is composed of the A site and B site (Walker *et al.*, 1982). Mutations of this motif in CPMV rendered the virus nonviable (Peters *et al.*, 1994). On the basis of conserved motifs, cellular and viral RNA and DNA helicases have been classified into a number of superfamilies (Caruthers and Mckay, 2002). The NTBM containing proteins of *Sindbis*-like viruses and potyviruses are similar to eukaryotic translation initiation factor (eIF4A) that have RNA-dependent ATPase and RNA helicase activity (Lain *et al.*, 1989). The NTBM-containing proteins of picorna-, como- and nepoviruses are related to *Simian virus-40* (S40) larger T antigen, a protein containing RNA and DNA helicase activity (Gorbalenya *et al.*, 1990).

RNA helicase, RNA stimulated ATPase and RNA binding activities have been demonstrated for the NTBM-containing proteins from a few potyviruses and flaviviruses (Caruthers and McKay, 2002; Fernandez *et al.*, 1995). For example, the NTBM-containing protein CI from *Plum pox virus* (a potyvirus) has been shown to have an RNA helicase activity and an RNA binding activity (Fernandez and Garcia, 1996; Lains *et al.*, 1990). Some helicases need a cofactor to enhance the RNA unwinding activity. For example, *Hepatitis C* viral helicase/proteinase NS3 has a polynucleotide-stimulated NTPase activity, a 3'-5' unwinding activity and a single stranded RNA binding activity. NS3 alone is a poor helicase on RNA, but the activity is enhanced by a cofactor NS4A. In contrast, NS3 alone is a highly processive helicase on DNA. Phylogenetic analysis suggests that this robust DNA helicase may have evolved in HCV to affect host DNA (Wolk *et al.*, 2000; Pang *et al.*, 2002). Recent experiments have shown that NS3 specifically interacts with the 3' terminal sequence of viral positive- and negative-stranded RNA (Banerjee and Dasgupta, 2001). NS4A is an integral membrane protein and interacts with NS3. Possibly, the NS3-NS4A complex bound to either the positive- or negative-stranded 3' UTR may anchor RNA-protein complexes to the cytoplasmic membranes (Wolk *et al.*, 2000; Pang *et al.*, 2002).

PV 2C protein is a putative helicase. Mutations in the conserved amino acids of the NTP-binding motifs A and B abolish or greatly reduce RNA synthesis. However, efforts to detect RNA helicase activity have not been successful (Mirzayan and Wimmer, 1994). The PV 2C is a multifunctional protein and some of these functions include ATPase and GTPase (Rodriguez and Carrasco, 1993), membrane binding (Teterina et al., 1997; Suhy *et al.*, 2000 and references therein) and RNA binding activities ( Banerjee and Dasgupta, 2001).

**1.3.2.1.3 Proteinase**

As discussed above, RNA viruses in many families express their genomes in ways which involve the synthesis and subsequent cleavage of precursor polyprotein and viral proteinases play a central role in polyprotein processing (see section 1.2.1). The regulation of proteolytic cleavage of precursors containing the polymerase may affect the activity of these polymerases. In addition to the proteolytic function, proteinases have other functions during initiation of RNA synthesis (Li *et al.*, 1997; Cornell and Semler, 2002). PV 3C proteinase interacts with a 5'-proximal cloverleaf structure to promote positive stranded RNA synthesis, and this interaction is enhanced when 3C is in the context of the 3CD polyprotein (Andino *et al.*, 1993; Cornell and Semler, 2002). The NIa proteolytic domain of TEV interacts specifically with NIb polymerase and binds TEV viral RNA, suggesting the viral RNA template is delivered to the polymerase through a NIa proteinase domain-RNA interaction (Schaad *et al.*, 1997). PV viral proteinase 3CD (intermediate precursor) binds the cloverleaf–like structure of the viral RNA that is required for replication. It has been proposed that 3CD binding of viral RNA at the cloverleaf structure may have at least two functions: (i) recruitment of polymerase 3D to the viral RNA template; (ii) regulation of replication initiation and translation. This will be discussed below.

#### 1.3.2.1.4 Capping and Methylation Enzymes

Some viruses, e.g., alpha-like, corona-like and flavi-like viruses possess capped genomic RNA. Replication of these viruses requires viral encoded capping and methylation enzymes. BMV RNA1 1a protein contains methyltransferase domain at the N-terminus and a helicase domain at its C-terminus. Mutations of the conserved domains rendered the virus unable to replicate (Sullivan and Ahlquist, 1997).

#### 1.3.2.1.5 Genome-linked virus proteins (VPgs)

Genome-linked virus proteins (VPgs) are virus-encoded proteins that are covalently linked by a phosphodiester linkage to the 5' terminal nucleotide of the virus RNA. These viruses include the picorna-like and sobemo-like supergroups. Although viruses in these group have VPg at 5' end, the amino acid that links the VPg to the RNA has been identified for only a few of them. A tyrosine residue was shown to link the VPg to the viral RNA for both picornaviruses and plant potyviruses. In *Tobacco vein mottling virus*, replacement of this tyrosine is lethal for viral replication (Murphy *et al.*, 1996). Some viruses, e.g., CPMV, link VPg to the viral RNA by a serine residue. Mutational analysis has demonstrated that the structure of the N-terminal end of VPg containing the serine is crucial for virus replication (Carette *et al.*, 2002). *Grapevine fanleaf virus* (GFLV) and *Tobacco ringspot virus* also link VPg to viral RNA by a serine residue (Mayo and Robinson, 1996, Zalloua *et al.*, 1996). The 5' VPg is essential for infectivity of some viral RNAs but not others (Mayo *et al.*, 1982). This conclusion comes from experiments in which the viral RNA is treated with proteinase K and assayed for infectivity. The infectivity of RNA of ToRSV was abolished by the treatment, while that of *Arabis mosaic virus* was only decreased (Mayo *et al.*, 1982). The infectivity of the comoviral RNA molecules did not change after the

treatment (Goldbach and Wellink, 1996). In addition, the VPg is thought to act as a primer for the initiation of viral RNA synthesis ( Xiang *et al.*, 1997). This suggestion is supported by the following evidences from experiments using PV as a model: **(i)** VPg can be uridylylated in reactions containing a poly(A) template, UTP and 3D polymerase (Paul *et al.*, 1998); **(ii)** VPg is found covalently linked to the 5' end of newly synthesized negative and positive strands of PV (Wimmer *et al.*, 1993); **(iii)** VPgpUpU can be synthesized in membrane-bound replication complexes isolated from infected cells and elongated to longer VPg RNA molecules (Takeda *et al.*, 1986; Vartapetian *et al.*, 1984); **(iv)** VPg can act as a primer in the form of VPg-pUpUppp, which can anneal to the 3' terminus of negative strand RNA (Crawford and Baltimore, 1983); **(v)** polymerase 3D binds with high affinity to the membrane bound viral protein 3AB but uridylylates only the VPg (3B). Mutation analysis of the polymerase showed that surface amino acid residues required for VPg uridylylation overlap with the sites for interaction with the VPg domain of 3AB (Pathak *et al.*, 2002).

#### 1.3.2.1.2 *Cis*-acting viral proteins

Nonstructural proteins (NSP) of (+) ssRNA viruses play catalytic and regulative roles in the replication process. In most cases, these NSPs can be provided using a helper virus expressing the proteins *in trans* (Towner *et al.*, 1998; Li and Carrington, 1995). However, mutations in some coding region are noncomplementable *in trans*. For example, genome of CPMV (CPMV) has two molecules B-RNA and M-RNA. B-RNA encodes all the nonstructural proteins required for replication and B-RNA can replicate independently. Replication of mutant B-transcripts could not be supported with co-inoculated B-RNA in protoplasts, suggesting that replication of a B-RNA molecule is tightly linked to its translation (Wellink *et al.*, 1994). M-RNA does not support its own

replication, but requires the viral replicative functions encoded by B-RNA *in trans*. Alternative initiation of translation on M-RNA gives coterminal polyproteins, which are processed into the 48 kDa/58 kDa movement protein(s) and capsid proteins. Mutations in the 58 kDa coding region in M-RNA can not rescued by wild-type M-RNA in the presence of B-RNA, indicating that replication of M-RNA depends on translation of the 58 kDa protein from the very same M-RNA molecule (Van Bokhoven *et al.*, 1993). *Cis*-acting functions have also been reported for PV (an coding region between 2A-amino acid 66 and 3D-amino acid 28) (Novak and Kirkegaard, 1994), *Rubella virus* (200 kDa polyprotein precursor) (Liang and Gillam, 1999), TEV NIa proteinase (Schaad *et al.*, 1996) and *Alfafa mosaic virus* (coat protein) (Neeleman and Bol, 1999). These results suggest that translation and replication of the genomes of these viruses are tightly coupled. The molecular basis for coupling between translation and replication of genomic RNA is not clear, but several possibilities have been proposed (Novak and Kirkegaard, 1994). One explanation is the formation of a functional template. The newly synthesized *cis*-acting proteins might interact with the RNA from which it is being translated to enable the RNA to become a functional template for negative stranded RNA synthesis.

#### 1.3.2.1.3 *Cis*-acting RNA elements required for RNA replication

The genomes of positive-stranded RNA viruses contain essential *cis*-acting sequences that function as recognition signals for viral RNA replication. (+) ss RNA viruses show a wide variation in the terminal structures of these RNAs (e.g., cap structure or genome-linked proteins (VPg) at 5' end and a poly (A) tail or tRNA-like structure at the 3' end). Moreover, the untranslated regions (UTR) at 3' and 5' end of the RNA of many viruses can be folded into a characteristic secondary or tertiary structure and contain conserved motifs that have been shown to be involved

in virus replication. The *cis*-acting nucleotide sequences required for BMV and PV replication are well characterized (Xiang *et al.*, 1997; Sullivan and Ahlquist, 1997).

The RNA genome of PV contains a long 5' UTR, a single open reading frame, a short 3' UTR and a poly (A) tail. The VPg is linked to 5' end of the viral RNA. As discussed above, initiation of PV RNA synthesis is coupled to uridylylation of VPg, whereby the resulting VPgpUpU serves as a primer for viral RNA synthesis (Xiang *et al.*, 1997). Cellular mRNA carrying 3'-terminal poly (A) are abundantly present in the cytoplasm of host cells, which requires signals within viral RNA that would directs uridylylation exclusively to the viral genome. PV contains a few *cis*-acting sequences important in virus replication (Xiang *et al.*, 1997; Rieder *et al.*, 2000).

PV contains two independent domains at the 5' UTR: a cloverleaf structure and the large internal ribosomal entry site (IRES). Recent studies indicate that 5' terminal cloverleaf RNA is required *in cis* for the initiation of RNA synthesis (Xiang *et al.*, 1997). PCBP binds to both the 5' end cloverleaf structure that is required for viral RNA replication and to the IRES that is required for viral RNA translation. Binding of the proteinase-polymerase intermediate precursor 3CD to the cloverleaf-like RNA dramatically increases the affinity of PCBP for the cloverleaf structure. Binding of PCBP to the IRES is required for translation, indicating that dynamic ribonucleoprotein (RNP) on the cloverleaf mediate the switch from translation to replication (Gamarnik and Andino, 1998; Xiang *et al.*, 1997). The 3' UTR and the associated poly (A) tail are important *cis*-acting determinants in the initiation of negative-stranded RNA synthesis (Teterina *et al.*, 2001 and references therein). In addition, recent experiments suggest that an RNA stem-loop structure within the polyprotein-encoding region functions as a *cis* replication element (CRE). Analogous elements in other picornaviruses including human *Rhinovirus* type 14, *Theiler's virus* and *Encephalomyocarditis* indicates that they are important for replication (Rieder *et al.*, 2000 and

references therein). All the CRE sequences identified so far contain an AAACA motif. In PV, it has been demonstrated that the first two nt of this motif in CRE is a primary template for the synthesis of VPgpUpU *in vitro* (Paul *et al.*, 2000). If this is also the case in infected cells, the question remains to be how the primer VPgpUpU is being translocated to the 3' poly (A) tail of plus stranded RNA or the 3'-terminal $UUUUAA_{OH}$ of minus stranded RNA (Rieder *et al.*, 2000 and references therein). It has been suggested that the different *cis*-acting sequences are brought in proximal conformation to regulate replication initiation and translation (Xiang *et al.*, 1997; Rieder *et al.*, 2000).

Another well-studied example is BMV. BMV has three genomic RNAs. Each RNA has a 5' cap and a tRNA-like 3' end. Each RNA contains several-loops and pseudoknots immediately upstream of the tRNA-like structure. The loops, pseudoknots and tRNA-like structure are required for viral RNA replication (Sullivan and Ahlquist, 1997). Furthermore, although the sequences at the 3' termini of RNAs 1, 2, and 3 are very similar, reciprocal exchanges cause aberrant replication, suggesting a requirement for compatibility with the upstream sequences (Guggal *et al.*, 1992). *Cis*-acting sequences are also required for the assembly of replication complexes. BMV RNA1 encoded 1a induces spherules that have been shown to be the replication site (Schwartz *et al.*, 2002). 1a protein can bring polymerase 2a and RNAs into the replication site (Chen and Ahlquist, 2000). 1a interacts with the intergenic region of the RNA3 to induce RNA3 association with cellular membrane (Sullivan and Ahlquist, 1999). 1a also interacts with the 5' terminal stem -loop of RNA2 and induce RNA2 association with cellular membrane (Chen *et al.*, 2001). Moreover, it has been demonstrated that 1a-induced stabilization and membrane association of RNA3 are closely linked to inhibition of RNA3 translation and stimulation of negative stranded RNA3 synthesis (Sullivan and Ahlquist, 1999). The action of 1a on RNA3 is similar to the action of 3CD

on the cloverleaf structure. Therefore, the *cis*-acting sequences are not only involved in replication but also regulate the switch between translation and replication.

Taken together, these results indicate that the sequences at the 5' and 3' end of the viral genome and other *cis*-acting elements are required for negative stranded RNA synthesis. This suggests that initiation of negative stranded RNA synthesis requires direct interactions between distal RNA structures at the termini of the genomic RNA. As mentioned above, in a current model of translation initiation of cell mRNAs, the 3' and 5' end of mRNA are held in a closed-loop conformation. Thus, circularization of viral RNA genomes may be necessary for both translation and replication (Sullivan and Ahlquist, 1997; Rieder *et al.*, 2000).

### 1.3.2.2 Host factors involved in virus replication

Viruses replicate in a restricted number of hosts and tissues, indicating that cellular factors present only in certain tissues (or hosts) are involved in the viral cycle (Andino *et al.*, 1999). The limited coding capacity of (+) ss RNA necessitates utilization of host factors for virus replication. In this section, we will review host proteins and intracellular membranes that are involved in virus replication.

#### 1.3.2.2.1 Host proteins involved in virus replication

Many cellular proteins appear to be essential for virus replication (Andino *et al.*, 1999; Lai, 1998; Xiang *et al.*, 1997; Buck, 1996). However, their exact function remains to be determined. Cellular proteins involved in replication can be put into two groups: (i) cellular proteins that regulate the activity of the viral RdRp; (ii) cellular proteins that interact with cis-acting regulatory viral RNA sequences. An example of the first group of host factor is eukaryotic translation

initiation factor eIF-3 that is tightly bound to the BMV 2a protein (RdRp) and stimulates the RdRp activity (Quadt *et al.*, 1993). An example of the second group of host factor is PCBP which binds to PV: both the 5'end cloverleaf structure which is required for viral RNA replication and IRES which is required for viral RNA translation. Binding of 3CD to the cloverleaf-like RNA dramatically increases the affinity of PCBP for this RNA element, indicating that dynamic ribonucleoprotein (RNP) interaction with the cloverleaf mediate the switch from translation to replication initiation (Gamarnik and Andino, 2000).

**1.3.2.2.2 Replication complexes associated with membranes**

Replication of the genome of all characterized positive-stranded RNA viruses occurs in large complexes which are associated with intracellular membranes (Buck, 1996). Many positive-stranded RNA viruses induce extensive proliferation and modification of intracellular membranes in their hosts which often results in the accumulation of numerous membranous vesicles. Double-stranded RNA replication intermediates and viral replication factors are associated with the membranous vesicles which are thought to be the site of the replication (Carette *et al.*, 2000; Carette *et al.*, 2002; Gosert *et al.*, 2002; Schaad *et al.*, 1997). The requirement for intact membranes for successful virus replication has also been demonstrated using cell-free replication systems (Barton *et al.*, 1995; Molla *et al.*, 1993; Wu *et al.*, 1992). The membrane may be an essential part of the replication complexes required for its organization and function (Buck, 1996). For example, *Semiliki Forest virus* (SFV) capping enzyme requires association with anionic membrane phospholipids for its activity, indicating that the protein is adapted to function only in a membranous environment (Ahola *et al.*, 1999). BMV replication occurs on the perinuclear region of the ER. Mutation of host $\Delta$9 fatty acid desaturase inhibits BMV replication between template recognition and RNA synthesis, emphasizing the importance of compatibility of the membrane

composition with RNA replication (Lee *et al.*, 2001). PV protein 2C has an amphipathic helix at its N-terminus which has been shown previously to be essential for membrane association. Mutations of the protein in the N-terminal sequence predicted to disrupt the amphipathic helix were lethal, suggesting that membrane association is important for the function of 2C. PV infection induces formation of vesicles to promote efficient replication of the virus. By use of detergent treatment it was shown that the virus-induced vesicles are not necessary for elongation of viral RNA but are required for initiation of viral plus-stranded RNA synthesis (Egger *et al.*, 1996). This suggests that the vesicles play more important roles than just being a simple carrier; it may organize and arrange all the components involved in initiation of replication so that it can proceed in a highly ordered way.

**1.3.2.2.2.1 Replication complexes of different viruses associated with distinct vesicles**

Different viruses modify distinct intracellular membranes for the assembly of their replication complexes, including the chloroplast (Prod'homme *et al.*, 2001), mitochondrial membrane (Miller and Ahlquist, 2002), vacuolar membrane (Van Der Heijden *et al.*, 2001) and ER membranes (Buck, 1996). Although some viruses belong to the same supergroup, they may modify different intracellular membranes. For example, SFV, BMV and *Alfalfa mosaic virus* all belong to the alphavirus-like supergroup. SFV replication takes place on the cytoplasmic surface of cytopathic vacuoles derived from endosomes and lysosomes (Kujala *et al.*, 2001). BMV viral RNA synthesis occurs on perinuclear ER (Chen *et al.*, 2001). The *Alfalfa mosaic virus* replication complex has been found associated with vacuolar membranes (Van Der Heijden *et al.*, 2001).

Although membranes of the ER are involved in the replication of several viruses, viruses may use different mechanisms to modify the ER membranes. PV replicates its RNA on the surface

of membrane vesicles budded from the ER, resulting in disorganization of the organelles of the secretory route in late infection (Suhy *et al.*, 2000). CPMV infection induces a massive proliferation of the ER. The proliferated membranes are often located near the nucleus and are connected to the ER network. Remarkably, the cortical ER and Golgi remained essentially unaffected in CPMV- infected cells (Carrette *et al.*, 2000). *Tobacco mosaic virus* replication induces redistribution of ER-derived membranes and the cortical ER morphology was highly perturbed (Reichel and Beachy, 1998). Inhibition of vesicle trafficking between ER and Golgi was found to inhibit GFLV, and PV replication, suggesting that replication requires a functional secretory transport system. Cerulenin, a drug inhibiting *de novo* lipid synthesis also inhibited GFLV, PV and CPMV, suggesting that their replication requires continuous lipid biosynthesis (Carette *et al.*, 2000; Ritzenthaler *et al.*, 2002 and references therein).

(+) ss RNA viruses induce cellular vesiculation, but the morphology of the vesicles are different. Many animal and plant (+) RNA viruses in the alphaviruses induce membrane-bound spherules. For example, BMV 1a induces perinuclear membrane-bound spherules (Schwartz *et al.*, 2002). The viral RNAs and polymerase 2a are sequested into the spherules in which the viral RNAs are in a membrane-associated, nuclease-resistant state. The 1a-induced spherules with their necks connecting to the outer nuclear membrane become the factories for virus replication. While replication of many (+) RNA viruses involves BMV-like spherules, some induce alternate membrane structures. Replication of PV takes place on the surface of double membrane vesicles originating from the ER (Suhy *et al.*, 2000). Although a single vesicle is capable of initiating and sustaining plus-stranded RNA synthesis, PV-induced vesicles have a high tendency to accumulate into high-order rosette-like structures. The active replication complexes are tightly enclosed and protected in the interior of the rosette, whereas only mature progeny plus stranded RNA is present

on the surface of the rosette (Egger *et al.*, 1996). Similar rosette structures have been identified in GFLV infected tissues (Ritzenthaler *et al.*, 2002). The morphological differences may reflect differences in the replication of different genomic RNA or differences in recruiting membranes for the formation of replication complexes.

**1.3.2.2.2.2 Viral anchoring proteins**

As mentioned above, distinct types of membranes are involved in the replication of different viruses, indicating the establishment of specific interactions between host membranes and viral proteins. Viral RNA replication complexes contain the viral RNA dependent RNA polymerase, accessory viral proteins, viral RNA and host proteins. One or several viral proteins are thought to act as a membrane anchor(s) for the complex while other viral replication factors are brought into the complex either as part of larger polyproteins or through protein-protein and protein RNA interactions with the membrane anchor. All viral membrane proteins identified so far are integral membrane proteins. In some cases, the membrane proteins associate with membrane by transmembrane domains. For example, PV3AB and TEV 6 k2 proteins are transmembrane proteins and have been suggested to play a role as membrane anchors for the replication complex as will be discussed in detail below. In other cases, proteins required for replication are associated with membranes by an amphipathic helix (Teterina *et al.*, 1997; Brass *et al.*, 2002; Ahila *et al.*, 2000). SFV encoded nsP1 contains the enzymatic guanine-7-methyltransferase and guanylytransferase activities that are necessary for capping of the viral RNA (Ahola *et al.*, 1999). The NSP1 binds the membrane by an amphipathic helix that interacts with negatively charged phospholipids. Palmitoylation of nsP1 enhances membrane affinity (Ahila *et al.*, 1999). In some cases, the viral polymerase directs itself to membrane by its C-terminal or N-terminal tail, leaving most of the

protein exposed to the cytoplasmic face. For example, *Hepatitis C virus* RdRp associates with membranes by its C-terminal hydrophobic insertion sequence (Schmidt-Mende *et al.*, 2001). *Flock house virus* RNA polymerase associated by its N-termnal hydrophobic insertion sequence (Miller and Ahlquist, 2002).

Although the viral proteins to act as membrane anchors have been proposed, the mechanisms by which the replication components are brought to the specific types of membranes are poorly understood. The membrane anchoring proteins for PV and TEV have been well characterized, as discussed below.

#### 1.3.2.2.2.2.1 The *Poliovirus* membrane-anchor proteins

PV3AB$^{VPg}$ is an integral membrane protein (Towner *et al.*, 1996; Teterina *et al.*, 1997). It has been demonstrated that generation of 3AB *in trans* was not able to complement the defective replication complex in which the mutation is in the hydrophobic domain of membrane-associated 3AB. However, co-translation of the large precursor P3 (3ABC$^{Pro}$D$^{Pol}$) precursor protein allowed rescue of RNA replication. This result indicates that a large precursor containing 3AB$^{VPg}$ rather than the mature viral cleavage product may be required for the formation of the viral RNA replication complex (Towner *et al.*, 1998). 3AB$^{VPg}$ and 3CD$^{Pro}$ specifically bind to the 5' terminal cloverleaf structure of the viral RNA. 3AB has been shown to stimulate the autocleavage of 3CD$^{Pro}$. The autocleavage of 3CD$^{Pro}$ into 3C$^{Pro}$ and 3D$^{Pol}$ is necessary for polymerase activity (Molla *et al.*, 1994). The VPg could be generated from the membrane-bound 3AB by the proteolytic activity of 3CD$^{Pro}$ (Andino *et al.*, 1990; Parsley *et al.*, 1997; Plotch and Palant, 1995).

PV 2C (a putative helicase), a C-terminal cleavage product of 2BC is an integral membrane protein. The membrane-targeting signal of 2C is an amphipathic helix at its amino terminal region (Teterina *et al.*, 1997). 2C and 2BC proteins specifically interact with the 3' cloverleaf structure of negative stranded RNA (Banerjee *et al.*, 2001). It is tempting to believe that PV 2C/2BC proteins anchor the negative strand to the cytoplasmic membrane, thus allowing initiation of positive stranded RNA synthesis to occur (Banerjee *et al.*, 2001). Moreover, initiation of positive stranded RNA synthesis is likely to required unwinding activity to melt the double-stranded RNA structure at the 3' end (Banerjee and Dasgupta, 2001). Consistent with this role, 2C and its precursor 2BC migrate to the rough ER where they attach to virus-induced smooth membrane vesicles that bud off and become the site of viral RNA synthesis (Bienz *et al.*, 1992, Porter, 1993; Teterina *et al.*, 1997; Suhy *et al.*, 2000).

Taken together, PV 3 AB and 2C are membrane anchors to bring replication proteins and PV RNA templates to the site of viral RNA synthesis and complex. These proteins are multifunctional and facilitate the formation of replication complex.

#### 1.3.2.2.2.2 The *Tobacco etch virus* membrane-anchor protein

TEV 6k2 protein (Schaad *et al.*, 1997) is an integral membrane protein. The 6k2 protein membrane-targeting signal consists of a central hydrophobic domain and flanking charged residues. It has been shown that the protein can target to ER-derived membranes independently and is associated with the viral replication complex (Schaad *et al.*, 1997). As mentioned earlier, despite their required presence in the membrane-bound replication complex, both replication proteins $NIa^{VPg\text{-}Pro}$ and $NIb^{pol}$ mainly accumulate in the nucleus of TEV-infected plants. The 6k2 protein is produced from polyprotein processing (Fig. 1.2). The membrane-binding activity of the 6k2 protein overrides the nuclear localization signal of $NIa^{VPg\text{-}Pro}$ (Restrepo-Hartwig and Carrington, 1992). Direction of the protein to ER-derived replication sites may involve precursors containing the 6k2 protein domain (either 6k2- NIa or a larger precursor). The $NIa^{VPg\text{-}Pro}$ proteolytic domain binds both TEV RNA and $NIb^{pol}$ (Daros and Carrington, 1997; Li *et al.*, 1997), indicating the polymerase is delivered to the viral RNA template through $NIa^{VPg\text{-}Pro}$. The 6k2 protein-containing precursor is further processed into mature proteins and intermediate precursors (Carrington and Dougherty, 1987).

#### 1.3.2.2.2.3 Viral proteins with vesicle-inducing and membrane-altering properties

Many (+) ss RNA viruses modify intracellular membranes of their host cell to create a membrane compartment for viral RNA replication. Modifications include proliferation and reorganization of intracellular membranes. The generation of vesicles associated with replication

complexes is induced by specific viral membrane proteins. BMV 1a can induce the formation of spherules in the ER membrane on its own, which are similar to the spherules induced by BMV infection (Schwartz *et al.*, 2002). PV3A and 2C, 2BC have been shown to induce vesicles when expressed individually (Porter, 1993; Teterina *et al.*, 1997; Suhy *et al.*, 2000). CPMV 32 kDa and 60 kDa proteins, when expressed individually in cowpea protoplasts, were found to be associated with membranes mainly derived from the ER (Carette *et al.*, 2002). Furthermore, expression of either 32 kDa or the 60 kDa was shown to induce aggregates. The aggregates induced by the 32 kDa were connected with the cortical ER network, while the aggregates induced by the 60 kDa were found near the nucleus. Both types of aggregates resembled the regions of proliferative ER membranes induced in CPMV-infected cells, although the aggregates induced in CPMV-infected cells were generally larger. Possibly, the combined action of the 32 kDa and 60 kDa is necessary to induce the proliferations of the ER. However, it is currently unknown whether the observed changes in ER morphology induced by 32 kDa and 60 kDa correspond to the formation of small membranous vesicles in infected cells.

Taken together, these results suggest that viral membrane proteins induce membrane modifications. However, the cellular mechanism underlying this vesiculation is unclear. It remains unclear whether vesicle induction and formation is an intrinsic property of the viral proteins or whether the viral proteins activate cellular vesiculation processes. Recent experiments have revealed that the C-terminal domain of CPMV 60 kDa interacts in the yeast two-hybrid system with VAP27, which is a SNARE-like protein localized in ER membranes upon transient expression (Carette *et al.*, 2002). Possibly, the binding of 60 kDa with VAP27 disturbed the proposed function of VAP27 in fusion of the transport vesicles with the ER membrane (Wei *et al.*, 2001; Pouwels *et al.*, 2002) and resulted in ER proliferation. However, the binding of 60k with VAP27 still needs

to be confirmed in CPMV-infected cells. Another mechanism may be that the tight association of 32 kDa and 60 kDa with ER membrane triggers a stress response. However, CPMV infection did not result in an increase in the level of BiP mRNA in protoplasts (Carette *et al.*, 2002). It is unlikely that this stress response is responsible for the ER membrane proliferations. Two mechanisms have been proposed for PV induced vesiculation.

### 1.3.3 Concluding remarks

In summary, (+) ssRNA viruses have evolved remarkable strategies, by which a single viral RNA can be selectively amplified into many RNA progeny. In chapter 1.2, we have reviewed the intracellular membrane system and membrane proteins. In chapter 1.3, we have reviewed viral and host factors involved in (+) ss RNA virus translation and replication. In some cases, *trans*-acting elements are required for both translation and replication. For example, PCBP binds both to the cloverleaf and IRES in PV and participates in viral life cycle at two stages: translation and replication. *Cis*-acting elements required for translation and RNA replication are also not independent. For example, IRES sequences of picornaviruses are also required for replication, in addition to viral protein translation (Borman *et al.*, 1994). These structures appear to act in concert with each other, which is in line with the idea that translation and replication may be coupled (Egger *et al.*, 2000).

## 1.4 Formation of replication complexes in the *Comoviridae*

### 1.4.1 Similarity in genomic organization of the picorna-like supergroup

The *Comoviridae* family is a member of picorna-like virus supergroup which also comprises *Picornaviridae* and *Potyviridae* (Goldbach and Wellink, 1996; Buck, 1996; Koonin and Dolja,

1993). Fig.1.4 summarizes the similarities in genomic organization and sequence that have been revealed between the following viruses: PV (*Enteroviruese, Picornaviridae*), TEV, (*Potyvirus, Potyviridae*), CPMV (*Comovirus, Comoviridae*) and GFLV (*Nepovirus, Comoviridae*). These viruses have the following features in common: (i) a viral RNA genome-linked protein VPg at their 5' terminus and a poly(A) tail at their 3' terminus; (ii) each RNA contains a single open reading frame and translates its proteins as a polyprotein, which is cleaved into functional proteins; (iii) the arrangement of nonstructural domains is similar within the polyproteins and these proteins have similar functions and share conserved amino acid motifs. The genomic organization of the non-structural proteins of all members of the picorna-like supergroup is similar, consisting of the NTB-VPg-Pro-Pol; (iv) all picorna-like viruses use a serine-like proteinase for proteolytic processing of most of the polyprotein cleavage sites although some additional proteinases are also involved in proteolytic processing; (v) they all contain a (putative) transmembrane domain between the helicase and VPg domain. These viruses also have distinct features, in addition to the common features discussed above. For example, potyviruses differ from other viruses in the picorna-like supergroup in the following aspects: (i) potyviruses have rod-shaped particles, other viruses have icosahedral particles; (ii) both the full length $NIa^{VPg\text{-}Pro}$ and the mature VPg (21 kDa) have been found linked to the viral genome. In contrast, the VPgs of other viruses in this supergoup are about 3 kDa; (iii) as mentioned in chapter 1.3.2.1.2, the helicases in potyviruses and the helicases in other viruses in the supergroup belong to different superfamily.

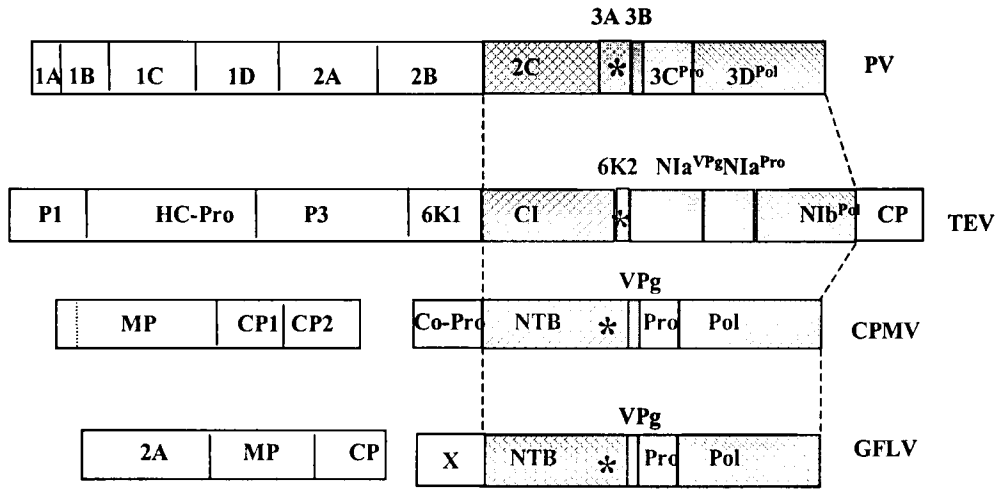


**Fig. 1.4. Comparison of the genomic organization of members of the picorna-like supergroup.** The genomic organization of *Poliovirus* (PV), *Tobacco etch virus* (TEV), *Cowpea mosaic virus* (CPMV) and *Grapevine fanleaf virus* (GFLV) is shown. The viral polyproteins are shown with boxes. The vertical lines through the polyproteins indicate the cleavage sites. The vertical dotted line indicates an alternative translation initiation in the CPMV genome. The name of the domains for the different mature proteins is indicated within each polyprotein. The hydrophobic domain is represented as an asterisk. For clarity, coding regions are not drawn to scale. The conserved NTB-VPg-Pro-Pol domain in each virus group is shown with the dotted lines. Regions of similar functions are indicated nu boxes with similar shading. NTB: protein containing a NTP binding motif, VPg: viral genome linked protein, Pro: proteinase, Pol: RNA-dependent RNA polymerase, MP: movement protein, CP: coat protein.

### 1.4.2 Formation of replication complexes in the *Comoviridae*

ToRSV is a member of the nepovirus genus in the *Comoviridae*. Little information was known about ToRSV replication. In this section, we will discuss the replication of the members of the *Comoviridae*: CPMV (*Comovirus*) and GFLV (*Nepovirus*). In comparison to PV and TEV, the replication of comoviruses is complicated by the fact that the two molecules of RNA need to be replicated.

#### 1.4.2.1 CPMV replication

As discussed above, CPMV B-RNA encodes all the proteins required for replication. M-RNA encodes the capsid and movement proteins that are indispensable for virus cell to cell movement. B-RNA can replicate in protoplasts independently. However, the replication of M-RNA depends on viral proteins encoded by B-RNA. In addition, M-RNA encodes a 58 kDa protein that is important for its replication (Goldbach and Wellink *et al.*, 1996; Van Bokhoven *et al.*, 1993) (Fig. 1.3). The 5' and 3' UTRs of CPMV genomic RNA species have extensive sequence homology. Exchange of the 5' and 3' UTR of M-RNA with those of B-RNA did not reduce the capacity of these RNAs to be replicated (Van Bokhoven *et al.*, 1993), indicating that the 5' and 3' UTRs of M-RNA do not determine the ability of this to be replicated. Protoplasts transfected with an expression vector containing the entire 200 kDa coding sequence from B-RNA (32 kDa-NTB-VPg-Pro-Pol), were active in supporting replication of co-inoculated M-RNA. However, replication of M-RNA was not observed in protoplasts transfected with expression vectors containing the 170 kDa (NTB-VPg-Pro-Pol), 110 kDa (Pro-Pol) or 87 kDa (Pol) coding sequences (Fig. 1.3). Since the 32 kDa protein is the only additional protein, this indicates that the 32 kDa protein plays a crucial role in achieving viral RNA replication. Surprisingly, despite the ability to support

replication of M-RNA, a CPMV-specific RNA polymerase activity dependent on exogenous added template RNAs could not be detected in extracts of protoplasts transfected with expression vectors containing the 200 kDa coding sequence (Van Bokhoven *et al.*, 1993).

CPMV infection induces characteristic cytopathological structures which consist of an amorphous matrix of electron-dense material traversed by rays of small membrane vesicles. Autoradiography in conjunction with electron microscopy on the sections of CPMV-infected leaves revealed that replication of the CPMV RNA genome is associated with these membranous vesicles (Carette *et al.*, 2000 and references therein). The majority of the replication proteins in CPMV-infected cells were immunolocalized not to the vesicles but to the adjacent electron-dense structures (Goldbach and Wellink, 1996). It was proposed that the replication complexes are disposed of in these electron-dense structures after taking part in RNA replication located on the membranes (Van Bokhoven *et al.*, 1993). These observation suggest that only a small part of the replication proteins in CPMV-infected cells is present in active replication complexes (Carette *et al.*, 2002 and references therein). In CPMV-infected plant cells, the ER undergoes dramatic morphological changes. The replication proteins, including the viral polymerase (110 kDa), VPg-containing proteins, 32 kDa protein, are always found in close association with proliferated ER membranes (Carette *et al.*, 2000). Distribution of replication proteins in protoplasts infected with CPMV carrying a particular mutation in the VPg was dispersed over the cytoplasm, suggesting that the VPg may be involved in protein-protein interactions that are important for the formation and the stabilization of the replication complexes (Carette *et al.*, 2001). Early plus stranded RNA accumulates at numerous distinct subcellular sites distributed throughout the cytoplasm which rapidly coalesce into a large body often located near the nucleus (Carette *et al.*, 2002). Combined localization of CPMV viral RNA and proteins in CPMV-infected protoplasts revealed that CPMV

plus-stranded RNA colocalizes with the viral polymerase (110 kDa), VPg-containing proteins, the 32 kDa protein. The subcellular sites for the colocalization are believed to correspond with the cytopathic structure consisting of electron-dense materials and clusters of small membrane vesicles. It still remains unknown whether the 110 kDa polymerase and the viral RNA are associated specifically with vesicles and /or the electron-dense material due to the limited resolution of fluorescence microscopy compared to electron microscopy (Carette *et al.*, 2002).

A virus-specific RNA-dependent-RNA-polymerase activity present in crude membrane fraction from CPMV-infected leaves is able to elongate RNAs of positive sense from *in vivo* initiated replication intermediates (Carette *et al.*, 2002 and references therein). Although the 87 kDa protein contains the domain specific for RNA-dependent RNA polymerase (RdRp), the proteinase-polymerase precursor 110 kDa (24 kDa+87 kDa) protein is the only viral protein present in highly purified replicase preparations capable of elongating nascent viral RNA chains (Goldbach and Wellink, 1996), suggesting that fusion to the 24 kDa proteinase is required for RNA polymerase activity. In contrast, PV polymerase 3D has an RdRp activity as a mature protein, while the 3CD proteinase-polymerase precursor is not active to elongate nascent viral RNA chains (Cornell and Semler, 2002 and references therein).

Taken together, a model for the formation of the site of CPMV has been proposed (Pouwels *et al.*, 2002). As mentioned above, the 200 kDa polyprotein encoded in RNA1 is rapidly cleaved into the 32 kDa and 170 kDa proteins (Goldbach and Wellink, 1996 and references therein). The 32 kDa/170 kDa complex is specifically targeted to the ER membrane via a localization signal residing in the 32 kDa protein. Interaction of the 32 kDa with membranes may change the 32 kDa/170 kDa conformation and triggers further proteolytic cleavage of the 170 kDa protein. At this stage, the 60 kDa protein (NTB-VPg) is released and inserted in the ER membrane, thereby

anchoring the replication complex to the membrane. The M-RNA is thought to be brought to the replication site through the action of the M-RNA encoded 58 kDa protein which acts in a *cis*-fashion (Van Bokhven *et al.* 1993). It was proposed that the N-terminal domain of the 58 kDa protein anchors M-RNA to the replication machinery through specific RNA-protein and protein-protein interactions. However, no experimental evidence yet is available to support this hypothesis.

### 1.4.2.2 GFLV replication

GFLV RNA1 encodes proteins required for its replication. GFLV RNA1 can replicate independently of RNA2 (Viry *et al.*, 1993). RNA2 encodes proteins needed for encapsidation and virus cell-to cell movement (Ritzenthaler *et al.*, 1995). RNA2 of GFLV is replicated *in trans* by the RNA1-encoded replication machinery.

GFLV replication induces a depletion of the cortical ER, together with distribution of ER-derived membranes to generate a perinuclear viral compartment where replication takes place. Inhibiting de novo synthesis of phospholipids or inhibiting vesicle trafficking between the ER and the Golgi was found to inhibit GFLV replication. These observations imply that GFLV replication requires ER-Golgi integrity and de novo lipid synthesis (Ritzenthaler *et al.*, 2002). GFLV RNA1 is sufficient to cause the complete cytopathic effect (Gaire *et al.*, 1999). Similarly to PV-induced vesicles, GFLV-induced vesicles resemble the vesicles that traffic along the secretory pathway both by size and their morphology. In PV and GFLV, some of the vesicles were aggregated into well-organized 'rosette-like structures' (Rust *et al.*, 2001, Ritzenthaler *et al.*, 2002). The viral proteins containing VPg, newly synthesized RNA and double-stranded replicative forms have been shown to colocalize at the ER (Ritzenthaler, *et al.*, 2002). Similarly to CPMV, protein 2A is necessary for the replication of its own RNA (RNA2) (Gaire *et al.*, 1999). It is associated with membrane

structures and is thought to be recruited by the RNA1-encoded replication machinery (Gaire *et al.*, 1999). It was proposed that the 2A moiety of polyprotein P2 could mediate the transport of the nascent P2-RNA2 complexes from their initial location in the cytosol to the replication sites where viral RNAs replication and P2 cleavage take place (Gaire *et al.*, 1999; Ritzenthaler, *et al.*, 2002).

### 1.4.2.3 Common features in the formation of replication complexes of the picorna-like supergroup

Various aspects of the formation of replication complexes of PV (*Picornaviridae*) and TEV (*Potyviridae*) have been reviewed in chapter 1.3.2. While there are a number of differences among the models for the formation of replication complexes, they have common features.

(i) All picorna-like viruses characterized so far have been shown to replicate in association with membranes derived from the ER (Carette *et al.*, 2000; Ritzenthaler *et al.*, 2002; Rust *et al.*, 2001).

(ii) Replication viral proteins induce host membrane modifications. For example, CPMV RNA1or GFLV RNA1 are sufficient on their own to induce membrane modifications (Carette *et al.*, 2002; Suhy *et al.*, 2000; Gaire *et al.*, 1999). This is in contrast to TMV, for which the movement protein is responsible for ER modifications (Reichel and Beachy, 1998).

(iii) For several picorna-like viruses, replication proteins have been shown to be brought to ER-like membranes through polyproteins containing the membrane-anchor domain. In the replication complex, the polyprotein(s) is (are) processed coordinately into cleavage products with functions distinct from those of their precursor proteins (Xiang *et al.*,1997; Goldbach and Wellink, 1996).

**1.5 Genomic organization and gene expression of nepoviruses**

As mentioned above, nepoviruses have a bipartite genome consisting of two molecules of positive stranded RNA (Fig. 1.4). In all the nepoviruses identified so far, the 3- termini (and in some cases also the 5' termini) of the two RNAs display considerable sequence homology or even complete identity (Ritzenthaler *et al.*, 1991; Mayo and Robinson, 1996). In ToRSV, large regions of homology between RNA1 and RNA2 are present at both the 5' and the 3' ends of the RNA. Each RNA contains an open reading frame beginning at position 78. The 5' terminal 459 nucleotides of both RNAs are identical and the following 447 nucleotides are identical at 75.8% of the nucleotide positions. Therefore, the coding region at the N-terminus of the RNA1 encoded polyprotein contains extensive homologies to the coding region at the N-terminus of the RNA2 encoded polyprotein. At the 3' terminal, 1533 nucleotides of RNA1 and RNA2 are identical with the exception of only 3 nucleotide positions. Rott *et al* have speculated that this high level of homology is the result of RNA recombination taking part during replication (Rott *et al.*, 1991a). In agreement with this speculation, Le Gall *et al* have found that the 3' non-translated region of *Grapevine chrome mosaic virus* RNA-1 was transferred to *Tomato black ring virus* (TBRV) virus RNA2 in pseudorecombinant isolates. It was proposed that the common occurrence of RNA recombination and the resulting identity of the two genomic RNAs might be characteristics of nepoviruses (Le Gall *et al.*, 1995).

Based on the size of RNA2, the occurrence and extent of the identity between the 3' untranslated regions of RNA1 and RNA2 (Le Gall *et al.*, 1995), and serological relationships between the viruses, nepoviruses have been divided into three subgroups (A, B and C) (Wellink *et al.*, 2000). The same group is produced when each criteria is considered separately. Nepoviruses

of subgroups A (e.g., GFLV) and B (e.g., TBRV) have smaller RNA-2 than nepoviruses of subgroup C (e.g., ToRSV).

### 1.5.1 Polyprotein processing in subgroup A/B of nepoviruses

Proteinases of subgroup A/B of nepoviruses are serine-like proteinases similar to the picornaviruses 3C proteinases and comoviruses proteinases. However, the conserved His residue found in the substrate-binding pocket of the proteinases of other picorna-like virus group is replaced by a Leu in the substrate-binding pocket of the proteinases in subgroupA/B nepoviruses. This may explain why the cleavage sites present on the polyproteins of nepoviruses A/B differ from those of the polyprotein of other members of the picorna-like virus supergroup.

In contrast to rapid co-translational polyprotein processing in PV, CPMV and TEV, polyproteins of nepoviruses are relatively inefficiently cleaved by the proteinase *in vitro* (Mayo and Robinson, 1996; Demangeat *et al.*, 1992).

GFLV RNA-1 encodes a 253 kDa polyprotein. The polyprotein is processed by the proteinase into intermediate and mature proteins (Margis *et al.*, 1991). Polyprotein processing using a partial cDNA *in vitro* revealed that VPg-Pro-Pol can be processed into VPg-Pro and Pol (Margis *et al.*, 1994). Cleavage between VPg and Pro is very inefficient *in vitro* (Margis *et al.*, 1994). The Pro or the VPg -Pro precursor can cleave *in trans* at a cleavage site between X-NTB present on the RNA-1 encoded polyprotein. The RNA-2 encoded polyprotein can be cleaved *in trans* into 2A, $2B^{MP}$, and $2C^{CP}$ in the presence of RNA-1 translation products containing the proteinase domain or the mature proteinase alone (Margis *et al.*, 1993; Demangeat *et al.*, 1992). The processing of RNA2 polyprotein does not apparently requires a proteinase cofactor (Margis *et al.*, 1991). Efficiency of processing is regulated by processing of the proteinase precursors. The

mature proteinase is more effective than the VPg-Pro precursor at processing the RNA2 encoded polyprotein. However, the VPg-Pro precursor was more effective than the mature proteinase at processing the RNA-1 polyprotein *in trans* ( Margis *et al*, 1994).

TBRV RNA1 encoded 250 kDa polyprotein is cleaved in *cis* by the proteinase into several mature proteins and intermediate precursors. The VPg-Pro-Pol precursor is very stable and is not cleaved further *in vitro* (Hemmer, *et al.*, 1995). This precursor is also detected as a stable product *in vivo* (Demangeat *et al.*, 1992). The VPg-Pro-Pol precursor can cleave the RNA2 encoded 150 kDa polyprotein *in trans* (Hemmer *et al.*, 1995). Similar to GFLV, proteinase precursors were found to have different proteolytic activities. However, the processing events in TBRV are different from GFLV: (i) in contrast to GFLV, *trans*-cleavage was not detected in the RNA1 encoded polyprotein (Hemmer *et al.*, 1995); (ii) the VPg-Pro-Pol cleaves RNA2-derived precursors *in trans* more effectively than the Pro-Pol protein (Hemmer *et al.*, 1995).

Taken together, these results suggest regulation of the proteolytic activity of proteinase by processing of the proteinase precursors is a common mechanism in nepoviruses of subgroup A/B and subgroup C (see below). This type of regulation was also found for PV 3C proteinase (Ypma-Wong, 1988). As mentioned above, the N-terminal 32 kDa protein of CPMV RNA1 polyprotein acts as a proteinase cofactor. Although amino acid homology have been identified between the N-terminal 50 kDa protein of the nepovirus RNA1 encoded polyprotein and the N-terminal 32 kDa protein (Rott *et al.*, 1995; Vos *et al.*, 1988; Ritzenthaler *et al.*, 1991), the evidence available does not suggest that the N-terminal 50 kDa protein plays a similar role (Hemmer *et al.*, 1995; Demangeat *et al.*, 1992).

### 1.5.2 Nepoviruses subgroup C

ToRSV, *Black currant reversion associated nepovirus*, *Peach rosette mosaic virus*, *Cherry leafroll virus* and *Blueberry leaf mottle* virus belong to the nepoviruses Subgroup C. Of the subgroup C nepoviruses, the complete genomic sequence is available for ToRSV and *Black currant reversion associated nepovirus* (Rott *et al.*, 1991b, 1995; Pacot-Hiriart *et al.*, 2001; Latvala-Kilby and Lehto, 1999). ToRSV is the only member of nepoviruses subgroup C for which the polyprotein processing has been well characterized (Wang and Sanfacon, 2000; Wang *et al.*, 1999; Carrier *et al.*, 1999 and 2001).

### 1.5.2.1 ToRSV genomic organization

ToRSV genome consists of two RNAs (RNA-1 and RNA-2) (Fig. 1.5). Each RNA encodes a polyprotein (P1and P2). P1 and P2 are processed into functional intermediate and mature products by the RNA1-encoded 3C-like proteinase. P1 contains X1, X2, a putative NTP binding protein (NTB), the VPg, the 3C-like proteinase (Pro) and the RNA-dependent RNA polymerase (Pol) (Rott *et al.*, 1995; Wang *et al.*, 1999; Wang *et al.*, 2000). Thus, the proteinase processes P1 at five cleavage sites *in vitro* and the precise location of the NTB-VPg, VPg-Pro and Pro-Pol cleavage sites has been determined experimentally. The RNA2-encoded polyprotein P2 contains X3, X4, the movement protein (MP) and the capsid protein (CP).

The N-terminal region of ToRSV P1 contains two putative distinct protein domain X1 and X2 (Wang and Sanfacon, 2000). This is in contrast to nepoviruses subgroup A/B and to comoviruses which contain only one protein domain upstream of the NTB. The putative X1 protein contains an alanine-rich sequence which is also present in other nepoviruses. The X2 protein has similarities with CPMV 32 kDa protein (a proteinase cofactor). The present evidence does not

support a role of X2 in regulation of the ToRSV proteinase activity in a similar manner (Wang and Sanfacon, 2000a; Wang *et al.*, 1999).

As mentioned above, ToRSV P1 contains the domains for proteins likely to be involved in replication including the NTB, VPg, Pro and Pol (Rott *et al.*, 1995; Wang *et al.*, 1999; Wang *et al.*, 2000; Hans and Sanfacon, 1995). The NTB has sequence elements similar to those found in known RNA helicases (Gorbalenya and Koonin, 1989) and has a putative transmembrane domain at its C-termini (Rott *et al.*, 1995). Therefore, ToRSV NTB corresponds to CPMV NTB, PV 2C-3A and TEV CI-6k2 (Fig. 1.1). This suggests that the NTB or a larger polyprotein containing NTB may act as a membrane anchor for the replication complex.

The N-terminal region of P2 contains two putative proteins X3 and X4 (Carrier *et al.*, 2001). In contrast, only one protein domain is present upstream of MP in N-terminal region of P2 in other characterized nepoviruses (Margis *et al.*, 1994). The X3 protein contains extensive regions of homology to the X1 protein domain at the N-terminus of P1 (Wang and Sanfacon, 2000), including an alanine-rich motif also present in the N-terminal region of other nepovirus P1 polyproteins (Mayo and Robinson, 1996). X3 protein also contains several proline motifs, which are also present in GFLV 2A, and CPMV M-RNA encoded 58 kDa protein, which has been shown to be involved in RNA2 replication (Gaire *et al.*, 1999; Van Bokhoven *et al.*, 1993). It is not known at this point whether X3 plays a similar role in the replication of ToRSV RNA2. X4 does not have similarity to other known proteins (Carrier *et al.*, 2001), and its putative function remains a mystery.

ToRSV coat protein (CP) and putative movement protein (MP) have been characterized (Sanfacon *et al.*, 1995; Wieczorek and Sanfacon, 1993). The movement protein co-localize with tubular structures containing virus-like particles found in or near the cell wall. These tubular

structures are probably involved in virus movement from cell to cell (Wieczorek and Sanfacon, 1993) and are similar to tubular structures induced by the movement proteins of CPMV and GFLV (Goldbach *et al.*, 1994; Belin *et al.*, 1999).

The genomic organization of ToRSV is based on *in vitro* studies and on the detection of several proteins (MP, CP and VPg) in plants. This will need to be confirmed by detection of other viral proteins ( in particular the proteins at the N-terminus of each polyprotein)and by functional analysis once infectious ToRSV cDNAs become available.

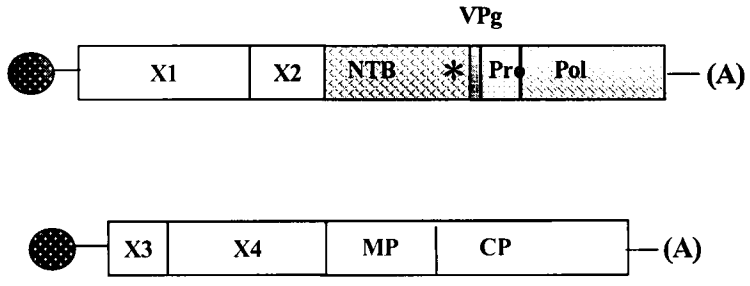


**Fig. 1.5. Predicted genomic organization of ToRSV.** The viral polyproteins are shown with boxes. The vertical lines through the polyproteins indicate cleavage sites identified by *in vitro* studies. The name of the domains for the different mature proteins is indicated within each polyprotein. The putative transmembrane domain is shown as an asterisk. The single lines horizontal show non-coding sequences. The hatched circles indicate the VPg protein. NTB: putative NTP binding protein, VPg: viral protein genomic linked, Pro: proteinase, Pol: putative polymerase, MP: movement protein, CP: coat protein.

### 1.5.2.2 Characteristics of proteolytic processing

#### 1.5.2.2.1 ToRSV proteinase

The ToRSV proteinase is a serine-like proteinase which is related to the 3C proteinase of picornaviruses and the 3C-like proteinase of comoviruses and potyviruses. The catalytic triad probably consists of His, Asp (or Glu) and Cys. Substitution of His with Asp resulted in a loss of proteolytic processing (Hans and Sanfacon, 1995; Wang *et al.*, 1999). The ToRSV proteinase has more overall homology at the amino acid sequence level to the proteinase from nepoviruses of subgroup A/B than to the proteinase of picornaviruses, comoviruses and potyviruses. However, the ToRSV proteinase contains a His residue in its substrate-binding pocket, which is similar to the proteinases of picornaviruses, comoviruses and potyviruses instead of the Leu residue present in the substrate-binding pocket of Nepoviruses of subgroups A/B (Mayo and Robinson, 1996; Ryan and Flint, 1997). Changing the His to a Leu caused a loss of proteolytic activity (Hans and Sanfacon, 1995), indicating that the His residue is important for proteolytic processing.

Recently, active recombinant ToRSV proteinases have been expressed and partially purified using an *E. coli* expression system, either as a mature proteinase (Pro) or as a precursor (VPg-Pro). The mature proteinase (Pro) was found to be more active than VPg-Pro in processing P2-derived polyproteins *in trans* (Chisholm *et al.*, 2001). This is similar to the differential proteolytic activity observed between the VPg-Pro and Pro of other nepoviruses and of PV 3C and 3CD of proteinase. Apart from the function of cleavage of polyprotein, the proteinase (Pro) of ToRSV has been shown to interact with the eukaryotic translation initiation factor elF4E from *Arabidopsis thaliana in vitro* (Leonard *et al.*, 2002). The presence of VPg domain on the VPg-Pro precursor increased the binding affinity of Pro for the initiation factor. Therefore, regulation of the cleavage at the VPg-Pro site may be involved in regulating the different activities of Pro. Initiation of translation of

cellular mRNAs is mediated by an interaction between the cap-binding protein complex composed of factors elF4E, eIF4A and eIF4G, and the cap structure present at the 5' end of mRNAs. The genome of ToRSV does not have a cap structure at its 5' end. Instead, VPg is linked to the 5' end of ToRSV genome . Initiation of translation by ToRSV must therefore use a cap-independent mechanism. As mentioned earlier, the current model for translation of cellular mRNA is through the formation of protein bridge between the 5' termini and 3' termini. It is reasonable to believe that ToRSV viral RNA also forms a closed-loop by protein bridge or other interactions. In PV and TEV, 3C-like proteinases have RNA-binding activity (Daros and Carrington, 1997; Cornell and Semler, 2002). This raise the possibility that the ToRSV proteinase and elF4E may also bind viral RNA and may serve as a bridge between the viral RNA. In this current model, the interaction between Pro and elF4E would promote the assembly of the translation complex on the viral RNA and possibly the circularization of the viral genome. Alternatively, as mentioned above, elF4E is required for initiation of translation of cellular mRNAs interaction between ToRSV proteinase and elF4E may be involved in inhibition of host translation.

**1.5.2.2.2 Cleavage events mediated by the 3C-like proteinase**

As mentioned above, the ToRSV P1 and P2 polyproteins are processed by a 3C-like proteinase at specific cleavage sites. The proteolytic processing of ToRSV encoded polyproteins has been characterized using partial clones and *in vitro* translation systems (Wang *et al.*, 1999; Wang and Sanfacon, 2000;Carrier *et al.*, 1999).

(i) Cleavage site specificity

The consensus sequence of cleavage sites of P1 and P2 is (Cys-Val)-Gln/(Ser, Gly), which is similar to the Gln/(Ser,Gly) consensus of picornaviruses, potyviruses and comoviruses but

not to those from nepoviruses of subgroups A/B (Carrier *et al.*, 1999). Substitution of conserved amino acids at the -2, -1 and +1 positions resulted in a significant reduction of proteolytic processing *in vitro* in cleavage site between Pro-Pol (*cis* cleavage) and in cleavage site between X-MP (*trans* cleavage) (Carrier *et al.*, 1999).

(ii) Cleavage events mediated by the 3C-like proteinase

Proteolytic processing of polyproteins derived from P1 occurs predominantly *in cis* (Wang *et al.*, 1999; Wang and Sanfacon, 2000). Furthermore, neither the Pro nor the VPg-Pro could cleave *in trans* P1-derived substrate containing the cleavage site delineating the X1, X2, NTB and VPg domains. The proteolytic processing of NTB-VPg-Pro or larger precursor *in vitro* resulted in VPg-Pro accumulation *in vitro* and in *E. coli*, suggesting cleavage between VPg-Pro is very inefficient (Wang *et al.*, 1999). Similarly, inefficient cleavage at the VPg-Pro site was observed for two other nepoviruses (GFLV and TBRV) (Margis *et al.*, 1994; Hemmer *et al.*, 1995).

The mature proteinase or VPg-Pro of ToRSV has been shown to be active in the cleavage of polyprotein P2 *in trans,* indicating processing of P2 does not apparently requires a proteinase cofactor as the 32 kDa protein of CPMV (Chisholm *et al.*, 2001).

### 1.5.2.3 NTB-VPg -membrane association *in vitro*

Amino acid sequence deduced from the nucleotide sequence of several isolates revealed the presence of a conserved glycosylation consensus sequence (N-M-T) on the VPg domain (Wang and Sanfacon, 2000b). Surprisingly, direct microsequencing of the VPg protein linked to the genomic RNA purified from virus particles revealed that there was a replacement of Thr with an Ala in the glycosylation consensus (Wang, Ph.D thesis; Wang *et al.*, 1999). We do not have an explanation

for this discrepancy. However, the glycosylation site in the VPg can be used as a convenient references point to study the topological orientation of NTB-VPg in membranes.

NTB contains a putative transmembrane domain at its C-terminus followed by a highly hydrophilic and basic VPg. To study whether NTB-VPg could associate with membrane outside of the viral genome context, an *in vitro* membrane assay was used. Translation of plasmid pT7 NTB-VPg in the presence of canine microsomal membranes resulted in the production of glycosylation at the consensus glycosylation site at VPg, suggesting NTB-VPg-membrane association *in vitro* and a lumenal location for the VPg (Wang, Ph.D thesis). As will be discussed in the introduction in chapter 4, possible signal processing of the NTB-VPg protein was also observed *in vitro*. This data suggest that the NTB-VPg protein has the ability to associate with membranes and stimulated our interest to study this membrane association in the context of the ToRSV replication complexes in infected plants.

### 1.6 Summary

In this review, we have examined the intracellular membrane system and the ss (+) RNA virus strategies for gene expression and replication. In particular, we have described the current knowledge about the mechanisms of formation of membrane-associated replication complexes. When this study was initiated, very little was known about the formation of nepovirus replication complexes.

The overall goal of this thesis is to provide new information on the assembly of nepovirus replication complexes with membrane and in particular, to characterize the membrane association of ToRSV NTB-containing precursors.

To realize this goal, this thesis has been designed to achieve the following objectives.

(1) To characterize the association of NTB containing precursors with membrane and their subcellular localization in infected plants

(2) To determine the subcellular localization of viral RNA replication (i.e. does it co-fractionate with NTB containing proteins on sucrose gradients?)

(3) To detect ER modification in ToRSV infected plant cells

(4) To determine the topology of proteins containing the NTB domain in the membranes

(5) To characterize membrane association of NTB-VPg outside of the context of the viral genome using an *in vitro* membrane association assay and a protoplast transfection assay.

# CHAPTER 2

# MATERIALS AND METHODS

## 2.1 Infection of plants and protoplasts.

ToRSV was propagated routinely in *Cucumis sativus* var. Straight Eight. *Nicotiana benthamiana* transgenic plants expressing the green fluorescent protein (GFP) targeted to the lumen of the ER were generously provided by D. Baulcombe (John Innes Centre, UK). Plants were inoculated at the 5-7 leaf stage using 40 µl of fresh leaf extracts of ToRSV-infected cucumber plants diluted 1:10 in phosphate-buffered saline (PBS) as described previously (Wieczorek and Sanfacon, 1993). Mesophyll protoplasts from the ER-GFP *Nicotiana benthamiana* plants and from *Plumbaginifoliae* were prepared and transfected with 10 µg of purified ToRSV viral RNA or with 20 µg plasmids by polyethylene glycol-mediated transfection as described previously (Wieczorek and Sanfacon, 1995). When labeling of protoplasts was required, 25 µCi [$^{35}$S] methionine was added at 18 h post-transfection to samples of 3 x$10^5$ protoplasts resuspended in 0.5 ml of culture medium. The labelling was allowed to proceed for 6 hrs before the protoplasts were collected and analyzed by immunoprecipitation (see below).

## 2.2 Membrane fractionation.

Leaf tissue from ToRSV-infected *Cucumis sativus* was used for the isolation of a crude membrane fraction as described previously [50mM Tris-HCl, 0.1 mm or 3mM MgCl2, 1mM EDTA, 1mM dithiothreitol (DTT), 0.1% BSA, 13% sucrose, 5 µg/ml leupeptin and 2 µg/ml aprotinin] (Schaad *et al.*, 1997). Briefly, one gram of tissue was ground in 4 ml of homogenization buffer (Schaad *et al.*, 1997). Nuclei, chloroplast, cell wall and debris were removed by

centrifugation at 3,700 x g at 4 $^0$C for 10 min. The supernatant (S3) was centrifuged at 30,000 x g at 4 $^0$C for 30 min, resulting in soluble (S30) and crude membrane (P30) fractions. The P30 fraction was resuspended in homogenization buffer with the aid of a Dounce homogenizer and centrifuged again at 30,000 x g for 20 min at 4 $^0$C, resulting in washed crude membrane fraction P30-2.

Membranes present in S3 or P30-2 fractions were fractionated on 20-45 % sucrose gradients containing the respective homogenization buffer as described above. The gradients were subjected to centrifugation at 143,000 x g for 4 h at 4 $^0$C. The sucrose gradient was subdivided into 13 fractions that were analyzed by immunoblotting or RdRp assays (see below). Ribosomal RNAs were extracted from 50 µl of gradient fractions using phenol-chloroform and precipitated with ethanol.

To concentrate and purify the intracellular membranes from sucrose gradient fractions, fractions 4-6 from a sucrose gradient obtained in the presence of 3 mM $MgCl_2$ were pooled. The membranes were collected by centrifugation at 140,000 x g for 45 min, resuspended in buffer (50 mM Tris-HCl, pH 8.0; 10 mM KCl; 1 mM EDTA) and the presence of viral proteins in the purified membranes was examined by immunoblotting (see below). These purified membranes were used for the proteinase K experiments (see below).

**2.3 Immunoblot analysis.**

Samples were separated by SDS-polyacrylamide gel electrophoresis (SDS-PAGE, Laemmli, 1970) and the proteins were transferred to Sequi-blot$^{TM}$ PVDF membranes (Bio-Rad) as described (Wieczorek and Sanfacon, 1993). The membranes were blocked with PBS containing 5 % skim milk powder and incubated with the primary antibodies (diluted in PBS buffer) for 1 h at room temperature. The anti-NTB, anti-VPg, anti-MP and anti-CP antibodies were described previously (Sanfacon *et al*, 1995; Wang *et al.*, 1999; Wieczorek and Sanfacon, 1993). The anti-Bip

and anti-$\beta$-xylosyl were gifts from M. Chrispeels (U. of California, San Diego) and A. Sturm (Friedrich Miescher Institute), respectively. Membranes were incubated with the secondary antibodies (goat anti-rabbit lgG) which were conjugated to either horseradish peroxidase (Amersham, Inc.) or alkaline phosphatase (Sigma), for 1 h at room temperature, and developed with a substrate for chemiluminescence (ECL plus, Amersham, Inc., for the peroxydase-conjugated antibodies) or for colorimetric detection (NBT-BCIP, Invitrogen, for the alkaline phosphatase-conjugated antibodies).

**2.4 RNA-dependent RNA polymerase ( RdRp ) activity assays.**

RdRp assays using endogenous templates present in membrane-enriched fractions from infected plants were conducted as described previously (Schaad *et al.*, 1997). Briefly, gradient fractions or resuspended P30-2 fractions were mixed with an equal volume of 2x RdRp buffer (Schaad *et al.*, 1997) containing [$\alpha$-$^{32}$P]UTP and incubated for 1 h at 24 $^0$C. The products were resuspended in 10 µl of deionized $H_2O$ and 5 µl of each sample was digested with RNase A (1.25 µg/ml, Sigma) in the presence of 233 mM NaCl, 3.3 mM TrisHCl, pH 7.4 and 10 mM EDTA at 30 $^0$C for 15 min. The RNase A-treated products were then incubated with proteinase K (5 mg/ml ) in the presence of 2 % SDS at 37 $^0$C for 30 min. For inhibition of host transcription assay, actinomycin D (50 µg/ml) and DNase I (12.5 U/ml) were added to the reaction. The products were analyzed by electrophoresis on a 1 % agarose gel, followed by autoradiography. As controls, ToRSV single-stranded RNA was extracted from purified virus particles and ToRSV double-stranded RNA was purified from infected leaves (Eastwell *et al.*, 1996). The purified ssRNAs and dsRNAs were run on the same agarose gel along with the RdRp reactions. Dot-blot hybridizations were performed using the labeled RdRp products from reactions containing P30-2 fractions from

infected and non-infected plants as probes. Plus- and minus-strand transcripts specific to a 1.7 kb region of RNA2 were synthesized by digestion of pT7-X-MP (Carrier *et al.*, 1999) with the appropriate restriction enzyme followed by *in vitro* transcription using T3 RNA polymerase for the plus-stranded transcript and T7 RNA polymerase (Invitrogen) for the minus-stranded transcript. One μg of each transcript was fixed to a Zeta-Probe blotting membrane (Bio-Rad) by baking at 80 $^0$C for 1 h and hybridized with heat-denatured RdRp products as recommended by the supplier (Bio-Rad).

**2.5 Immunofluorescent analysis of transfected protoplasts.**

Immunofluorescent staining of transfected protoplasts was performed essentially as described (Carette *et al.*, 2000). Briefly, protoplasts harvested at 30 h post-transfection were allowed to settle on poly-L-lysine-coated coverslips for 2 min. One volume of fixing solution (Carette *et al.*, 2000 ) was then added to the protoplast suspension. After incubation for 15 min, the coverslips were immersed in fixing solution and allowed to incubate for another 30 min. The cells were washed three times with PBS and permeabilized with a 0.5% Triton X-100 solution in PBS for 10 min. Nonspecific antibody binding was reduced by incubation for 10 min in blocking solution (Carette *et al.*, 2000). Subsequently, the protoplasts were incubated for 1 h with the anti-NTB antibodies (diluted 1: 5000 in blocking solution). After 5 washes with PBS, the protoplasts were incubated with goat anti-rabbit antibodies conjugated to Cy3 (Jackson Immuno Research Laboratories, diluted 1: 250 in blocking buffer) for 1 h. After 5 washes with PBS, the coverslips were mounted on microscope slides using the ProLong Antifade kit (Molecular Probes, Inc.).

**2.6 Fluorescence microscopy.**

Protoplasts were viewed by fluorescence microscopy using an Axiophot microscope

(Zeiss). For detecting GFP fluorescence, a BP 450-490 exciter filter/LP520 barrier filter set was used. For detecting Cy3 fluorescence, a BP 546/12 exciter filter/LP 590 barrier filter set was used. Photomicrographs were taken using Kodak Ektachrome 160 film. For analysis of infected plant tissues, leaf disks containing infection sites were excised and mounted as live tissue on microscope slides and investigated immediately. A Bio-Rad Micro Radiance confocal microscope was used to obtain the images.

**2.7 Membrane protein extraction analysis.**

Crude membrane fractions (P30) were resuspended in 0.1 M $Na_2CO_3$, pH 10.5 or 1 M KCl. For each extraction, the samples were incubated for 30 min on ice, then subjected to centrifugation at 30,000 x g at 4 $^0$C for 30 min. The pellets (P30-2) were resuspended in protein loading buffer (Laemmli, 1970) in a volume equal to that of the corresponding supernatant. Triton X-114 phase partitioning was performed as previously described (Bordier, 1981). The volumes of the final aqueous and detergent-soluble phases were equalized. The samples were then analyzed by immunoblotting as described above.

**2.8 Structure predictions.**

The secondary structure of NTB-VPg was predicted using methods available at the website (http://npsa-pbil.ibcp.fr/cgi-bin/npsa) (Combet *et al.*, 2000). Prediction of the topological orientation of NTB-VPg was conducted using the Transmembrane Hidden Markov Model algorithm (Krogh *et al.*, 2001) (www.cbs.dtu.dk/services/TMHMM/TMHMM2.0).

**2.9 Proteinase K protection assays.**

Samples enriched in membrane-bound NTB-VPg were obtained as described above by

purifying membranes using an ultracentrifugation step of pooled fractions from a sucrose gradient obtained in the presence of 3 mM $MgCl_2$. Aliquots of the resuspended membranes were incubated with proteinase K (0.5 mg/ml) for 6 min at room temperature in the absence or presence of 0.4 % triton X-100. The samples were then incubated with phenylmethylsulfonyl fluoride (0.2 mg/ml) for 8 min on ice and analyzed by immunoblotting as described above.

**2.10 Plasmid constructions.**

pBI 525 is a plant transient expression vector (originally obtained from Dr. Crosby, Plant Biotechnology Institute, Saskatoon, Sask. Canada). pBBI 525, a modified version of plasmid pBI 525 was originally described previously (Sun *et al.*, 2000) and provided by Dr. Martin, USDA-Corvallis, Oreg.). Plasmid pT7cNTB-VPg, pT7cNTB-VPg (T/A) and pT7cNTB-VPg ΔTMD were made by Dr. Wang (Wang, Ph.D thesis). To construct plasmid pBBI 525- cNTB-VPg, a NcoI-Bgl II fragment containing cNTB-VPg from pT7 cNTB-VPg (Wang, Ph.D thesis) was ligated into the Nco I -BamH I sites of plasmid PBBI525. pBBI cNTB-VPg (T/A) and pBI cNTB-VPg ( ΔTMD1) were obtained as described for pBI cNTB-VPg.

**2.11 *In vitro* transcription and translation.**

*In vitro* transcription and translation of the plasmid pT7cNTB-VPg (T/A) was performed using a TNT T7 coupled rabbit reticulocyte lysate system (Promega) following the manufacture's recommendations. [$^{35}$S] methionine-labelled translation products were synthesized for 1h at 30 $^0$C. Where indicated, 1 µl canine microsomal membranes was added to a 12.5 µl reaction (Promega).

In some experiments, run off transcripts were first synthesized from linearized plasmids

synthesized using a standard rabbit reticulocyte lysate system (Promega) following the manufacture's recommendations.

For membrane sedimentation analyses, 30 ul NTE buffer (100 mM NaCI, 10 mM Tris-HCI, pH 8.0, 1 mM EDTA) was added after completion of *in vitro* translation, followed by centrifugation at 20,000 x g for 15 min. Supernatant fractions were collected (S1) and pellets were resuspended in 100 µl 4M urea and incubated for 30 min on ice, followed by centrifugation at 20, 000 x g for 30 min. The supernatant (S2) and pellet (P2) fractions were collected.

**2.12 Immunoprecipitation.**

Immunoprecipitations were conducted as described previously (Hans and Sanfacon, 1995). Briefly, pelleted [$^{35}$S] methionine-labeled protoplasts or *in vitro* translation mix were resuspended in 1 vol. of dissociation buffer (125 mM Tris-HCl pH 6.8, 25% β-mercaptoethanol, 10% SDS), boiled for 3 min and diluted 10 fold with PBS-TDS buffer (PBS buffer, 1% Triton-100, 0.5% deoxycholic acid, 0.1% SDS) (Hans and Sanfacon, 1995). 10 µl of polyclonal antibody against NTB or antibody against VPg was added. Samples were incubated overnight at 4 $^{0}$C and then incubated with Protein G-Sepharose CL-4B (Sigma) for 1 h at 4 $^{0}$C with rotatory shaking. The immunoprecipitates were washed five times in PBS-TDS buffer, resuspended in 25 µl of dissociation buffer, analyzed on SDS-PAGE gel and visualized by autoradiography.

# CHAPTER 3

# *CHARACTERIZATION OF* MEMBRANE ASSOCIATION *OF VIRAL* PROTEINS CONTAINING THE NTB DOMAIN IN *TOMATO RINGSPOT VIRUS* INFECTED PLANTS[1]

## 3.1 Introduction

The putative NTP-binding protein (NTB) of ToRSV contains a stretch of hydrophobic residues at its C-terminus, suggesting that it may act as a membrane anchor for the replication complex. In this chapter, we wish to determine whether NTB containing proteins are present in infected plant cells in association with intracellular membranes and with replication complex. First, we have determined whether proteins containing NTB domain co-fractionated with ER marker and with ToRSV specific RdRp activity in sucrose gradients. Then we have examined the severe changes in the morphology of the ER in plants infected with ToRSV. The subcellular location of the NTB-VPg protein was also investigated by immunostaining. Finally, proteinase K assays using purified membranes from infected plants were used to study topology of the NTB containing proteins.

---

[1]Part of this chapter is contained in the following publication: Han, S. and Sanfacon, H. 2003. *Tomato ringspot virus* proteins containing the NTB domain are transmembrane proteins that associate with the endoplasmic reticulum and co-fractionate with replication complexes. J. Virology. **77:** 523-34.

## 3.2 Results

### 3.2.1 Various viral proteins containing the NTB domain are detected in crude membrane fractions.

To determine if the NTB protein or larger polyproteins containing the NTB domain are present in infected plants, membrane enriched fractions (P30 fractions) of ToRSV-infected and healthy plant cell extracts were analyzed by immunoblotting using two previously described antisera: polyclonal antisera raised against a fusion protein containing the middle region of NTB and polyclonal antisera raised against a synthetic peptide corresponding to the central region of VPg (Wang *et al.*, 1999, see Fig. 3.1A ). The bands were visualized using a chemiluminescent based detection assay. The anti-NTB antibodies did not recognize any plant proteins in the healthy control, while the anti-VPg antibodies cross-reacted with several plant proteins in the healthy control (a predominant protein with a molecular mass of approximately 110 kDa and a protein of approximately 75 kDa). Several protein bands were detected with the anti-NTB and anti-VPg antibodies in infected but not in healthy P30 fractions (see Fig. 3.1B). These proteins were not detected in S30 fractions corresponding to the cytosolic fraction (data not shown). A predominant band with an apparent molecular mass of approximately 69 kDa was detected with both antibodies and corresponds to the NTB-VPg polyprotein. The mature NTB protein has a calculated molecular mass of 66 kDa and would migrate very closely to the 69 kDa NTB-VPg on SDS-polyacrylamide gels. It was therefore possible that the NTB protein was also present in infected plants but that the chemiluminescent detection method did not allow the resolution of the two closely spaced protein bands. To test this, we conducted new immunoblotting experiments with the same extracts using a colorimetric based detection method. The colorimetric detection was less sensitive than the chemiluminescent detection.

However the resolution of closely spaced protein bands was improved (Fig. 3.1C). Using this method, a protein of approximately 66 kDa was detected in addition to the 69 kDa NTB-VPg. The 66 kDa protein was recognized by the anti-NTB antibodies but not by the anti-VPg antibodies and therefore probably corresponded to the mature NTB (Fig 3.1C). Other viral proteins detected by the anti-NTB antibodies were present in much smaller amounts and their relative concentration varied from extract to extract. The apparent molecular masses of these proteins were 90 kDa, 110 kDa and 130 kDa (Fig. 3.1B). The 90 kDa protein was also detected by the anti-VPg antibodies. Detection of the 110 kDa protein by the anti-VPg antibodies was obscured by cross-reaction of the antibodies with a 110 kDa protein also present in the healthy plant extract. The 90 kDa and 110 kDa proteins may correspond to the X2-NTB-VPg and NTB-VPg-Pro polyproteins, respectively. The 130 kDa band was only partially recognized by the anti-VPg antibodies, raising the possibility that it may consist of a mixture of two proteins, only one of which contains the VPg domain. Based on its apparent molecular mass the 130 kDa protein may correspond to a polyprotein containing the X1-X2-NTB-VPg (possibly mixed with X1-X2-NTB). Alternatively, it may be a dimer form of NTB-VPg (possibly mixed with a dimer form of NTB). The precise nature of these proteins could not be determined as antisera against other domains of the P1 polyprotein were not available. These results show that several viral proteins containing the NTB domain are present in membrane-enriched fractions and are consistent with the suggestion that the NTB protein is a membrane-associated protein.

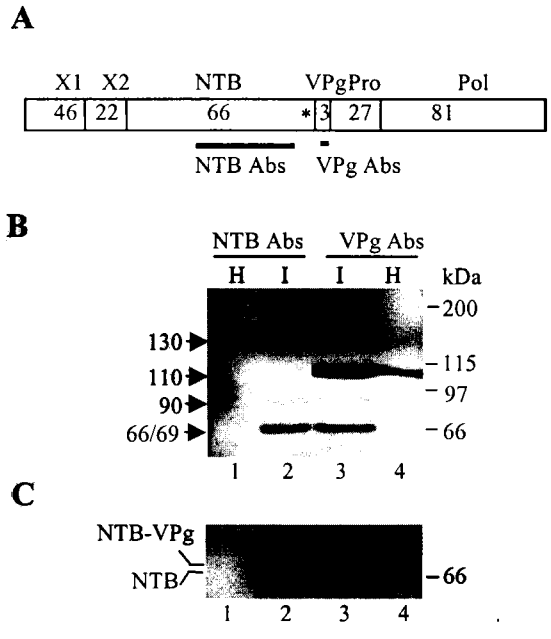


**Fig. 3.1. Immunodetection of viral protein precursors containing NTB.**
(A) Schematic diagram of the ToRSV RNA1-encoded polyprotein. Identified cleavage sites are indicated by vertical lines and the putative function of individual domains is indicated above the diagram. The hydrophobic domain at the C-terminus of the NTB domain is represented as an asterisk. The regions of the NTB and VPg domains present in the fusion protein or peptide used as antigens to raise the corresponding antibodies (Abs) are shown below the diagram. (B) Immunoblot analysis of crude membrane fraction (P30) from healthy (H) or ToRSV-infected (I) plants. The proteins were separated by SDS-PAGE (8% polyacrylamide), detected by antibodies raised against the NTB (NTB Abs) or the VPg (VPg Abs), and developed using the chemiluminescence detection system as described in Materials and Methods. Arrows on the left side of the gel point to proteins detected by the NTB Abs in the infected but not in the healthy extracts and the numbers associated with the arrows indicate the estimated molecular mass of these proteins (in kDa). Migration of molecular mass standards is shown on the right side of the gel. (C) Detection of the NTB and NTB-VPg proteins using the colorimetric detection system. Only the relevant portion of the gel is shown.

### 3.2.2 Viral proteins containing NTB co-fractionate with endoplasmic reticulum-derived membranes in sucrose gradients.

To characterize further the type of membranes to which the NTB protein attaches, cellular membranes from ToRSV-infected leaves were fractionated on sucrose gradients. Extracts from infected leaves were obtained as described in Materials and Methods and clarified by a single centrifugation at 3,000 x g to eliminate the majority of the cell wall and debris. The resulting S3 fraction was then analyzed on 20-45% sucrose gradients in the presence or absence of 3 mM $MgCl_2$. The presence of 3 mM $MgCl_2$ in the extraction buffer preserves the integrity of the association of ribosomes with the rough ER (rER) while in the absence of $MgCl_2$, the association of ribosomes with the rER is disrupted, resulting in a shift of rER-containing fractions towards the top of the gradient (Wienecke and Robinson, 1982). In this experiment, we chose to analyze S3 fractions to ensure that all intracellular membranes (including Golgi membranes) were present in the extracts. Sucrose gradient fractions were analyzed by immunoblot assay using antibodies raised against the Bip protein (a marker of the ER, Staehelin, 1997) and against proteins containing xylose $\beta$, 1→2 mannose modifications (a marker of the medial- and trans-Golgi, Zhang and Staehelin, 1992). Two peaks containing Bip were detected in gradients derived from infected leaves extracted in the presence of 3 mM $MgCl_2$ (Fig. 3.2A, Bip), a result previously described by others ( Schaad *et al.*, 1997). These two peaks were also detected in gradients derived from healthy leaves although the concentration of Bip was lower in these gradients (data not shown). The peak containing Bip at the bottom of the gradient (fractions 1 to 6) was shifted towards the top of the gradient in the absence of $MgCl_2$ (fractions 8 to 12) suggesting that these fractions contain rER. The proteins containing $\beta$-xylosyl were detected near the top of the gradient (fractions 9 to 13) in the

presence or absence of $MgCl_2$ indicating that these fractions contained the Golgi apparatus (Fig. 3.2A, $\beta$-xylosyl). Immunoblotting of the sucrose gradient fractions was also conducted using the anti-NTB antibodies. The 66/69 kDa band was found in fractions 4 to 6 in gradients obtained from extracts prepared in the presence of 3 mM $MgCl_2$ and shifted up to fractions 9 to 12 in the gradient obtained from extracts prepared in the absence of $MgCl_2$ (Fig. 3.2A, NTB). This shift was similar to that observed with the bottom Bip-containing peak and suggested that proteins contained in the 66/69 kDa band were associated with membranes having properties in common with the rER. The 66/69 kDa peak in the gradient obtained from extracts prepared in the presence of 3 mM $MgCl_2$ (fractions 4 to 6 with a maximum in fraction 5) was slightly displaced compared to the bottom Bip-containing peak in the same gradient (fractions 1 to 6 with a maximum in fractions 4 and 5). One possible interpretation of this observation is that the viral proteins contained in the 66/69 kDa peak were associated with only a sub-population of the rER-derived membranes present in infected plants. The distribution of the 66/69 kDa band was compared with that of the movement protein (MP, present in tubular structures in the cell wall, Wieczorek and Ssanfacon, 1993) and the coat protein (CP). Antibodies raised against the MP detected a protein of the expected size for the mature movement protein in a few fractions at the bottom of either gradient (fractions 1 to 3), suggesting that these fractions were enriched in residual cell wall material that was not eliminated at the clarification step (Fig. 3.2A, MP). The CP was detected in a broader area of the sucrose gradients (Fig. 3.2A, CP, fractions 1 to 7). The MP and CP-containing peaks did not shift towards the top of the gradient in the absence of $MgCl_2$ indicating that these proteins did not associate with rER-derived membranes and did not co-fractionate with the 66/69 kDa peak.

Using immunoblot analysis of the diluted sucrose gradient fractions with the anti-NTB

antibodies, we could detect the predominant 66/69 kDa band but not other larger proteins containing NTB. To further analyze the nature of the NTB-containing proteins associated with the intracellular membranes contained in fractions 4 to 6 (gradients prepared in the presence of 3 mM $MgCl_2$), the membranes were purified and concentrated by an ultracentrifugation step (see Materials and Methods). Immunoblotting experiments using these purified membranes revealed the presence of the NTB-VPg polyprotein (69 kDa protein detected by the anti-NTB and anti-VPg antibodies), and of the 130 kDa and 90 kDa proteins (also detected by both antibodies, Fig. 3.2B). These proteins were not present in controls prepared in a similar manner using sucrose gradients containing extracts from non-infected (healthy) plants. The 110 kDa plant protein that cross-reacted with the anti-VPg antibodies in the healthy and infected P30 extracts (Fig. 3.1), was not detected by these antibodies in the healthy or infected purified membranes (Fig. 3.2B), because this protein separated to different fractions in the sucrose gradient (data not shown). These results suggested that NTB-VPg and possibly other proteins containing the NTB domain were associated with membranes having properties in common with the rER.

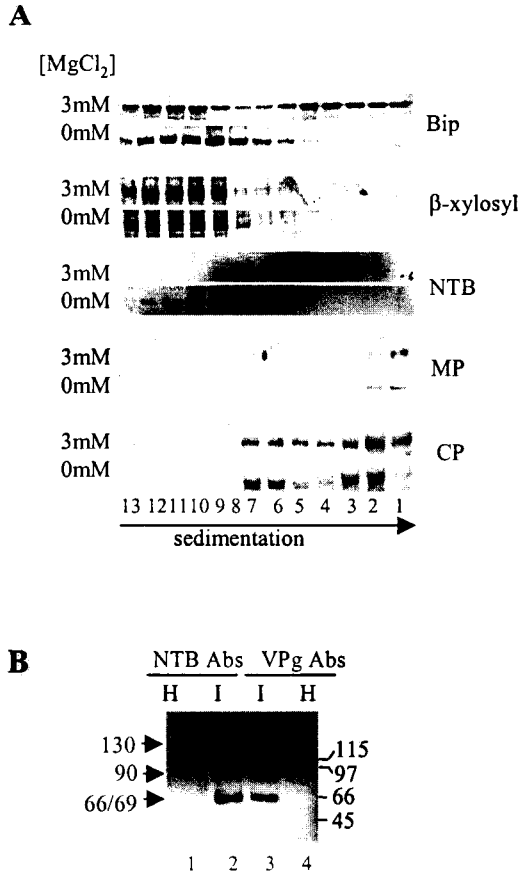


**Fig. 3.2. Western blot analyses of fractions from sucrose density gradients.**
(A) Tissue extracts were prepared and fractionated on a 20-45 % sucrose density gradient in the presence or absence of 3 mM $MgCl_2$. The direction of sedimentation is shown, with fraction 13 representing the top of each gradient. The proteins from each fraction were separated by SDS-PAGE (12% polyacrylamide), detected by antibodies raised against Bip, NTB, β-xylosyl containing proteins, MP and CP and developed using the chemiluminescence-based secondary antibody system. The relevant portion of each immunoblot is shown. In the NTB immunoblot, the predominant 66/69 kDa band (corresponding to the NTB and NTB-VPg proteins) is shown. In the β-xylosyl immunoblot, only β-xylosyl-containing proteins with apparent molecular masses of approximately 50kDa are shown. The concentration of $MgCl_2$ used in each sucrose gradient is shown on the left side of the gels. (B) Fraction 4-6 from the 3 mM $MgCl_2$ gradient prepared with ToRSV-infected (I) plant extracts were pooled, concentrated by ultracentrifugation and resuspended in buffer as described in Material and Methods. Equivalent sucrose gradient fractions were also used to prepare purified membranes from healthy plants (H). Proteins were separated by SDS-PAGE (15% polyacrylamide) and detected by immunoblotting using anti-NTB and anti-VPg antibodies. Migration of molecular mass standards (in kDa) is shown on the right side of the gel and arrows on the left side of the gel point to the proteins detected by the anti-NTB and anti-VPg antibodies. The estimated molecular masses (in kDa) are indicated by the numbers associated with the arrows.

### 3.2.3 Viral RNA synthesis activity co-fractionates with proteins containing NTB.

We next investigated whether RdRp activity co-fractionated with the NTB-containing proteins and with the rER. As a first step, we established a ToRSV RdRp assay using endogenous templates present in washed membrane-enriched fractions (P30-2 fractions) from healthy or infected plants. The [$\alpha$-$^{32}$P]UTP labeled RNA products were separated by electrophoresis in 1% agarose under non-denaturing conditions. In infected membrane fractions, an RNA product was synthesized that migrated to a position corresponding to that of ToRSV dsRNAs purified from infected plants (Fig. 3.3A, lane 1). The band was rather diffuse indicating that it may represent a mixture of RNA1 and RNA2. Due to their large and similar size, the dsRNA products of RNA1 (7.2 kb) and RNA2 (8 kb) purified from infected plants are not resolved into two separate bands on agarose gels (data not shown). The labeled band was not detected in the RNA products synthesized in membrane fractions derived from healthy plants (lane 2). The labeled RNA was also synthesized in the presence of DNase I (which degrades endogenous DNA) and actinomycin D (which inhibits transcription) indicating that it was not derived from DNA-dependent host transcription (lane 3). The RNA product was resistant to RNase A digestion confirming that the labeled RNA was double-stranded RNA produced by an RNA-dependent RNA polymerase and not a single-stranded polyU extension synthesized through the action of a terminal uridylyl transferase (lane 5). To confirm that the labeled dsRNAs were specific to ToRSV, hybridization experiments were conducted using the labeled RdRp products from infected membrane fractions as a probe and ToRSV minus and plus strand synthetic RNA2 transcripts bound to a filter (Fig. 3.3B). A strong hybridization was detected with (-) strand synthetic RNA2, indicating that the ToRSV (+) strand was synthesized from the endogenous templates. In contrast, the labeled RdRp products hybridized very weakly

to ToRSV (+) stranded RNA2, suggesting that ToRSV (-) strand was synthesized at very low levels (if at all). As expected, the products synthesized using non-infected tissue extracts did not hybridize with either of the RNA transcripts. Similar results were obtained using synthetic RNAs derived from ToRSV RNA1 (data not shown). Other studies have also shown that only dsRNA replication products are observed in replication assays using extracts from plants infected with other picorna-like viruses, including another nepovirus (*Grapevine chrome mosaic virus*, GCMV, subgroup II, Le Gall *et al.*, 1997), a comovirus [cowpea infected with CPMV, Eggen *et al.*, 1988] and a potyvirus (*Plum pox virus*, Martin and Garcia, 1991). Analysis of the RdRp products of other plant picorna-like viruses has revealed that (+) stranded RNA is synthesized predominantly; i.e., the (-) strand is synthesized at very low levels or not at all (Le Gall *et al.*, 1997; Eggen *et al.*, 1988; Martin and Garcia, 1991 ; Schaad *et al.*, 1997).

Membrane-enriched fractions (P30-2) from ToRSV-infected tissues were separated by sucrose gradient analysis in the presence of 3 mM $MgCl_2$ as described above. In this experiment we chose to analyze P30-2 fractions that were enriched in ER membranes to allow a better separation of the membranes on the sucrose gradients and to increase the concentration of membranes present in each sucrose gradient fraction. Analysis of the RdRp activity in the different fractions revealed a peak of activity in fractions near the bottom of the gradient (fractions 1 to 4, Fig. 3.3C). Proteins containing NTB co-fractionated with the peak of ToRSV RdRp activity (only the 66/69 kDa protein band is shown in the figure). The 66/69 kDa protein band was also detected by the anti-VPg antibodies confirming the presence of NTB-VPg in these fractions. As shown above, proteins containing NTB also co-fractionated with a peak containing Bip at the bottom of the gradient. Noticeably, the 66/69 kDa protein (and Bip marker) sedimented faster in this gradient than in the gradient prepared with clarified extracts

(S3 fractions, Fig. 3.2A). Similar differential sedimentation of the Bip marker were also obtained by others when comparing gradients prepared using concentrated purified P30-2 fractions or more diluted S3 fractions (Schaad *et al.*, 1997). Extraction of ribosomal RNAs from the different fractions confirmed that the bottom peak containing Bip also contained ribosomal RNA suggesting the presence of rough ER in these fractions. Taken together, the results presented in Fig. 3.2 and 3.3 indicated that the proteins containing NTB co-fractionated with replication complexes associated with membranes having properties of the rough ER.

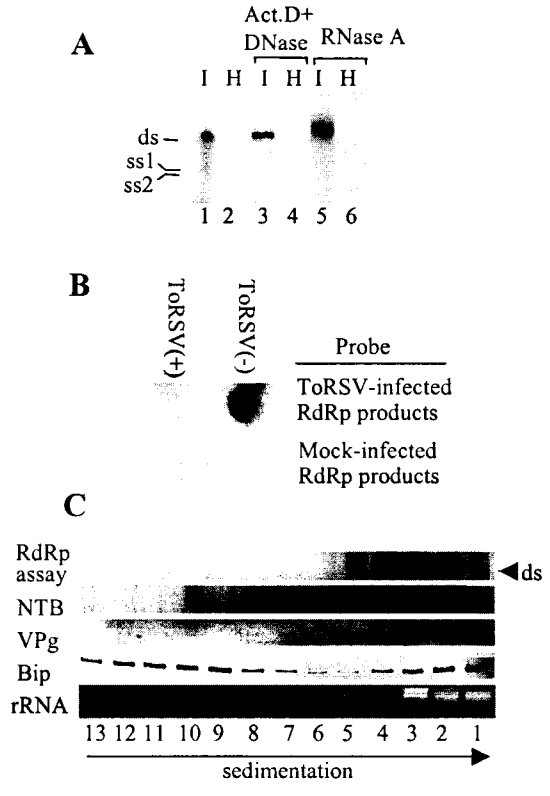


**Fig. 3.3. Analysis of membrane-bound ToRSV RdRp activity.**
(A) Detection of [α- $^{32}$P]UTP-labeled RdRp products synthesized using P30-2 fractions from ToRSV-infected (I) and healthy (H) plants. The RdRp products were separated on 1 % agarose gels. Total products (lanes1 and 2) , DNase I- and actinomycin D-resistant products (lanes 3 and 4) and RNase A-resistant products (lanes 5 and 6 ) are shown. The migration of ToRSV single-stranded RNA1 and RNA2 (ss1 and ss2, respectively) and double-stranded (ds) RNAs purified from infected plants (the ds forms of RNA1 and RNA2 do not separate on 1 % agarose gels and migrate as one diffuse band) is shown on the left side of gel. In lane 5, the presence of 2 % SDS in the proteinase K digestion buffer used after the RNase A treatment interfered slightly with the migration of the sample resulting in a slower migration of the dsRNA products. (B) Dot blot hybridization analysis of labeled RdRp products using P30-2 fractions from ToRSV-infected (I) and healthy (H) plants. Transcripts corresponding to the positive (+) or negative (-) strand of a region of ToRSV RNA2 were synthesized *in vitro* as described in Materials and Methods and blotted onto Zeta-Probe membranes (Bio-Rad ). The polarity of the ToRSV transcripts is indicated at the top of the panel. (C) Fractionation of RdRp activity, proteins containing NTB or VPg, Bip and ribosomal RNAs in a 20-45 % sucrose gradient using P30-2 extracts from ToRSV-infected tissue. Each fraction was analyzed for RNase A-resistant RdRp activity (top), subjected to immunoblot analysis using anti-NTB, anti-VPg and anti-Bip antibodies and tested for the presence of ribosomal RNA (rRNA). For the anti-NTB and anti-VPg antibodies, only the portion of the gel containing the predominant 66/69 kDa band is shown.

### 3.2.4 ToRSV infection induces morphological changes of the ER.

To investigate whether infection by ToRSV induces morphological changes of the ER we used transgenic *N. benthamiana* plants which express GFP targeted to the lumen of the ER. GFP fluorescence was examined in epidermal cells of leaves from ToRSV-infected plants and mock-inoculated plants by confocal fluorescence microscopy. As described by others (Carette *et al.*, 2000; Schaad *et al.*, 1997), green fluorescence was associated with the cortical ER network and with the nuclear envelope in healthy plant cells (Fig. 3.4A, the green fluorescence has been converted to white in the black and white figure). In contrast, the morphology of the ER was drastically altered in ToRSV-infected epidermal cells (Fig. 3.4B and 4C). Large bodies of fluorescence were observed which were often (but not always) located in close proximity to the nucleus (Fig. 3.4C). These morphological changes were found in clusters of cells (probably corresponding to foci of infection) in inoculated leaves 4 days post-inoculation and in systemically infected leaves 7 days post-inoculation, i.e. before obvious symptoms developed in the leaves. Once lesions became necrotic, the cells were in general too damaged to allow a clear visualization of the ER structure. However, ER aggregates were visible in cells surrounding the necrotic lesions. The ER aggregates were never observed in mock-inoculated plants. Taken together, these results suggest that the formation of ER aggregates is a consequence of ToRSV infection.

Changes in the morphology of the ER were also observed by epifluorescence microscopy in live mesophyll protoplasts prepared from ER-GFP transgenic *N. benthamiana* transfected with ToRSV viral RNA. In mock-transfected protoplasts, the green fluorescence was in general very weak. However, the cortical ER network was visible (Fig. 3.5A. panel 1) and in some cases, a perinuclear weak green fluorescence was also observed (data not shown).

In protoplasts transfected with ToRSV RNA (30 hrs post-inoculation), large bodies of fluorescence were observed in 10 to 15% of the protoplasts (which corresponds to the percentage of protoplasts successfully infected by ToRSV as measured in a separate experiment, see below). In some cases, the fluorescence appeared as several large aggregates in the protoplast (panel 2) and in other cases it appeared as a halo around the nucleus (panel 3). Therefore, morphological changes in the ER were also induced in protoplasts after infection with ToRSV viral RNA.

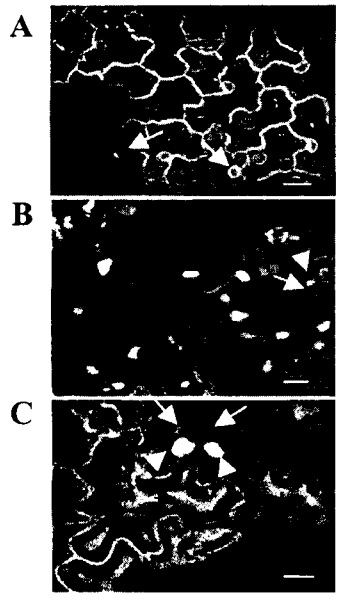


**Fig. 3. 4. Confocal fluorescence micrograph of mock-infected (A) or ToRSV-infected (B and C) epidermal cells of ER-GFP transgenic *N. benthamiana.***

(A) Epidermal cells of a mock-inoculated leaf (B and C) Epidermal cells of a ToRSV-inoculated leaf (4 days post-inoculation) showing aggregates of ER-GFP fluorescence. (C) Close-up of two ToRSV-infected epidermal cells showing a perinuclear location of the ER-GFP aggregates. The bars on the figures represent 20 μm. Arrows point to nuclei. In this black and white figure, the green GFP fluorescence is shown in white over the dark background.

### 3.2.5 Proteins containing NTB co-localize with ER membranes in infected protoplasts.

To determine whether the proteins containing NTB co-localize with ER membrane aggregates in infected plant cells, protoplasts prepared from ER-GFP *N. benthamiana* were transfected with viral RNA, fixed at 30 hrs post-inoculation and immunostained with anti-NTB antibodies. The use of goat anti-rabbit-Cy3 as secondary antibodies allowed us to simultaneously visualize the red fluorescence (Cy3) associated with the anti-NTB antibodies and the green fluorescence from the ER-GFP. Although some red autofluorescence from the chloroplasts remained after the fixation procedure, the Cy3 red fluorescence was much more intense and easily distinguishable from the chloroplasts autofluorescence [compare non-infected protoplast on the right of Fig. 3.5B-1 (panel NTB) to ToRSV-infected protoplast on the left of the figure]. Using epifluorescence microscopy, the percentage of protoplasts successfully infected by ToRSV was estimated by analyzing the number of protoplasts displaying the Cy3 red fluorescence and therefore expressing proteins containing NTB. In approximately 15 % of the protoplasts, a successful ToRSV infection was established. In ToRSV-infected protoplasts, the NTB-associated red fluorescence was localized in one or several large fluorescent bodies per cell (Fig. 3.5B-1, protoplast on the left of the picture, and Fig. 3.5B-2). In approximately 90 % of the ToRSV-infected protoplasts, the aggregates of red fluorescence associated with the anti-NTB antibodies co-localized with aggregates of green fluorescence associated with the ER-GFP as shown in the digitally superimposed image (Fig. 3.5B, Merge). These results are in agreement with the sucrose gradient fractionation studies presented above and confirm the suggestion that proteins containing NTB associate with membranes derived from the ER.

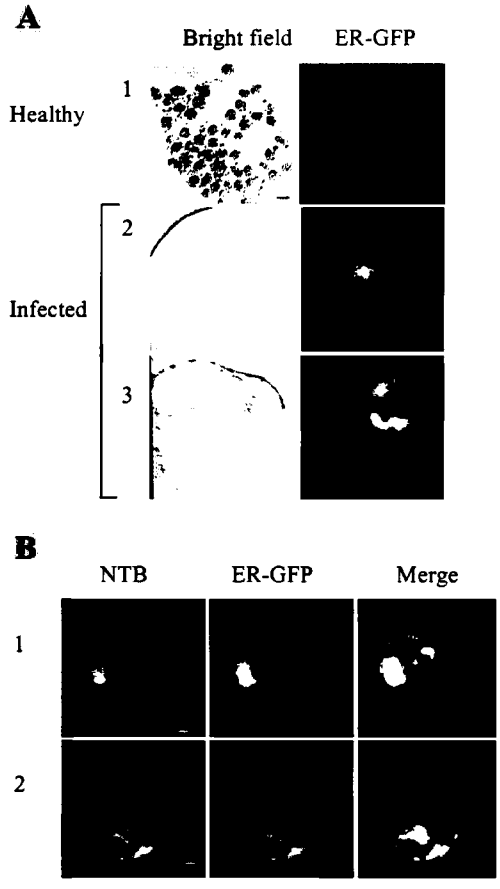


**Fig. 3.5. Immunofluorescence localization of viral proteins containing NTB in infected protoplasts.** (A) Visualization of ER-GFP in mock-transfected (1) and ToRSV-transfected (2 and 3) live protoplasts. Micrographs in each horizontal row show brightfield and ER-GFP fluorescence. (B) Immunofluorescence localization of proteins containing NTB in ToRSV-transfected protoplasts. The protoplasts were fixed and immunostained with anti-NTB and Cy3-conjugated secondary antibodies. Micrographs in each horizontal row show the Cy3 fluorescence corresponding to the location of the NTB protein (NTB), the ER-GFP fluorescence (ER-GFP) and the digitally superimposed images where green and red signals that coincide produce a yellow signal (Merge). In panel 1, two protoplasts are present in the picture. In the protoplast on the left, a successful infection by ToRSV was established and NTB specific fluorescence is detected. The protoplast in the right is apparently not infected and NTB fluorescence is not detected. The bars on the figure represent 10 μm.

### 3.2.6 Proteins containing NTB are integral membrane proteins.

To further characterize the nature of the association of NTB-containing proteins with cellular membranes, membrane-enriched fractions (P30) were extracted with different agents known to dislodge peripheral, lumenal or integral membrane proteins. Treatment with 1M KCl solubilizes peripheral proteins while integral and lumenal proteins remain associated with the membranes (Schaad *et al.*, 1997). Under high pH conditions (0.1M $Na_2CO_3$, pH 10.5), membrane vesicles are converted to open membrane sheets allowing the release of peripheral and lumenal proteins but not of integral membrane proteins (Fujiki et al., 1982; Howell and Palade, 1982 ). Finally, membrane-enriched fractions were subjected to a Triton X-114 phase partition analysis. Integral membrane proteins partition to the detergent phase while other proteins are found in the aqueous phase (Bordier, 1981).

After treatment with the various agents, the membranes were collected by centrifugation and analyzed by immunoblotting. The immunoblots were probed sequentially with antibodies against NTB, VPg and Bip (a soluble ER lumenal protein) (Fig. 3.6 ). In these experiments, the proteins containing NTB including NTB-VPg (revealed by both the anti-NTB and anti-VPg antibodies) remained associated with the membrane pellet following extraction with 0.1 M $Na_2CO_3$, pH 10.5 and 1 M KCl. Furthermore, they partitioned into the detergent fraction after extraction with Triton X-114 (Fig. 3.6 A and B). In contrast and as expected, the lumenal Bip protein was released into the supernatant fraction after treatment with 0.1 M $Na_2CO_3$, pH 10.5, remained in the pellet after treatment with 1 M KCl and partitioned into the aqueous phase after extraction with Triton X-114. Taken together, these results indicate that the proteins containing NTB are associated with cellular membranes as true integral membrane proteins.

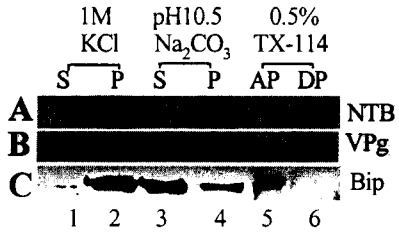


**Fig.3. 6. Extraction and immunoblot analysis of proteins containing NTB from infected plants.** The P30 fraction from infected plants was extracted with 1 M KCl or 0.1 M $Na_2CO_3$ (pH 10.5) and subjected to centrifugation at 30,000 x g, yielding S30 (S) and P30 (P) fractions (lanes 1-4). The total P30 fraction was also separated into aqueous phase (AP) and detergent-soluble phase (DP) after treatment with Triton X-114 (lanes 5 and 6). The supernatant and pellet fraction or aqueous phase and detergent phase were loaded on 12% SDS-polyacrylamide gels in equivalent amounts and analyzed by immunoblotting using anti-NTB, anti-VPg and anti-Bip antibodies and the chemiluminescence-based secondary antibody system. Only the portion of the gel containing the predominant 66/69 kDa band is shown.

### 3.2.7 The VPg domain of proteins containing NTB and VPg is protected from proteinase K digestion by its association with cellular membranes.

I have shown above that several NTB-containing proteins are strongly associated with ER-derived membranes. The predominant proteins in membrane-enriched fractions were the mature NTB and the NTB-VPg polyprotein (see Fig. 3.1). The presence of the NTB-VPg polyprotein in association with replication complexes was confirmed by its detection using anti-NTB and anti-VPg antibodies (see Fig. 3.3). Because of the suggested role of the VPg as a primer in viral RNA replication in the related picornaviruses (Paul *et al.*, 1998), it was of interest to study the topology of NTB-VPg in the membranes. In an attempt to predict the possible topology of NTB-VPg, the deduced amino acid sequence was analyzed with the Transmembrane Hidden Markov Model algorithm (TMHMM, Krogh *et al.*, 2001). As expected, a *trans*-membrane domain was predicted at the C-terminus of the protein. The region of NTB upstream of the putative *trans*-membrane domain was predicted to be localized on the cytoplasmic face of the membranes (100% prediction, data not shown). Interestingly, the C-terminal segment of NTB-VPg containing the VPg domain was predicted to be on the lumenal face of the membrane (60% prediction) (Fig. 3.7A ). The C-terminal hydrophobic domain was previously suggested to be a *trans*-membrane domain (Rott *et al.*, 1995). This domain consists of two hydrophobic stretches of 19 a.a. and 20 a.a. separated by a single charged Lys residue (Fig. 3.7 C). Lys residues were also present at the C- and N-termini of the hydrophobic domain. As stretches of 20-25 non-polar amino acids have been shown to be a sufficient length to span the hydrophobic lipid bilayer (Lemmon *et al.*, 1997), the sequence of the ToRSV putative *trans*-membrane domain suggested that it could either adopt a hairpin structure and span the membrane twice, or that it could span the membrane only once.

To study the topology of proteins containing the NTB and VPg domains, samples enriched in membrane-bound NTB-VPg were treated with proteinase K. Using this technique, only portions of the proteins which are exposed to the cytoplasmic face should be susceptible to the proteinase. In contrast, parts of the proteins embedded in the membrane are protected from digestion unless the membranes are solubilized by a detergent. I have shown above that intracellular membranes purified from sucrose gradient fractions contain the NTB-VPg polyprotein along with smaller amounts of other larger proteins recognized by the anti-NTB and anti-VPg antibodies (Fig. 3.2B). These samples, which did not contain substantial amounts of plant proteins cross-reacting with the anti-NTB or anti-VPg antibodies were used to conduct the proteinase K protection assays. To test the efficiency of the proteinase K protection assay, we used the Bip ER lumenal protein as a control (Fig. 3.7D, lanes 1-3). Immunoblotting of samples collected prior to the proteinase K digestion allowed the recognition of the full-length 70 kDa protein by the anti-Bip antibodies. Small amounts of a 31 kDa fragment that may represent a degradation product of the protein were also detected. As expected, the 70 kDa protein (and 31 kDa protein) were protected from degradation in the absence of the detergent but were degraded in the presence of Triton X-100. Small amounts of two 30 kDa fragments were resistant to proteinase K digestion in the presence or absence of Triton X-100. Therefore this resistance to proteinase digestion was not due to membrane protection. Very similar results were described in studies using Kar2p which is a yeast ER lumenal protein homologous to Bip (Den Boon *et al.*, 2001). The immunoblots were stripped of the anti-Bip antibodies and reprobed sequentially with the anti-NTB antibodies raised against the central region of NTB and with the anti-VPg antibodies. In samples collected prior to the proteinase K digestion, only the predominant 66/69 kDa protein is shown (Fig. 3.7D, lanes 4 and 7). The anti-NTB

antibodies failed to detect any protected fragments in the presence or absence of detergent suggesting that the region of the NTB protein which is recognized by the antibodies is exposed to the cytoplasmic face of the membrane (lanes 4-6). Interestingly, an 8 kDa segment was detected by the anti-VPg antibodies when the proteinase K digestion was performed in the absence of detergent (lane 8). This fragment was completely digested when Triton X-100 was added to the reaction (lane 9). A proteinase K protection experiment was also performed on the purified membrane samples from non-infected plant extracts. The anti-VPg antibodies did not detect any protected fragment in the presence or absence of Triton X-100 (lanes 11 and 12). The size of the 8 kDa protected fragment corresponds to the predicted size for a fragment containing the putative *trans*-membrane domain at the C-terminus of the NTB (with a calculated molecular mass close to 5 kDa) followed by the entire VPg domain (3 kDa, see Fig. 2.7B). This result confirms the prediction that the central portion of the NTB domain is exposed to the cytoplasmic face of the membranes while the VPg domain adopts a lumenal orientation in at least a portion of the molecules.

**Fig. 3.7. Predicted structure of the NTB-VPg polyprotein and proteinase K treatment of membrane-enriched fractions from sucrose gradients.**
(A) Prediction of topology of NTB-VPg using the Transmembrane Hidden Markov Model algorithm. The shaded area represents the predicted transmembrane domain. The light grey line indicates the probability for each residue to be at the cytoplasmic face of the membrane. The black line indicates the probability for each residue to be at the lumenal side of the membrane. The position of the start of the VPg is indicated by an arrow above the graphic. (B) Graphical summary of the prediction for the 620 amino acids of NTB-VPg. The light grey square, the asterisk and the black square represent the putative amphipathic α-helix, the putative *trans*-membrane domain and the VPg, respectively. (C) Amino acid sequence of the putative *trans*-membrane domain. Positively charged amino acids are shown in bold and two hydrophobic stretches are underlined. The NTB-VPg cleavage site downstream of the *trans*-membrane domain is shown by the arrow. (D) Proteinase K protection assays using membrane-enriched fractions from ToRSV-infected plants. Purified membranes from Fig. 2B were subjected to proteinase K (Prot. K) digestion in the absence (-) or presence (+) of Triton X-100. The proteins were separated by SDS-PAGE (18% polyacrylamide), analyzed by immunoblotting using anti-Bip (lanes1-3), anti-NTB (lanes 4-6) and anti-VPg (lanes 7-12) antibodies and developed using the chemiluminescence-based secondary antibody system. The arrowhead points to the 8 kDa protected fragment detected by the anti-VPg antibodies. Migration of molecular mass standards is shown on the right side of the gels.

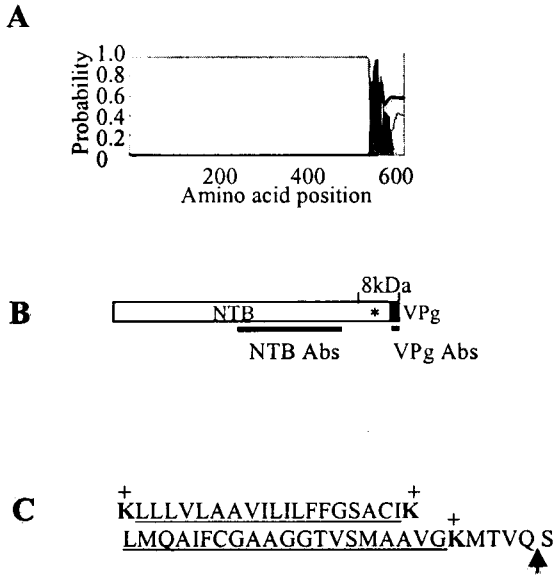
A
Probability
1.0
0.8
0.6
0.4
0.2
0
200
400
600
Amino acid position
B
8kDa
NTB
VPg
NTB Abs
VPg Abs
C
KLLLVLAAVILILFFGSACIK
LMQAIFCGAAGGTVSMAAVGKMTVQS
D
Bip
NTB
VPg
Infected
Prot. K
Triton
66-
45-
31-
21-
14.5-
6.5-
1 2 3 4 5 6 7 8 9 10 11 12

### 3.2.8 Sequence comparison and structure prediction

The experiments described above allowed the identification of a membrane anchor within the C-terminus of the NTB. To see if the potential membrane anchor is well conserved in the picorna-like virus supergroup, I have analyzed the deduced amino acid sequence of the NTB-VPg polyprotein of different viruses using hydropathy plots.

First, I wanted to see if the hydrophobic domain is conserved in nepoviruses. Since the cleavage site at the N-terminus of the NTB has not been defined in some nepoviruses, I compared hydropathy plots using only the C-terminal portion of NTB-VPg. Analysis of the hydrophobicity profile of NTB-VPg revealed the presence of conserved hydrophobic domains immediately upstream of the hydrophilic VPg domain in nepoviruses (Fig. 3.8).

Second, the hydrophobicity profile was also examined for the entire ToRSV NTB-VPg (Fig. 3.9). The analysis also reveals that the NTB domain contains an additional hydrophobic domain at its N– terminus in addition to the already identified hydrophobic sequence at its C-terminus (Fig. 3.9). A similar hydrophobic region was also noted in the N-terminal region of the CPMV NTB-VPg. Hydrophobic domains immediately upstream of the hydrophilic VPg domain were also observed upon analysis of the entire CPMV NTB-VPg and PV 2C-3A-3B (Fig. 3.9).

We have used several prediction methods to analyze the possible secondary structure of ToRSV NTB-VPg in the region of the short N-terminal hydrophobic domain (see Materials and Methods). An α-helix was predicted for the segment of amino acids 37-54 (numbered from the first amino acid of the NTB domain). An α-helix projection of this segment revealed the presence of a putative amphipathic helix (Fig. 3.10).

An α-helix was also predicted for the segment of amino acids 42-59 of the CPMV NTB-VPg (numbered from the first amino acid of the NTB domain). An α-helix projection of this segment also revealed the presence of a putative amphipathic helix (Fig. 3.10). Finally, it should be noted that PV 2C also contains an amphipathic helix at its N-terminus which has been identified and has been shown to be important for membrane association (Paul *et al.*, 1994). These results show that ToRSV NTB-VPg, CPMV NTB-VPg and PV 2C-3AB share similarity domains possibly involved in membrane association.

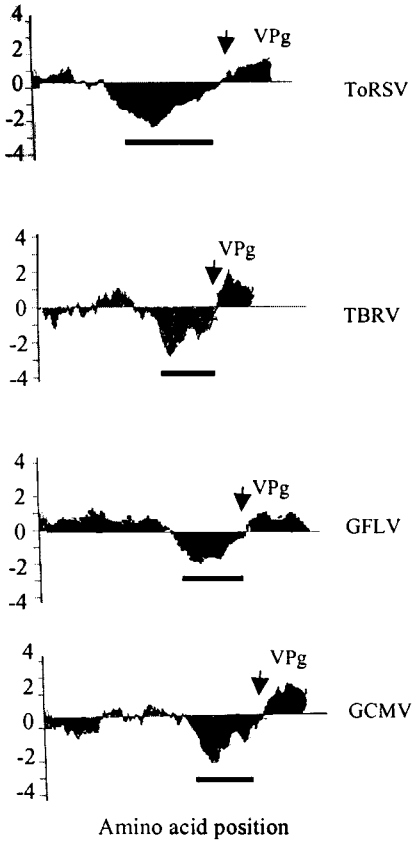


**Fig. 3.8. Kyte-Doolittle hydropathy plots for C-terminal sequences of NTB-VPg in nepoviruses.** The hydropathy plots are derived from analysis of the C-terminal sequences of NTB-VPg in nepoviruses using the Kyte-Doolittle program. Positive values represent hydrophilic regions, and negative values represent hydrophobic regions. The underlined regions indicate the conserved hydrophobic domain. The position of the start of the VPg domain is indicated by an arrow above the graphics.

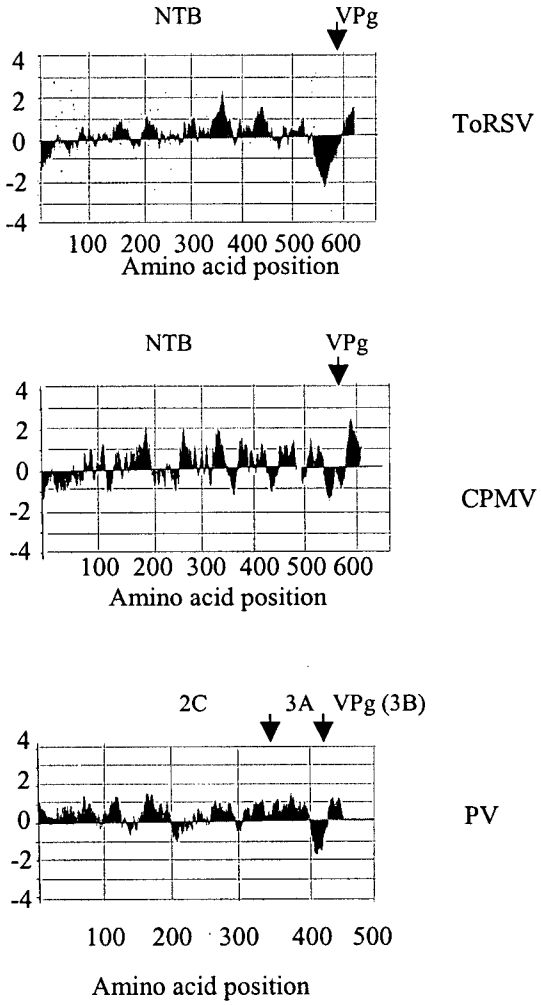


**Fig. 3.9. Kyte-doolittle hydropathy plots for ToRSV NTB-VPg, PV 2C-3A-3B and CPMV NTB-VPg.** The hydropathy plots are derived using kyte-doolittle program. Positive values represent hydrophilic regions, and negative values represent hydrophobic regions. The underlined regions indicate the conserved hydrophobic domain. The position of the start of the VPg domain is indicated by an arrow above the graphics.

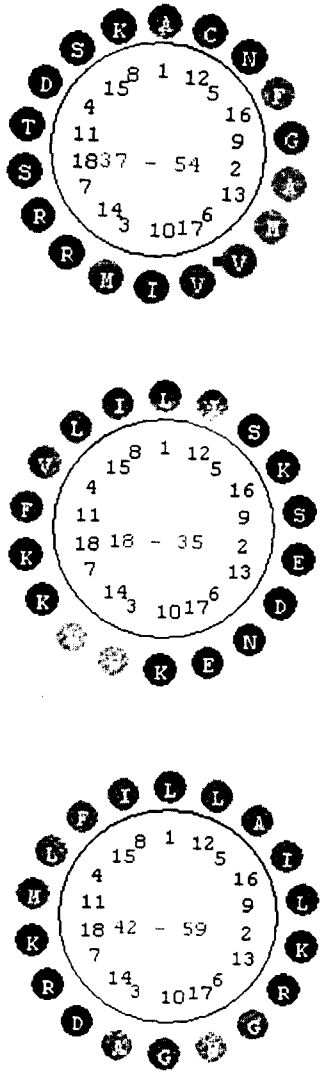


**Fig. 3.10. Helical wheel diagrams of putative amphipathic helices at the N-termini of ToRSV NTB, PV 2C and CPMV NTB.** The following amino acid sequences were used in the prediction: ToRSV, amino acids 37-54; PV, amino acids 18-35; CPMV, amino acids 42-59. The blackened shaded and light-grey shaded letters correspond to polar and hydrophobic residues, respectively.

## 3.3 DISCUSSION

In this study, I have shown that several proteins containing the NTB domain are present in membrane-enriched fractions isolated from infected plant leaves. Among these proteins, the mature NTB and the NTB-VPg polyprotein were abundant in all the extracts tested. The accumulation of NTB-VPg suggests that it is a stable intermediate in the processing pathway. The cleavage sites on the RNA1-encoded polyprotein (including the NTB-VPg cleavage site) are not processed in *trans* by the proteinase *in vitro* (Carrier *et al.*, 1999; Wang and Sanfaçon, 2000). Therefore, the NTB and NTB-VPg proteins detected in infected plant extracts are likely to be produced by alternative *cis*-processing pathways of the P1 polyprotein. Such alternative processing strategies have also been suggested for the closely related CPMV (Goldbach and Wellink, 1996). *In vitro*, the ToRSV NTB-VPg cleavage site is a predominant *cis*-cleavage site and accumulation of NTB-VPg is not detected. Rather the mature NTB and the VPg-Pro intermediate were shown to accumulate (Wang and Sanfaçon, 2000; Wang *et al.*, 1999). The accumulation of NTB-VPg in infected plants suggests that cellular factors (such as the membrane environment) modulate the recognition of the NTB-VPg cleavage site by the ToRSV proteinase.

The accumulation of ToRSV NTB-VPg in infected plants also raises the possibility that it may play an important role in the biology of the virus which may be distinct from that of the mature NTB. Because NTB-VPg co-fractionates with the viral replication complex, an active role of this protein in the replication of the virus seems probable. The accumulation of processing intermediates containing a putative membrane-anchor (such as the hydrophobic domain at the C-terminus of the NTB) and the VPg has been observed for several picorna-like viruses. The picornavirus 3AB, the TEV, 6K-NIa, the CPMV NTB-VPg (60K) proteins and

now the ToRSV NTB-VPg polyproteins are examples of such processing intermediates which accumulate in infected tissues (Agol *et al.*, 1999; Goldbach and Wellink, 1996; Restrepo-Hartwig *et al.*, 1994; Xiang *et al.*, 1997 and this study). The PV 3AB protein has been shown to play critical roles in the virus replication cycle and the presence of the VPg moiety (3B) on 3AB is essential for its activity (Agol *et al.*, 1999; Porter, 1993; Xiang *et al.*, 1997). Improving proteolytic cleavage at the 3A/3B site of *Hepatitis A virus* polyprotein results in impaired processing and particle formation (Kusov *et al.*, 1999) suggesting that accumulation of the 3AB protein is essential for the virus replication cycle. Future work will be necessary to dissect the possible biological function(s) of the ToRSV NTB-VPg polyprotein.

Using transgenic plants expressing GFP targeted to the ER, I showed that ToRSV infection induces drastic modifications of the ER. Large GFP-containing structures were found in infected tissues that often had a perinuclear location, and proteins containing NTB co-localize with these structures. Sucrose gradient fractionation analysis confirmed that proteins containing NTB co-fractionate with membranes derived from the rough ER that are active in viral replication. Nepovirus-infected cells are characterized by the presence of diffuse inclusions (containing membrane vesicles) often near the nuclei (Francki *et al.*, 1985). Recently, the replication activity of another nepovirus (GFLV) has been shown to be associated with ER-derived membrane structures very similar to the ones described in this study, and they were also located at a perinuclear location (Ritzenthaler *et al.*, 2002). Replication-associated proteins were also shown to co-localize at this site (Gaire *et al.*, 1999; Ritzenthaler *et al.*, 2002). Infection of ER-GFP plant cells by other picorna-like viruses (including CPMV and TEV) is also characterized with the induction of GFP-aggregates similar to the ones described here and the replication proteins of these viruses co-localize with the modified ER membranes (Carette

*et al.*, 2000; Carette *et al.*, 2002). Several viral proteins expressed outside the context of the virus genome have been shown to localize to intracellular membranes and to induce the alteration of the morphology of these membranes. For example, the morphology of ER and/or Golgi membrane is altered after expression of the PV 2C, 2BC (Cho *et al.*, 1994), 3A and 3AB (Datta and Dasgupta, 1994; Doedens and Kirkegaard, 1995), the TEV 6 kDa protein (Restrepo-Hartwig and Carrington, 1994) and the CPMV 60K and 32K proteins (Carette *et al.*, 2002). On the basis of sequence similarities with the PV 3A and 2C and the CPMV 60 kDa proteins, it is likely that NTB and/or proteins containing NTB are also responsible (at least in part) for the alterations of the ER morphology in ToRSV-infected cells. The association of the replication complex with membranes derived from the rough ER would provide opportunities for the coupling between the translation and the replication of the virus genome. Coupling between the viral translation, the formation of membranous vesicles and viral RNA synthesis is required for the formation of the PV replication complex (Egger *et al.*, 2000; Novak and Kirkegaard, 1994), although the mechanisms by which the virus regulates the switch from translation to replication are not yet clearly understood (Agol *et al.*, 1999; Barton *et al.*, 1999; Gamarnik and Andino, 1998).

I have shown that proteins containing NTB associate with membranes as integral membrane proteins suggesting that they may act as anchors for the ToRSV replication complex. Active replication complexes are presumed to assemble on the cytoplasmic face of the membranes (Schwartz *et al.*, 2002 and references therein). For BMV and possibly other viruses, the replication complexes are subsequently sequestered in cytoplasmic invaginations or spherules connected to the cytoplasm by a neck (Schwartz *et al.*, 2002). In agreement with this model,my analysis of the topology of the proteins containing NTB revealed that at least the

central part of the NTB domain is exposed to the cytoplasmic face of the membranes. The results of the proteinase K protection assay also revealed that an 8 kDa fragment containing the VPg domain is embedded in the membranes. Because NTB-VPg is one of the predominant proteins in the purified membranes used in the protection experiments (see Fig. 3.2B), it is likely that the protected fragment is mainly derived from NTB-VPg although we cannot exclude the possibility that digestion of other larger NTB- and VPg-containing polyproteins by the proteinase K may also result in the protection of this fragment. As mentioned above, the size of the protected fragment corresponds to the predicted size for a fragment containing the entire hydrophobic domain at the C-terminus of NTB followed by the VPg. This would suggest that the *trans*-membrane domain spans the membrane once, resulting in the lumenal location for the VPg. As the VPg is likely to play an active role in the replication of the viral RNA (possibly as a primer in RNA synthesis; Paul *et al.*, 1998), a lumenal location for the VPg may seem surprising. Recently, Ritzenthaler and colleagues demonstrated that small membranous vesicles contained in ER-enriched sucrose gradient fractions purified from GFLV-infected tissues could be immunotrapped by anti-VPg antibodies, suggesting that at least some of the VPg population is present on the cytoplasmic face of the membranes in GFLV-infected cells (Ritzenthalter *et al.*, 2002). Several points should be made that may help reconcile this apparently conflicting observation. First, my results do not exclude the possibility that NTB-VPg (or other proteins containing the NTB and VPg domains) displays a dual topology in the membranes. In recent years, it has become evident that certain cellular and viral *trans*-membrane proteins exhibit two or more distinct topological orientations which influence their biological functions (Lambert and Prange, 2001 and references therein). The TMHMM analysis of NTB-VPg gave a 100% prediction for a cytosolic-orientation of the region of NTB

upstream of the *trans*-membrane domain but only a 60% prediction for a lumenal-orientation of the VPg, suggesting that alternative topological orientations are possible. According to this prediction, the alternative topology would only be possible if the *trans*-membrane domain spans the membrane twice resulting in the VPg being exposed to the cytosol. As mentioned above, the presence of two adjacent hydrophobic stretches of 19-20 a.a. suggests that such a conformation is theoretically possible. Unfortunately, the proteinase K-protection assay used in this study would not allow us to detect proteins with this alternative topology. Indeed if the VPg was exposed to the cytoplasm, a 5 kDa fragment corresponding to the NTB *trans*-membrane domain would be protected from proteinase K digestion but would not be detected in my assay as the anti-NTB antibodies were not raised against this part of the protein. Additional experiments will be needed to investigate the possibility that other topological orientations of NTB-VPg (or other larger polyproteins) exist in infected plants. The second point is that NTB-VPg is probably not the donor for the VPg in infected plants. As discussed above, the NTB and NTB-VPg proteins are probably produced by alternative *cis*-processing events and therefore probably associate with the membranes after their release from the P1 polyprotein. As a consequence, the Pro and VPg-Pro (and/or Pro-Pol and VPg-Pro-Pol) are likely also produced in infected plants. The VPg-Pro or VPg-Pro-Pol are therefore possible donors for the active VPg as is suggested for CPMV (Peters *et al.*, 1995). We are currently raising polyclonal antibodies against the Pro and Pol domains in an attempt to detect such intermediates in infected plant cells. It should be noted that the VPg-Pro-Pol intermediate was detected in plants infected by *Tomato black ring virus* (TBRV, genus *Nepovirus*, subgroup B, Demangeat *et al.*, 1992) and that several large polyproteins containing VPg were also detected in ER-enriched fractions from GFLV-infected plant extracts (Ritzenthaler *et al.*, 2002). Finally, while it is

possible that the lumenal-orientation of the VPg in at least some of the membrane-associated proteins may play an important (as yet unknown) biological role, it may also represent a means to dispose of excess VPg and regulate the replication of the virus. Similarly, in TEV, the export of NIa (containing the VPg domain) in the nucleus has been suggested to help dispose of excess NIa in the cytoplasm and this process is tightly regulated by autoproteolysis (Restrepo-Hartwig and Carrington, 1992).

My results provide support for a role of the *trans*-membrane domain at the C-terminus of NTB in the association of proteins containing NTB with the membranes. In agreement with this, analysis of the hydrophobicity profile of NTB-VPg from a comovirus (CPMV) and three other nepoviruses (GFLV, GCMV and TBRV) also revealed the presence of large hydrophobic domains (40 to 50 residues) immediately upstream of the hydrophilic VPg domain (data not shown). The possible role of the putative amphipathic helix at the N-terminus of ToRSV NTB in the membrane-association remains to be determined. The ToRSV-encoded NTB-VPg shares similarities with picornavirus 2C and 3AB proteins (Fig. 3.11A). An amphipathic helix at the N-terminus of the 2C protein was shown to be essential for association of the protein with membranes (Agol *et al.*, 1999; Xiang *et al.*, 1997) and may be the functional equivalent of the putative N-terminal amphipatic helix in the ToRSV NTB domain. It was proposed that membrane association of the picornavirus replication complex is mediated by the 2C and 3AB proteins (Agol *et al.*, 1999; Xiang *et al.*, 1997), possibly in the form of larger 2C and 3AB-containing polyproteins. My results suggest that the NTB protein (as a mature protein or as a larger polyprotein) acts as an anchor for the replication complex. By analogy with the picornavirus proteins, we suggest a model in which NTB-VPg (and NTB) is attached to the membranes by both termini (Fig. 3.11B) with its central portion exposed to the cytoplasm and

accessible for protein-protein interactions with other viral (or plant) proteins. Further investigation of protein-protein interactions involved in ToRSV RNA replication should be helpful in defining the mechanism of replication complex assembly.

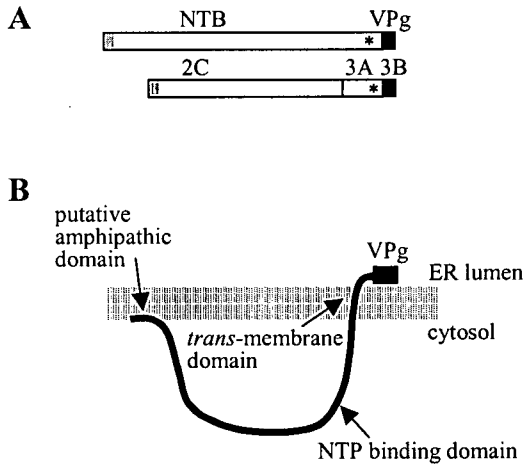


**Fig. 3.11 Model for the topology of NTB-VPg.**
(A) Schematic diagram of picornavirus 2C-3A-3B and ToRSV NTB-VPg. The light grey square, the asterisk and the black square represent the putative amphipathic α-helix, the *trans*-membrane domain and the VPg, respectively. (B) Model for the topology of ToRSV NTB-VPg. The N-terminal putative amphipathic α-helix is partly buried within membranes. The C-terminal *trans*-membrane domain spans the membrane once and VPg is buried within the ER lumen. The central part of NTB is exposed to the cytoplasmic face of the membranes.

# CHAPTER 4

# CHARACTERIZATION OF NTB-VPG MEMBRANE ASSOCIATION *IN VITRO* AND IN PROTOPLASTS.

## 4.1 Introduction

I have shown in the previous chapter that ToRSV proteins containing the NTB are associated with membranes derived from the ER in infected plants. The proteinase K digestion experiment revealed that a fragment containing VPg and the hydrophobic domain at the C-terminus of NTB is embedded in the membranes while the middle portion of the NTB domain is exposed to the cytoplasmic face. This result implied that NTB-VPg is a transmembrane protein with the VPg domain present on the lumenal face of the membranes, which raises the possibility that NTB-VPg is subject to modifications in the ER. After a protein is targeted to the ER membranes, two early events may occur in the transport process: the cleavage of signal peptides by the signal peptidase complex (SPC) and the addition of core oligosaccharides to Asn-X-Ser/Thr acceptor tripeptides by oligosaccharyltransferase (OST) (Dalbey *et al.*, 1997). Since the OST is an ER integral membrane protein and its active site faces the ER lumen, N-linked glycosylation generally indicates a lumenal location of at least the glycan attachment site (Doms *et al*, 1993). Therefore, introducing a consensus glycosylation site (NXT) has been extensively used for mapping protein topology in the membranes (Hasler *et al.*, 2000). Computer-assisted analysis of the NTB-VPg sequence deduced from the published sequence (Rott *et al.*, 1995) revealed that there was a glycosylation consensus sequence (N-M-T) on the VPg sequence. Amino acid sequence deduced from the nucleotide sequence of several isolates revealed that the glycosylation consensus (N-M-T) was conserved on the VPg sequence (Wang

and Sanfacon, 2000b). Surprisingly, direct microsequencing of the VPg protein linked to genomic RNA purified from virus particles revealed that there was a replacement of Thr (T) with an Ala (A) in the glycosylation consensus N-M-T (Wang, Ph.D thesis; Wang *et al.*, 1999). We do not have an explanation for this discrepancy yet. However, the glycosylation site in the VPg can be used as a convenient reference point for the study of the NTB-VPg topology in membranes.

ToRSV RNA1 encodes polyprotein P1. The P1 is cleaved into mature viral proteins and intermediate precursors. To study whether the NTB-VPg could associate with membrane on its own, canine pancreatic microsomal membranes were used for an *in vitro* membrane assay. Commercial microsomes have been isolated free from contaminating membrane fractions and stripped of endogenous membrane-bound ribosomes and mRNA. Microsomal membranes are ER-enriched microsomal vesicles and are widely used to study membrane-induced modifications such as signal peptide cleavage, membrane insertion, and glycosylation.

NTB-VPg and a truncated protein (cNTB-VPg) containing only the C-terminal half of the NTB domain followed by the entire VPg were analyzed (Wang, Ph.D thesis). Since cNTB-VPg (36 kDa) is smaller than NTB-VPg (70 kDa), it is easier to visualize any membrane-dependent modifications of the protein. Translation of plasmid pT7-cNTB-VPg in the presence of canine microsomal membranes resulted in the production of these additional proteins (39 kDa, 30 kDa and 9 kDa), in addition to the 36 kDa protein (cNTB-VPg). The 39 kDa protein was not produced from translation of a mutated derivative of plasmid pT7-cNTB-VPg in which the conserved T was replaced by an A in the VPg glycosylation site. A deglycosylation assay confirmed that the 39 kDa product is a glycosylated c-NTB-VPg protein in which the VPg domain is glycosylated at a consensus N-glycosylation site in the presence of microsomal

membranes (Wang, Ph.D thesis). Sequence analysis of the C-terminus of the NTB domain using the Signal P prediction program (Nilsson *et al.*, 1997) revealed that the NTB contains a cleavable signal sequence at its C-terminus (Fig. 4.1. A). Indeed, the predicted signal sequence contains a few positively charged amino acids, a hydrophobic sequence and a polar region. A (Alanine) is in position -1and M (Methionine) in position -3 upstream of the putative cleavage site. This raises the possibility that the 30 kDa and 9 kDa protein may be released from the cNTB-VPg protein by the signal peptidase complex (SPC) *in vitro*.

In this study, I address the following questions. (1) Can we map the position of the proteolytic cleavage of the cNTB-VPg observed *in vitro*? (2) Is the hydrophobic domain at the C-terminus of NTB essential for NTB-VPg membrane association and modifications? (3) Do cNTB-VPg modifications occur in protoplasts?

## 4.2 Results

### 4.2.1 The cNTB-VPg protein is processed by a proteolytic enzyme associated with membranes at a position upstream of the junction between NTB and VPg

To map the position of the membrane-associated proteolytic cleavage of cNTB-VPg observed *in vitro*, immunoprecipitation of the cleaved fragments was conducted using anti-VPg antibodies. Preliminary experiments revealed that anti-VPg antibodies could not immunoprecipitate the glycosylated form of the VPg (results not shown) suggesting that the epitopes recognized by these antibodies were masked by the glycosylation. We therefore performed the immunoprecipitation experiment using the T/A mutant in which glycosylation did not occur. Plasmid pT7-cNTB-VPg (T/A) was translated in the coupled TNT (transcription/translation rabbit reticulocyte system) in the presence and absence of canine

microsomal membranes (Promega) and the products were analyzed on 18% SDS-PAGE. As expected, two additional proteins were produced. The sizes of the proteins correspond to 30 kDa and 6 kDa. The 6 kDa protein was possibly the non-glycosylated form of the 9 kDa cleavage product observed with the wild-type cNTB-VPg and likely contained the VPg domain. To confirm that the 6 kDa protein contains the VPg domain, immunoprecipitation with anti-VPg antibodies was conducted. The VPg antibodies could immunoprecipitate the 36 kDa and 6 kDa proteins but not the 30 kDa protein (Fig. 4.1. C). The size of the small protein suggested that the cleavage occurred at a position 1 to 2 kDa upstream of the junction between the NTB and VPg domain (3 kDa VPg plus 1.6 kDa vector), which is consistent with the predicted signal peptidase cleavage site (Fig. 4.1. A). N-terminal sequencing of the small cleaved fragment containing VPg would be necessary to further define the cleavage site. However, the efficiency of cleavage observed varied from one batch of membranes to another. In recent batches of membranes, the cleavage event, although consistently observed, was less efficient. Unfortunately, the concentration of the small fragment released was too low to allow its purification for N-terminal sequencing.

**Fig. 4.1. The cNTB-VPg protein is processed by a proteolytic enzyme associated with membranes at a position upstream of the junction between NTB and VPg.** (A) Amino acid sequence and estimated position of the predicted cleavable signal sequence at the C-terminus of NTB. The ToRSV P1 polyprotein is shown at the top of the figure. Vertical lines indicate the cleavage sites recognized by the ToRSV protease. The black box represents the VPg coding region and the asterisk represents the putative transmembrane domain in the NTB coding region. The deduced amino acids sequence of the C-terminus of the NTB domain (along with the first amino acid of the VPg domain) is shown. The predicted signal peptidase cleavage site and viral protease NTB-VPg cleavage site are shown with an arrow-head and an arrow, respectively. Positively charged amino acid are indicated as (+). Bold amino acids are hydrophobic amino acids. The amino acids at the predicted -1 and -3 position are underlined. (B) Schematic representation of the proteolytic cleavage at the C-terminal end of the NTB domain. A schematic representation of the cNTB-VPg protein and the predicted cleavage products are shown with the calculated molecular mass of each region of the protein (VS: vector sequence). The horizonal dotted lines represent amino acids from the vector fused in frame with cNTB-VPg. (C) Identification of the two fragments generated by a membrane associated enzyme. *In vitro* transcription-translation of plasmid pT7-cNTB-VPg (T/A) was conducted in the presence (+) of canine microsomal membranes (lanes 2 and 3) or in the absence (-) of canine microsomal membranes (lanes 1 and 4). The translation products were labeled with [$^{35}$S] methionine. The translation products were immunoprecipitated with anti-VPg antibodies. The translation products (lanes 1and 2) and the immunoprecipitated products (lanes 3 and 4) were separated on SDS-PAGE (18% polyacrylamide) and visualized as described in Materials and Methods. The position of the precursor and the cleavage products are indicated on the right side of the gel. Positions of the molecular mass markers are indicated on the left side of the gel.

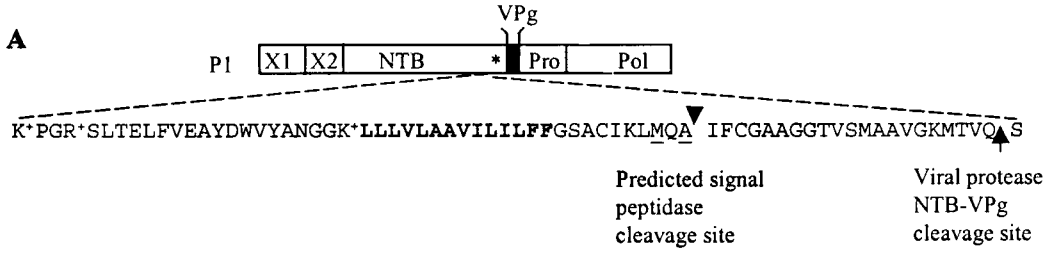
A
VPg
P1
X1
X2
NTB
*
Pro
Pol
K*PGR*SLTELFVEAYDWVYANGGK*LLLVLAAVILILFFGSACIKLMQA IFCGAAGGTVSMAAVGKMTVQ S
Predicted signal peptidase cleavage site
Viral protease NTB-VPg cleavage site

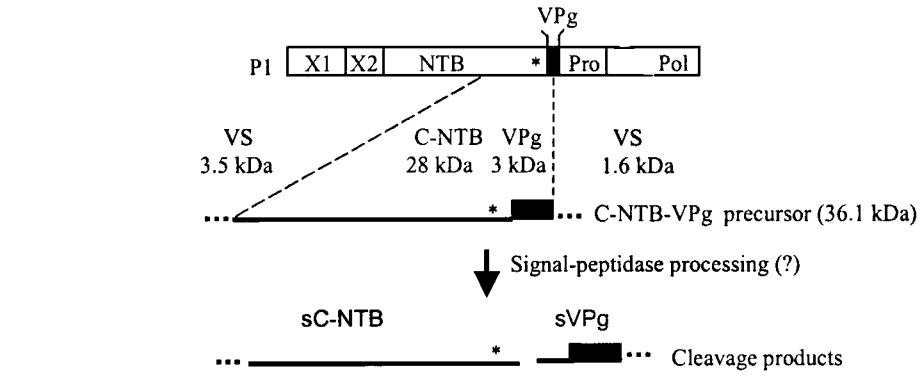
B
VPg
P1
X1
X2
NTB
*
Pro
Pol
VS
3.5 kDa
C-NTB
28 kDa
VPg
3 kDa
VS
1.6 kDa
C-NTB-VPg precursor (36.1 kDa)
Signal-peptidase processing (?)
sC-NTB
sVPg
Cleavage products

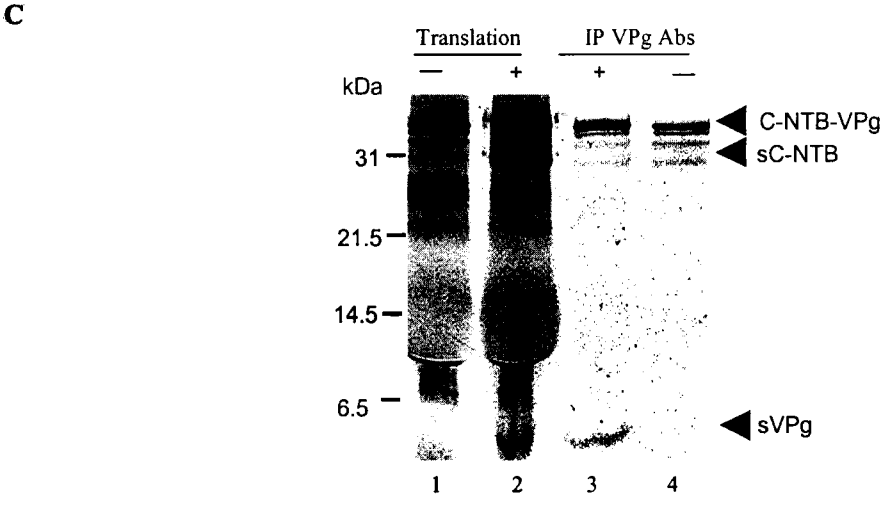
C
Translation
IP VPg Abs
—
+
+
—
kDa
31
21.5
14.5
6.5
C-NTB-VPg
sC-NTB
sVPg
1
2
3
4

### 4.2.2 cNTB-VPg protein associates with microsomal membranes as an integral membrane protein *in vitro*

The results shown above suggest that cNTB-VPg associates with microsomal membranes as an integral membrane protein with VPg on the lumenal side of the membranes. To test the association of cNTB-VPg with membranes directly, I established a membrane association assay. Translation of pT7-cNTB-VPg (T/A mutant) was conducted using a standard rabbit reticulocyte lysate in the presence or absence of membranes. Glycosylation at the consensus glycosylation site at VPg domain of NTB-VPg protein was not expected in this mutant. A 30 kDa product was produced in small amounts in the presence of membranes, in addition to the 36 kDa unmodified cNTB-VPg. Subsequently, membrane-associated materials were separated by centrifugation and resulted in a supernatant (S1) and pellet (P1) containing membrane-associated proteins. The P1 fraction was resuspended in 4M urea, a strong chaotropic agent that extracts peripheral membrane proteins and the solution was clarified by centrifugation to yield supernatant (S2) and pellet (P2). It was anticipated that only integral membrane proteins would remain in the P2 pellet. As shown in Fig. 4.2, the cNTB-VPg protein was found predominantly in the supernatant (S1) when translation was conducted in the absence of microsomal membranes. In contrast, a large portion of the protein remained in the pellet (P2) when translation was done in the presence of microsomal membranes. These results confirm the suggestion that cNTB-VPg associates with microsomal membranes as an integral membrane protein.

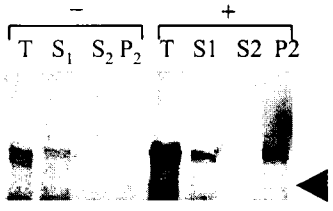


**Fig. 4 .2. cNTB-VPg associates with microsomal membranes.**
[$^{35}$S] methionine-labeled *in vitro* translation of plasmid pT7-cNTB-VPg (T/A) was conducted in the presence (+) or in the absence (-) of canine microsomal membranes. Subsequently, membrane sedimentation analyses were performed as described in the text. Supernatant (S) and pellet fractions (P) were applied in equivalent amounts, separated by SDS-PAGE (12% polyacrylamide) and visualized as described in Materials and Methods. The arrowhead points to the putative cleavage product.

### 4.2.3 Association of NTB-VPg protein with microsomal membranes *in vitro* requires the hydrophobic domain.

To determine the importance of the transmembrane domain in the association of the NTB-VPg protein with cellular membranes, a previously described mutant in which the entire transmembrane domain was deleted from the cNTB-VPg protein, was analyzed using the *in vitro* membrane binding assay (Wang, Ph.D thesis). Translation of cNTB-VPg and of the ΔTMD mutant was conducted using rabbit reticulocyte lysate in the presence (+) or absence (-) of membranes. As described in the previous section, cNTB-VPg was not modified in the absence of membranes. In contrast, cNTB-VPg was glycosylated and processed in the presence of membranes. As shown above, only a small portion of the protein remained in the supernatant (S1) with the majority of the protein present in the P2 fraction. This was specially true for the modified forms of the protein. In contrast, the ΔTMD mutant was not modified and remained mainly in the supernatant (S1) (Fig. 4.3). These results suggest that the transmembrane domain is required for NTB-VPg membrane association and modifications.

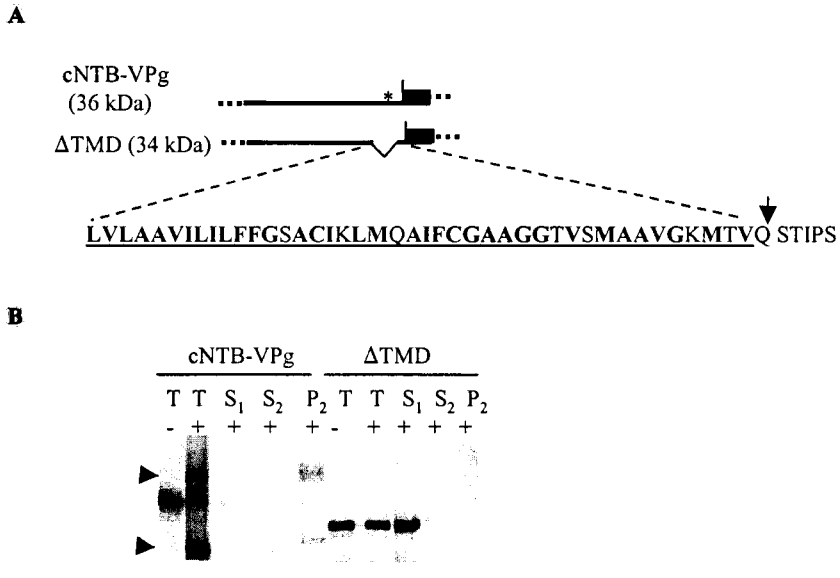


**Fig. 4.3. Association of NTB-VPg protein with microsomal membranes *in vitro* requires a hydrophobic domain.** (A) Schematic representation of the wild type and mutated cNTB-VPg protein which contains a deletion of the entire putative transmembrane domain (TMD). The dotted lines represent amino acids from the vector fused in frame with cNTB-VPg. The black box represents the VPg coding region and the asterisk represents the putative transmembrane domain in the NTB coding region. The amino acid sequence represents the region deleted in the ΔTMD mutant (underlined), the NTB-VPg cleavage site (vertical arrow) and a few amino acids in the VPg sequence. (B) [$^{35}$S] methionine-labeled *in vitro* translation of plasmid pT7-cNTB-VPg and its mutated derivative ΔTMD was conducted in the presence (+) or in the absence (-) of canine microsomal membranes. The modified proteins (glycosylated and processed) are shown by the arrowheads. Subsequently, membrane sedimentation analyses were performed as described in Materials and Methods. The supernatant (S) and pellet (P) fractions were applied in equivalent amounts, separated by SDS-PAGE (12% polyacrylamide) and visualized as described in Materials and Methods.

### 4.2.4 Detection of a putative N-terminal signal-processed protein from cNTB-VPg in protoplasts

Translation of pT7 cNTB-VPg in the presence of membranes resulted in cNTB-VPg glycosylation on the consensus glycosylation site of VPg and cleavage of cNTB-VPg by a membrane-associated enzyme, possibly SPC. I next wanted to determine if these modifications also occur in *vivo*. For this purpose, an expression cassette containing cNTB-VPg was inserted into the polylinker of expression plasmid pBBI525 as described in Materials and Methods (Sun and Sanfaçon, 2001). As controls, plasmids allowing the expression of cNTB-VPg (T/A) and cNTB-VPg ΔTMD *in vivo* were also prepared in the same vector.

The plasmids were transfected into protoplasts which were labeled for 6 h with [$^{35}$S] methionine at 18 h post-transfection. Extracts from transfected and mock-transfected protoplasts were prepared for immunoprecipitation with anti-NTB and anti-VPg antibodies. In mock-transfected protoplasts, a host protein cross-reacted with anti-NTB antibodies and anti-VPg antibodies (Fig. 4.4.C). However, these background bands were very faint. In protoplasts transfected with cNTB-VPg, a protein with an apparent molecular mass of 31kDa, corresponding to the size for the unmodified cNTB-VPg was immunoprecipitated with anti-NTB and anti-VPg antibodies. A protein with a similar size was also immunoprecipitated with both antibodies from extracts of protoplasts transfected with the cNTB-VPg (T/A) mutant. In addition to the cNTB-VPg precursor, a smaller protein with an apparent molecular mass of 26 kDa was detected with anti-NTB antibodies, but not with anti-VPg antibodies (Fig. 4.4.C). This smaller protein was also detected using extracts from protoplast transfected with cNTB-VPg (T/A), in addition to the precursor cNTB-VPg (T/A). The size of the protein was

consistent with the predicted size for a cleavage product released after processing at the putative signal peptidase cleavage site (Fig. 4. 4. C). The additional protein was not detected in extracts from protoplasts transfected with the ΔTMD mutant. Indeed, in the ΔTMD-transfected extracts only a protein of 28 kDa was detected corresponding to the predicted size for the unmodified ΔTMD protein. This suggested that the production of the additional protein depends on the presence of the putative transmembrane domain.

Taken together, these results suggest that the smaller protein detected with anti-NTB antibodies, but not with anti-VPg antibodies in protoplasts transfected with cNTB-VPg may be a cleavage product released after cleavage of cNTB-VPg by a membrane-associated enzyme. To confirm this, it would be useful to detect the other predicted cleavage product containing the VPg domain. Unfortunately, the level of expression was very low and a long exposure (several weeks) was needed to detect the proteins immunoprecipitated by NTB antibodies (Fig. 4.4.C). It would be difficult to detect this small fragment containing the VPg domain. If this protein is indeed released by a SPC enzyme in protoplasts, then I must conclude that the cleavage is very inefficient.

**Fig. 4. 4. Detection of a putative N-terminal signal-processed protein derived from cNTB-VPg in protoplasts**

(A) A schematic representation of the cNTB-VPg protein and of the predicted products of cNTB-VPg cleaved by a SPC is shown with the calculated molecular mass of each region of the protein (VS: vector sequence). The dotted lines represent amino acids from the vector fused in frame with cNTB-VPg. The black box represents the VPg coding region and the asterisk represents the putative transmembrane domain in the NTB coding region. (B) Schematic representation of the wild type and mutated cNTB-VPg proteins with the calculated molecular mass (before modification). The black box represents the VPg coding region. The dotted lines represent amino acids from the vector fused in frame with c-NTB-VPg. The consensus N-glycosylation sequence (NMT) in the VPg sequence is shown by an arrow. The T/A mutant is a replacement of the conserved threonine (T) at the consensus glycosylation site by an alanine (underlined). ΔTMD is a mutated cNTB-VPg protein that contained a deletion of the entire putative transmembrane domain. The underlined amino acids are deleted in ΔTMD. (C) The wild-type (WT) cNTB-VPg, ΔTMD and T/A mutant cloned in a plant expression vector were transfected in protoplasts which were labeled with [$^{35}$S] methionine for 6 h at 18 h post-transfection. The protoplasts were collected and processed for immunoprecipitation with anti-NTB and anti-VPg antibodies. The immunoprecipitated proteins were separated by SDS-PAGE (12% polyacrylamide) and visualized as described in Materials and Method. The additional smaller protein (the putative cleavage product of SPC) is shown by a dot on the right of the lane and by an arrowhead. The position of molecular mass markers is shown on the left side of the gel.

A

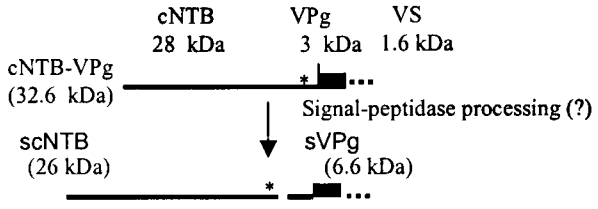
cNTB
28 kDa
VPg
3 kDa
VS
1.6 kDa
cNTB-VPg
(32.6 kDa)
Signal-peptidase processing (?)
scNTB
(26 kDa)
sVPg
(6.6 kDa)

B

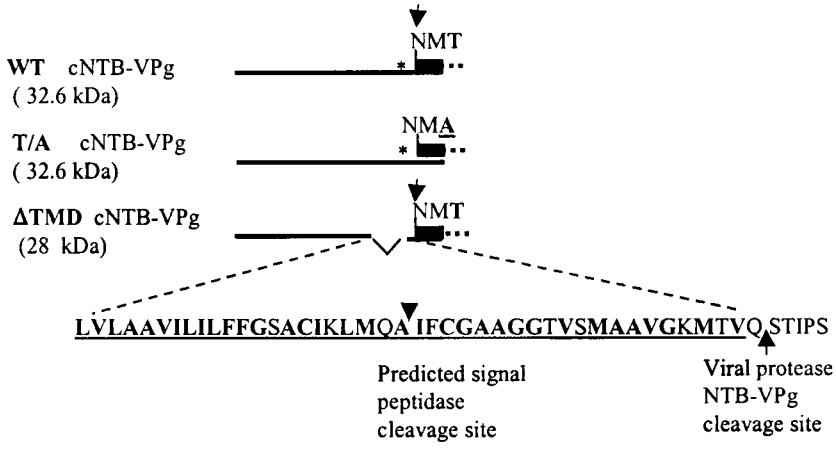
NMT
WT cNTB-VPg
( 32.6 kDa)
NMA
T/A cNTB-VPg
( 32.6 kDa)
NMT
ΔTMD cNTB-VPg
(28 kDa)
LVLAAVILILFFGSACIKLMQAIFCGAAGGTVSMAAVGKMTVQSTIPS
Predicted signal
peptidase
cleavage site
Viral protease
NTB-VPg
cleavage site

C

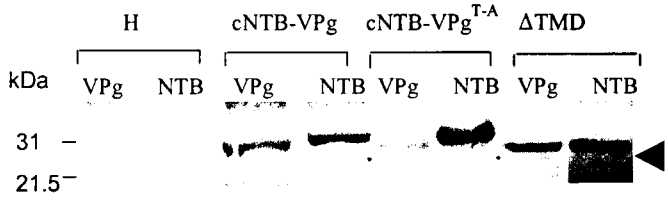
H
cNTB-VPg
cNTB-VPg T-A
ΔTMD
kDa
VPg
NTB
VPg
NTB
VPg
NTB
VPg
NTB
31
21.5

## 4.3 Discussion

The studies in the previous chapter implied that NTB-VPg is a transmembrane protein with the hydrophobic domain at the C-terminus of NTB embedded in the membranes and the VPg domain present on the lumenal face of the membranes. In this chapter, I have further studied how NTB-VPg associates with membranes. I have utilized a rabbit reticulocyte system and protoplasts to study membrane protein integration and processing. I focused my analysis on the role of the transmembrane domain and only C-terminal segments of the NTB-VPg protein (cNTB-VPg) were used in these experiments. In this study, I have shown that (i) NTB-VPg associates with membranes independently; (ii) the C-terminal fragment containing the transmembrane domain is sufficient for membrane association; (iii) the transmembrane domain is essential for membrane association; (iv) cNTB-VPg modifications *in vitro* (i.e., glycosylation in the VPg domain) suggest a topology similar to that observed in infected plants.

Translation of pT7-cNTB-VPg and pT7-NTB-VPg *in vitro* in the presence of microsomal membranes resulted in glycosylation at the consensus glycosylation site in the VPg domain of cNTB-VPg (Fig. 4.3 and data not shown). In contrast, transient expression of cNTB-VPg in protoplasts did not show cNTB-VPg glycosylation (i.e. the size of the wild-type protein is identical to that of the glycosylation mutant (T/A) suggesting that glycosylation did not occur). The reasons for this discrepancy are not known yet.

One possible explanation may be that the consensus glycosylation site in cNTB-VPg is not accessible to the OST in protoplasts. Possibly, canine microsomal membranes are different from plant ER-derived membranes. Recent experiments have shown that membrane phospholipid composition has a strong effect on topology of polytopic membrane proteins, suggesting membrane proteins may have different topologies and protein modifications *in vitro*

in the presence of canine microsomal membranes than in plants (Bogdanov, *et al.*, 2002). Efficient glycosylation requires a minimal distance (defined as the number of amino acids) between the C-terminal end of the transmembrane domain and the first Asn (Asn-X-Thr/Ser). This minimum distance has been shown to differ in experiments performed in *vitro* and *in vivo* (Haseler *et al.*, 2000). Discrepancies between *in vitro* and *in vivo* results were also documented for PV3A and 3AB (Datta and Dasgupta, 1994). A fraction of 3A and 3AB was glycosylated at a consensus N-glycosylation site amino terminal to the 3A hydrophobic domain when translated *in vitro* in the presence of microsomal membranes. However, protease sensitivity experiments on membrane extracts of infected cells demonstrated that the N-terminus of 3AB was cytoplasmic. Moreover, glycosylated forms of 3A and 3AB were not detected in extracts of *Poliovirus*-infected cells.

Alternatively, glycosylation may occur in protoplasts, but was not detected. One possibility is that the glycosylation efficiency of cNTB-VPg in protoplasts was too low to distinguish the glycosylated form from the unglycosylated form. The degree of protein glycosylation is probably determined by host factors such as the activity of glycosyl transferase. For example, differential glycosylation has been observed in prion protein expressed in different cells (Schroder et al., 1999). Another possibility is that the glycosylation at the consensus glycosylation site in the VPg of cNTB-VPg is coupled with the cleavage of cNTB-VPg by a membrane-associated enzyme *in vivo*. The cleaved glycosylated product containing the VPg domain would be too small to be detected on the SDS-PAGE (12% polyacrylamide) and would probably be present in very small amounts. Finally, it is possible that the glycosylated form of cNTB-VPg was excreted through the secretory pathway or degraded.

cNTB-VPg was cleaved by a membrane-associated enzyme (probably the SPC) *in vitro* and possibly *in vivo*. It would be important to determine whether signal processing also occurs on the full-length NTB-VPg. Indeed, removal of the cytoplasmic N-terminal tail may lead to a repositioning of the transmembrane domain and may have effects on signal processing (Hasler *et al.*, 2000). For example, N-terminal truncation of a membrane protein leads to exposure of a cryptic signal peptidase cleavage site present in the transmembrane domain (Hasler *et al.*, 2000). I have attempted to detect cleavage products of the full-length NTB-VPg protein. Unfortunately, several background proteins were found (presumably produced by internal initiation or premature termination) in the *in vitro* translation products even when translations were conducted in the absence of membranes. These background proteins are similar in size to the predicted size for cleaved products produced by SPC and it was therefore not possible to determine whether membrane-associated processing of NTB-VPg occurred *in vitro*, in spite of repeated attempts. Equally, I do not have evidence to determine whether signal processing of NTB-VPg occurs *in vivo*. In the previous chapter, I have shown that the mature NTB is detected in infected plants. The putative SPC cleavage site is very close to the viral proteinase cleavage site. Therefore, the mature NTB could be produced by a cleavage event conducted by either the putative SPC or the ToRSV 3C-like proteinase.

In summary, the data presented here are consistent with a model that NTB-VPg is a transmembrane protein with VPg domain present on the lumenal face of the membranes. Further experiments will need to be conducted to determine if NTB-VPg modifications occur in infected plants and to examine the mechanism by which NTB-VPg is targeted to ER-derived membranes.

# CHAPTER 5

## SUMMARY AND FUTURE PROJECT

In this thesis, I have characterized the membrane association of NTB containing viral proteins using extracts from ToRSV-infected plants (Chapter 3) and using a rabbit reticulocyte system with canine microsomal membranes and protoplasts (Chapter 4). The proteins containing the NTB domain cofractionated with markers of the ER and with ToRSV-specific RdRp activity in sucrose gradients. ToRSV induced severe changes in the morphology of the ER, and proteins containing the NTB domain were localized at the ER. The proteinase K protection assay using membrane fractions from ToRSV infected plants revealed that a fragment containing the VPg and the hydrophobic domain at the C-terminus of NTB is embeded in the membranes while the middle portion of the NTB domain is exposed to the cytoplasmic face. This implies that a putative transmembrane is involved in membrane association and results in VPg present at the lumenal face. *In vitro* membrane binding assay revealed that a C-terminal fragment of cNTB-VPg containing the putative transmembrane domain can associate with membranes. The putative transmembrane domain of the NTB is required for the cNTB-VPg membrane association. An *In vitro* glycosylation at the consensus glycosylation site in the VPg domain of NTB-VPg suggests a lumenal location for the VPg. This is in agreement with the results from infected plants. Taken together, my results provide evidence that proteins containing the NTB domain are transmembrane proteins associated with ER-derived membranes, and probably act as anchors for the replication compex.

Although my results have provided important information for understanding of the mechanisms employed by nepoviruses to assemble their replication complex on ER membranes, several important questions were also raised by this study. In the following sections, I will discuss these questions and possible future research projects aimed at addressing these questions

My results indicate that NTB-VPg or cNTB-VPg can associate with membranes *in vitro*. I have not determined whether these proteins could properly localize to the ER in plants. In Chapter 4, cNTB-VPg was expressed in protoplasts in a plant transient expression vector. Unfortunately, the level of expression was very low and a long exposure (several weeks) was needed to detect the proteins immunoprecipitated by the antibodies. To improve transfection efficiency and the level of protein expression, expression of individual viral proteins in the virus vector *(Potato virus X)* may be a good alternative. Using this approach, I could express NTB-VPg in ER-GFP plants and determine the subcellular localization of the expressed NTB-VPg using subcellular fractionation or immunostaining. If successful, I could then introduce mutations to further identify important regions of the NTB-VPg involved in proper ER targeting (see below). If increased expression levels are obtained, immunoprecipitation experiments could be conducted to further investigate possible modifications of NTB-VPg in *vivo*. I have determined that the transmembrane domain is important. However, I have not studied the potential role of a putative amphipathic helix at the N-terminus of NTB. To see if the putative amphipathic helix is involved in membrane association, at least two mutants should be made. In the first mutant, the transmembrane domain at the C-terminus of the NTB-VPg would be deleted. In the second mutant, the putative amphipathic helix and the putative transmembrane domain would be deleted. Expression of wild-type NTB-VPg, mutant 1 and mutant 2 in ER-GFP plants and analysis of the result with the two approaches mentioned above would reveal if the putative amphipathic helix is important for the membrane association. Such mutants could also be analyzed in the *in vitro* membrane association assay.

In sucrose gradients of homogenates of ToRSV-infected cells, my results indicate that the RdRp activity co-fractionates with ER-derived membranes. However, the active RdRp fraction may contain other membranes as well. To further confirm that the RdRp activity is located at the

ER membranes, the following approaches could be used: (i) immunoblotting using fractions from sucrose gradient with antibodies against other subcellular markers, such as markers from the chloroplasts, vacuoles and mitochondria; (2) labeling of the newly synthesized viral RNA with BrUTP (Sigma) in the presence of actinomycin D (an inhibitor for host transcription) in viral RNA infected ER-GFP protoplasts. (iii) detection of the double-stranded RNA (ds RNA) with antibodies against the double stranded RNA in viral RNA infected ER-GFP protoplasts. Immunostaining using anti-BrdU antibodies (Sigma) or anti-ds RNA antibodies can reveal if replication takes place at ER. In both cases, I would then examine whether the labeled RNA colocalizes with ER-GFP.

My results indicate that the VPg is buried in the ER lumen, but do not exclude the possibility that alternative conformations of the NTB-VPg or different precursors containing VPg in the cytoplasm may exist. To see if some of the population is also found on the cytoplasmic face of the membranes, sequence-specific antibody binding could be performed. Proteins with epitopes exposed to the outside of membranes can react to antibodies without addition of mild detergent to disrupt the membranes. In contrast, proteins with epitopes hidden inside the membranes cannot be recognized by antibodies without addition of detergent (Grgacic *et al.,* 2000). Therefore, immunoprecipitation in the presence or absence of detergent and immunoblot with anti-VPg Abs may show if the epitopes of the protein are inside or outside of the membranes, providing important information on possible alternative topology of the protein. Alternatively, in an attempt to visualize if there is VPg exposed to the cytoplasmic face, immunocytochemistry coupled with electron microscopy (IEM) could be used to observe vesicles. Formvar-coated electron microscopic grids would be first coated with affinity immunopurified anti-VPg Abs and then floated on aliquots of ER-enriched fractions. The bound material would be fixed and visualized with EM as described for another nepovirus (Rizenthaler *et al.*, 2002).

As mentioned above, ToRSV P1 contains the domains for proteins likely to be involved in replication including the NTB, VPg, Pro and Pol. These proteins may be brought to the membrane-associated complex as a polyprotein containing the NTB domain. Alternatively, these proteins may be brought to the membranes through protein-protein interactions. Even if viral proteins are initially brought to the membranes as large polyproteins, protein-protein interactions may be important to stabilize the complex. A few approaches, such as co-fractionation, co-immunoprecipitation and colocalization and the yeast two-hybrid system could be used to characterize these protein-protein interactions.

## REFERENCES

**Agol VI, Paul AV, Wimmer E.** 1999. Paradoxes of the replication of picornaviral genomes. Virus Res. **62:** 129-247.

**Ahlquist P.** 2002. RNA-dependent RNA polymerases, viruses, and RNA silencing. Science **296:** 1270-1273.

**Ahola T, Kujala P, Tuittila M, Blom T, Laakkonen P, Hinkkanen A, Auvinen P.** 2000. Effects of palmitoylation of replicase protein nsP1 on alphavirus infection. J. Virol. **74:** 6725-6733.

**Ahola T, Lampio A, Auvinen P, Kaariainen L.** 1999. Semliki Forest virus mRNA capping enzyme requires association with anionic membrane phospholipids for activity. EMBO J. **18:** 3164-3172.

**Allaire M, Chernaia MM, Malcolm BA, James MN.** 1994. Picornaviral 3C cysteine proteinases have a fold similar to chymotrypsin-like serine proteinases. Nature **369:** 72-6.

**Andino R, Boddeker N, Silvera D, Gamarnik AV.** 1999. Intracellular determinants of picornavirus replication. Trends Microbiol. **7:** 76-82.

**Andino R, Rieckhof GE, Achacoso PL, Baltimore D.** 1993. Poliovirus RNA synthesis utilizes an RNP complex formed around the 5'-end of viral RNA. EMBO J. **12:** 3587-3598.

**Andino R, Rieckhof GE, Baltimore D.** 1990. A functional ribonucleoprotein complex forms around the 5' end of poliovirus RNA. Cell **63:** 369-80.

**Banerjee R, Dasgupta A.** 2001. Specific interaction of hepatitis C virus protease/helicase NS3 with the 3'-terminal sequences of viral positive- and negative-strand RNA. J. Virol. **75:** 1708-21

**Banerjee R, Tsai W, Kim W, Dasgupta A.** 2001. Interaction of poliovirus-encoded 2C/2BC polypeptides with the 3' terminus negative-strand cloverleaf requires an intact stem-loop b. Virology **280:** 41-51.

**Barton DJ, Black EP, Flanegan JB.** 1995. Complete replication of poliovirus in vitro: Preinitiation RNA replication complexes require soluble cellular factors for the synthesis of VPg-linked RNA. J. Virol. **69:** 5516-5527.

**Barton DJ, Morasco BJ, Flanegan JB.** 1999. Translating ribosomes inhibit poliovirus negative-strand RNA synthesis. J. Virol. **73:** 10104-10112.

**Belin C, Schmitt C, Gaire F, Walter B, Demangeat G, Pinck L.** 1999. The nine C-terminal residues of the grapevine fanleaf nepovirus movement protein are critical for systemic virus spread. J. Gen. Virol. **80:** 1347-1356.

**Belsham GJ, Sonenberg N.** 1996. RNA-protein interactions in regulation of picornavirus RNA translation. Microbiol. Rev. **60:** 499-511.

**Bogdanov M, Heacock PN, Dowhan W.** 2002. A polytopic membrane protein displays a eversible topology dependent on membrane lipid composition. EMBO J. **21:** 2107-2116.

**Bordier C.** 1981. Phase separation of integral membrane proteins in Triton X-114 solution. J. Biol. Chem. **256:** 1604-1607.

**Borman AM, Deliat FG, Kean KM.** 1994. Sequences within the poliovirus internal ribosome entry segment control viral RNA synthesis. EMBO J. **13:** 3149-3157.

**Bradshaw RA.** 1989. Protein translocation and turnover in eukaryotic cells. Trends Biochem. Sci. **14:** 276-279.

**Brass V, Bieck E, Montserret R, Wolk B, Hellings JA, Blum HE, Penin F, Moradpour D.** 2002. An amino-terminal amphipathic alpha-helix mediates membrane association of the hepatitis C virus nonstructural protein 5A. J. Biol. Chem. **277:** 8130-8139.

**Brinton MA.** 2002. The molecular biology of west nile virus: A New Invader of the Western Hemisphere. Annu. Rev. Microbiol. **56:** 371-402.

**Buck KW.** 1996. Comparison of the replication of positive-stranded RNA viruses of plants and animals. Adv. Virus Res. **47:** 159-251.

**Bushell M, Sarnow P.** 2002. Hijacking the translation apparatus by RNA viruses. J. Cell. Biol. **158:** 395-9.

**Bustamante P, Hull R.** 1998. Plant virus gene expression strategies. Electronic Journal of Biotechnology.

**Carette JE, Guhl K, Wellink J, Van Kammen A.** 2002. Coalescence of the sites of cowpea mosaic virus RNA replication into a cytopathic structure. J. Virol. **76:** 6235-6243.

**Carette JE, Kujawa A, Guhl K, Verver J, Wellink J, Van Kammen A.** 2001. Mutational analysis of the genome-linked protein of cowpea mosaic virus. Virology **290:** 21-29.

**Carette JE, Stuiver M, Van Lent J, Wellink J, Van Kammen A .** 2000. Cowpea mosaic virus infection induces a massive proliferation of endoplasmic reticulum but not Golgi membranes and is dependent on *de novo* membrane synthesis. J. Virol. **74:** 6556-6563.

**Carette JE, Van Lent J, MacFarlane SA, Wellink J, Van Kammen A.** 2002. Cowpea mosaic virus 32- and 60-kilodalton replication proteins target and change the morphology of endoplasmic reticulum membranes. J. Virol. **76:** 6293-6301.

**Carette JE, Verver J, Martens J, Van Kampen T, Wellink J, Van Kammen A.** 2002. Characterization of plant proteins that interact with cowpea mosaic virus '60K' protein in the yeast two-hybrid system. J. Gen. Virol. **83:** 885-893.

**Carrier K, Hans F, Sanfaçon H.** 1999. Mutagenesis of amino acids at two tomato ringspot nepovirus cleavage sites: Effect on proteolytic processing *in cis* and *in trans* by the 3C-like protease. Virology **258:** 161-175.

**Carrier K, Xiang Y, Sanfaçon H.** 2001. Genomic organization of RNA2 of Tomato ringspot virus: processing at a third cleavage site in the N-terminal region of the polyprotein in vitro. J. Gen. Virol. **82:** 1785-1790.

**Carrington JC, Dougherty WG.** 1988. A viral cleavage site cassette: identification of amino acid sequences required for tobacco etch virus polyprotein processing. Proc. Natl. Acad. Sci.USA **85:** 3391-3395.

**Carrington JC, Freed DD.** 1990. Cap-independent enhancement of translation by a plant potyvirus 5' nontranslated region. J. Virol. **64:** 1590-1597.

**Carrington JC, Freed DD, Leinicke AJ.** 1991. Bipartite signal sequence mediates nuclear translocation of the plant potyviral NIa protein. Plant Cell. **3:** 953-962.

**Carrington JC, Freed DD, Oh CS.** 1990. Expression of potyviral polyproteins in transgenic plants reveals three proteolytic activities required for complete processing. EMBO J. **9:** 1347-1353.

**Carrington JC, Haldeman R, Dolja VV, Restrepo-Hartwig MA.** 1993. Internal cleavage and trans-proteolytic activities of the VPg-proteinase (NIa) of tobacco etch potyvirus in vivo. J. Virol. **67:** 6995-7000.

**Caruthers JM, McKay DB.** 2002. Helicase structure and mechanism. Curr. Opin. Struct. Biol. **12:** 123-33.

**Chen J, Ahlquist P.** 2000. Brome mosaic virus polymerase-like protein 2a is directed to the endoplasmic reticulum by helicase-like viral protein 1a. J. Virol. **74:** 4310-4318.

**Chen J, Noueiry A, Ahlquist P.** 2001. Brome mosaic virus Protein 1a recruits viral RNA2 to RNA replication through a 5' proximal RNA2 signal. J. Virol. **75:** 3207-3219.

**Chisholm J, Wieczorek A, Sanfaçon H.** 2001. Expression and partial purification of

recombinant tomato ringspot nepovirus 3C-like proteinase: comparison of the activity of the mature proteinase and the VPg-proteinase precursor. Virus Res. **79:** 153-164

**Cho MW, Teterina N, Egger D, Bienz K, Ehrenfeld E.** 1994. Membrane rearrangement and vesicle induction by recombinant poliovirus 2C and 2BC in human cells. Virology. **202:** 129-145.

**Clum S, Ebner KE, Padmanabhan R.** 1997. Cotranslational membrane insertion of the serine proteinase precursor NS2B-NS3(Pro) of dengue virus type 2 is required for efficient in vitro processing and is mediated through the hydrophobic regions of NS2B. J. Biol. Chem. **272:** 30715-30723.

**Cocquerel L, Wychowski C, Minner F, Penin F, Dubuisson J.** 2000. Charged residues in the transmembrane domains of hepatitis C virus glycoproteins play a major role in the processing, subcellular localization, and assembly of these envelope proteins. J. Virol. **74:** 3623-3633.

**Combet C, Blanchet C, Geourjon C, Deleage G.** 2000. NPS@: network protein sequence analysis (http://npsa-pbil.ibcp.fr/cgi-bin/npsa) Trends Biochem. Sci. **25:** 147-150.

**Cornell CT, Semler BL.** 2002. Subdomain specific functions of the RNA polymerase region of poliovirus 3CD polypeptide. Virology **298:** 200-213.

**Crawford NM, Baltimore D.** 1983. Genome-linked protein VPg of poliovirus is present as free VPg and VPg-pUpU in poliovirus-infected cells. Proc. Natl. Acad. Sci. USA **80:** 7452-7455.

**Dalbey RE, Lively MO, Bron S, Van Dijl JM.** 1997. The chemistry and enzymology of the type I signal peptidases. Protein Sci. **6:** 1129-1138.

**Daros JA, Carrington JC.** 1997. RNA binding activity of NIa proteinase of tobacco etch potyvirus. Virology **237:** 327-336.

**Das S, Dasgupta A.** 1993. Identification of the cleavage site and determinants required for poliovirus 3C $^{Pro}$-catalyzed cleavage of human TATA-binding transcription factor TBP. J. Virol. **67:** 3326-3331.

**Daros JA, Schaad MC, Carrington JC.** 1999. Functional analysis of the interaction between VPg-proteinase (NIa) and RNA polymerase (NIb) of tobacco etch potyvirus, using conditional and suppressor mutants. J. Virol. **73:** 8732-8740.

**Datta U, Dasgupta A.** 1994. Expression and subcellular localization of poliovirus VPg-precursor protein 3AB in eukaryotic cells: evidence for glycosylation *in vitro*. J Virol. **68:** 4468-4477.

**Demangeat G, Hemmer O, Reinbolt J, Mayo MA, Fritsch C.** 1992. Virus-specific proteins in cells infected with tomato black ring nepovirus: evidence for proteolytic processing *in vivo*. J. Gen. Virol. **73:** 1609-1614.

**Den Boon JA, Chen J, Ahlquist P.** 2001. Identification of sequences in *Brome mosaic virus* replicase protein 1a that mediate association with endoplasmic reticulum membranes. J. Virol. **75:** 12370-12381.

**Diez J, Ishikawa M, Kaido M, Ahlquist P.** 2000. Identification and characterization of a host protein required for efficient template selection in viral RNA replication. Proc. Natl. Acad. Sci. USA **97:** 3913-3918.

**Doedens JR, Giddings THJr, Kirkegaard K.** 1997. Inhibition of endoplasmic reticulum-to-Golgi traffic by poliovirus protein 3A: genetic and ultrastructural analysis. J. Virol. **71:** 9054-9064.

**Doedens JR, Kirkegaard K.** 1995. Inhibition of cellular protein secretion by poliovirus proteins 2B and 3A. EMBO J. **14:** 894-907.

**Doms RW, Lamb RA, Rose JK, Helenius A.** 1993. Folding and assembly of viral membrane proteins. Virology **193:** 545-562.

**Duggal R, Rao AL, Hall TC.** 1992. Unique nucleotide differences in the conserved 3' termini of brome mosaic virus RNAs are maintained through their optimization of genome replication. Virology **187:** 261-270.

**Eastwell KC, Bernardy MG.** 1996. Association of high molecular weight double-strand RNA with little cherry disease. Can. J. Plant Path. **18:** 203-208.

**Eggen R, Kaan A, Goldbach R, Van Kammen A.** 1988. Cowpea mosaic virus RNA replication in crude membrane fractions from infected cowpea and *Chenopodium amaranticolor*. J. Gen. Virol. **69:** 2711-2720.

**Egger D, Pasamontes L, Bolten R, Boyko V, Bienz K.** 1996. Reversible dissociation of the poliovirus replication complex: functions and interactions of its components in viral RNA synthesis. J. Virol. **70:** 8675-8683.

**Egger D, Teterina N, Ehrenfeld E, Bienz K.** 2000. Formation of the poliovirus replication complex requires coupled viral translation, vesicle production and viral RNA synthesis. J. Virol. **74:** 6570-6580.

**Epel BL.** 1994. Plasmodesmata: composition, structure and trafficking. Plant Mol. Biol. **26:** 1343-1356.

**Failla C, Tomei L, De Francesco R.** 1994. Both NS3 and NS4A are required for proteolytic processing of hepatitis C virus nonstructural proteins. J. Virol. **68:** 3753-3560.

**Fernandez A, Garcia JA.** 1996. The RNA helicase CI from plum pox potyvirus has two regions involved in binding to RNA. FEBS Lett. **388:** 206-210.

**Fernandez A, Lain S, Garcia JA.** 1995. RNA helicase activity of the plum pox potyvirus CI protein expressed in *Escherichia coli*. Mapping of an RNA binding domain. Nucleic Acids Res. **23:** 1327-1332.

**Francki RIB, Milne RG, Hatta T.** 1985. Nepovirus Group, p. 23-38. *In* Atlas of plant Viruses, Vol. II, CRC Press Inc., Boca Raton, Fla.

**Fujiki YA, Hubbard S, Fowler S, Lazarow PB.** 1982. Isolation of intracellular membranes by means of sodium carbonate treatment: application to endoplasmic reticulum. J. Cell Biol. **93:** 97-102.

**Fulton AB.** 1982. How crowded is the cytoplasm? Cell **30:** 345-357.

**Gaire F, Schmitt C, Stussi-Garaud C, Pinck L, Ritzenthaler C.**. 1999. Protein 2A of grapevine fanleaf nepovirus is implicated in RNA2 replication and colocalizes to the replication site. Virology **264:** 25-36.

**Gallie DR.** 2001. Cap-independent translation conferred by the 5' leader of tobacco etch virus is eukaryotic initiation factor 4G dependent. J.Virol. **75:** 12141-12152.

**Gamarnik AV, Andino R.** 1998. Switch from translation to RNA replication in a positive-stranded RNA virus. Genes Dev. **12:** 2293-2304.

**Goldbach R, Wellink J.** 1996. Comoviruses. Molecular Biology and Replication. p. 35-76. *In* B. D. Harrison and A .F. Murant (ed.), The plant viruses. Polyhedral virions and bipartite RNA genomes. Plenum, New York.

**Goldbach R, Wellink J, Verver J, Van Kammen A, Kasteel D, Van Lent J.** 1994. Adaptation of positive-strand RNA viruses to plants. Arch Virol Suppl **9:** 87-97.

**Gorbalenya AE, Koonin EV.** 1989. Viral proteins containing the purine NTP-binding sequence pattern. Nucl. Acids Res. **17:** 8413-8440.

**Gorbalenya AE, Koonin EV, Donchenko AP, Blinov VM.** 1988. A novel superfamily of nucleoside triphosphate-binding motif containing proteins which are probably involved in duplex unwinding in DNA and RNA replication and recombination. FEBS Lett **235:** 16-24.

**Gorbalenya AE, Koonin EV, Wolf YI.** 1990. A new superfamily of putative NTP-binding domains encoded by genomes of small DNA and RNA viruses. FEBS Lett. **262:** 145-148.

**Gosert R, Kanjanahaluethai A, Egger D, Bienz K, Baker SC.** 2002. RNA replication of mouse hepatitis virus takes place at double-membrane vesicles. J. Virol. **76:** 3697-3708.

**Hans F, Sanfaçon H.** 1995. Tomato ringspot nepovirus protease: characterization and cleavage site specificity. J. Gen. Virol. **76:** 917-927.

**Harris KS, Reddigari SR, Nicklin MJ, Hammerle T, Wimmer E.** 1992. Purification and characterization of poliovirus polypeptide 3CD, a proteinase and a precursor for RNA polymerase. J. Virol. **66:** 7481-7489.

**Haseloff J, Siemering KR, Prasher DC, Hodge S.** 1997. Removal of a cryptic intron and subcellular localization of green fluorescent protein are required to mark transgenic Arabidopsis plants brightly. Proc. Natl. Acad. Sci. U S A. **94:** 2122-2127.

**Hasler U, Greasley PJ, Von Heijne G, Geering K.** 2000. Determinants of topogenesis and glycosylation of type II membrane proteins. Analysis of Na,K-ATPase beta 1 and beta 3 subunits by glycosylation mapping. J.
Biol. Chem. **275:** 29011-22.

**Hemmer O, Greif C, Dufourcq P, Reinbolt J, Fritsch C.** 1995. Functional characterization of the proteolytic activity of the tomato black ring nepovirus RNA-1-encoded polyprotein. Virology **206:** 362-71.

**Howell KE, Palade GF.** 1982. Hepatic Golgi fractions resolved into membrane and content subfractions. J. Cell. Biol. **92:** 822-832.

**Jennings ML.** 1989. Topography of membrane proteins. Annu. Rev. Biochem. **58:** 999-1027.

**Joachims M, Van Breugel PC, Lloyd RE.** 1999. Cleavage of poly(A)-binding protein by enterovirus proteases concurrent with inhibition of translation in vitro. J. Virol. **73:** 718-27.

**Koonin EV, Dolja VV.** 1993. Evolution and taxonomy of positive-strand RNA viruses: implications of comparative analysis of amino acid sequences. Crit. Rev. Biochem.Mol. Biol. **28:** 375-430.

**Krausslich HG, Nicklin MJH, Toyoda H, Etchison D, and Wimmer E.** 1987. Poliovirus proteinase 2A induces cleavage of eukaryotic initiation factor 4F polypeptide p220. J. Virol. **61:** 2711-2718.

**Krogh A, Larsson B, Von Heijne G, and Sonnhammer ELL** 2001. Predicting transmembrane protein topology with a hidden Markov model: Application to complete genomes. J. Mol. Biol. **305:** 567-580.

**Kujala P, Ikaheimonen A, Ehsani N, Vihinen H, Auvinen P, Kaariainen L.** 2001. Biogenesis of the Semliki Forest virus RNA replication complex. J. Virol **75:** 3873-84.

**Kusov Y, Gaus-Muller V.** 1999. Improving proteolytic cleavage at the 3A/3B site of the hepatitis A virus polyprotein impairs processing and particle formation, and the impairment can be complemented *in trans* by 3AB and 3ABC. J. Virol. **73:** 9867-9878.

**Kutay U, Hartmann E, Rapoport TA.** 1993. A class of membrane proteins with a C-terminal anchor. *Trends Cell Biol.* **3:** 72-75.

**Laemmli UK.** 1970. Cleavage of structural proteins during assembly of the head of bacteriophage T4. Nature **227:** 680-685.

**Lai MM.** 1998. Cellular factors in the transcription and replication of viral RNA genomes: a parallel to DNA-dependent RNA transcription. Virology **244:** 1-12.

**Lain S, Riechmann JL, Garcia JA.** 1990. RNA helicase: a novel activity associated with a protein encoded by a positive strand RNA virus. Nucleic Acids Res. **18:** 7003-7006.

**Latvala-Kilby S, Lehto K.** 1999. The complete nucleotide sequence of RNA2 of blackcurrant reversion nepovirus. Virus Res. **65:** 87-92.

**Lain S, Riechmann JL, Martin MT, Garcia JA.** 1989. Homologous potyvirus and flavivirus proteins belonging to a superfamily of helicase-like proteins. Gene. **82:** 357-62.

**Lambert C, Prange R.** 2001. Dual topology of the hepatitis B virus large envelope protein: determinants influencing post-translational pre-S translocation. J. Biol. Chem. **276:** 22265-22672.

**Le Gall O, Candresse T, Dunez J.** 1995. Transfer of the 3' non-translated region of grapevine chrome mosaic virus RNA-1 by recombination to tomato black ring virus RNA-2 in pseudorecombinant isolates. J. Gen. Virol. **76:**1285-1289.

**Le Gall O, Candresse T, Dunez J.** 1997. An RNA-dependent-RNA-polymerase activity associated with grapevine chrome mosaic nepovirus infection. Arch. Virol. **142:** 151-156.

**Lee E, Stocks CE, Amberg SM, Rice CM, Lobigs M.** 2000. Mutagenesis of the signal sequence of yellow fever virus prM protein: enhancement of signalase cleavage *In vitro* is lethal for virus production. J. Virol. **74:** 24-32.

**Lee WM, Ishikawa M, Ahlquist P.** 2001. Mutation of host delta9 fatty acid desaturase inhibits brome mosaic virus RNA replication between template recognition and RNA synthesis. J. Virol.

**75:** 2097-2106.

**Lemmon MA, MacKenzie KR, Arkin IT, Engelman DM.** 1997. Transmembrane α-helix interactions in folding and oligomerization of integral membrane proteins. p. 3-23. *In* G. Von Heijne (ed.), Membrane protein assembly. Springer, Heidelberg, Germany.

**Leonard S, Chisholm J, Laliberte JF, Sanfaçon H.** 2002. Interaction *in vitro* between the proteinase of Tomato ringspot virus (genus Nepovirus) and the eukaryotic translation initiation factor iso4E from *Arabidopsis thaliana.* J. Gen. Virol. **83:** 2085-2089.

**Li XH, Carrington JC.** 1995 . Complementation of tobacco etch potyvirus mutants by active RNA polymerase expressed in transgenic cells. Proc. Natl. Acad. Sci.USA **92:** 457-461.

**Li XH, Valdez P, Olvera RE, Carrington JC.** 1997. Functions of the tobacco etch virus RNA polymerase (NIb): subcellular transport and protein-protein interaction with VPg/proteinase (NIa). J. Virol. **71:**1598-607.

**Liang Y, Gillam S.** 2001. Rubella virus RNA replication is cis-preferential and synthesis of negative- and positive-strand RNAs is regulated by the processing of nonstructural protein. Virology **282:** 307-19.

**Lyons T, Murray KE, Roberts AW, Barton DJ.** 2001. Poliovirus 5'-terminal cloverleaf RNA is required in cis for VPg uridylylation and the initiation of negative-strand RNA synthesis. J. Virol. **75:** 10696-10708.

**Lytle JR, Wu L, Robertson HD.** 2002. Domains on the hepatitis C virus internal ribosome entry site for 40s subunit binding. RNA **8:** 1045-1055.

**Machamer CE.** 1993. Targeting and retention of Golgi membrane proteins. Curr. Opin. Cell Biol. **5:** 606-12.

**Maia IG, Seron K, Haenni AL, Bernardi F.** 1996. Gene expression from viral RNA genomes. Plant. Mol. Biol. **32:** 367-391.

**Martin MT, and Garcia JA.** 1991. Plum pox potyvirus RNA replication in a crude membrane fraction from infected *Nicotiana clevelandii* leaves. J. Gen. Virol. **72:** 785-790.

**Margis R, Pinck L.** 1992. Effects of site-directed mutagenesis on the presumed catalytic triad and substrate-binding pocket of grapevine fanleaf nepovirus 24-kDa proteinase. Virology **190:** 884-888.

**Margis R, Viry M, Pinck M, Bardonnet N, Pinck L.** 1994. Differential proteolytic activities of precursor and mature forms of the 24K proteinase of grapevine fanleaf nepovirus. Virology **200:** 79-86.

**Margis R, Viry M, Pinck M, Pinck L.** 1991. Cloning and in vitro characterization of the grapevine fanleaf virus proteinase cistron. Virology **185:** 779-787.

**Mayo MA, Barker H, Harrison BD.** 1982. Specificity and properties of the genome-linked proteins of the nepovirus, J. Gen.Virol. **59:** 603-610.

**Mayo MA, Robinson DJ.** 1996. Nepoviruses: Molecular biology and replication. p. 139-185. *In* B.D. Harrison and A. F. Murrant (ed.), The plant viruses, Volume 5: Polyhedral virions and bipartite RNA genomes. Plenum Press, New York.

**Michel YM, Poncet D, Piron M,. Kean KM, Borman AM.** 2000. Cap-poly(A) synergy in mammalian cell-free extracts. Investigation of the requirements for poly(A)-mediated stimulation of translation initiation. J. Biol. Chem. **275:** 32268-32276.

**Miller DJ, Ahlquist P.** 2002 Flock house virus RNA polymerase is a transmembrane protein with amino-terminal sequences sufficient for mitochondrial localization and membrane insertion. J. Virol. **76:** 9856-9867.

**Mirzayan C, Wimmer E.** 1994. Biochemical studies on poliovirus polypeptide 2C: evidence for ATPase activity. Virology **199**:176-87.

**Molla A, Harris KS, Paul AV, Shin SH, Mugavero J, Wimmer E.** 1994. Stimulation of poliovirus proteinase 3Cpro-related proteolysis by the genome-linked protein VPg and its precursor 3AB. J. Biol. Chem. **269:** 27015-27020.

**Molla A, Paul AV, Wimmer E.** 1993. Effects of temperature and lipophilic agents on poliovirus formation and RNA synthesis in a cell-free system. J. Virol. **67:** 5932-5938.

**Murphy JF, Klein PG, Hunt AG, Shaw JG.** 1996. Replacement of the tyrosine residue that links a potyviral VPg to the viral RNA is lethal. Virology **220:** 535-8.

**Neeleman L, Bol JF.** 1999. Cis-acting functions of alfalfa mosaic virus proteins involved in replication and encapsidation of viral RNA. Virology **254:** 324-333.

**Nickel W, Brugger B, Wieland FT.** 1998. Protein and lipid sorting between the endoplasmic reticulum and the Golgi complex. Semin. Cell Dev. Biol. **9:** 493-501

**Nilsson I, Johnson AE, Von Heijne G.** 2002. Cleavage of a tail-anchored protein by signal peptidase. FEBS Lett. **516:** 106-108.

**Nilsson I, Von Heijne G.** 2000. Glycosylation efficiency of Asn-Xaa-Thr sequons depends both on the distance from the C terminus and on the presence of a downstream transmembrane segment. J. Biol. Chem. **275:** 17338-17343.

**Novak JE, Kirkegaard K.** 1994. Coupling between genome translation and replication in an RNA

virus. Genes Dev. **8:** 1726-1737.

**Pacot-Hiriart C, Latvala-Kilby S, Lehto K.** 2001. Nucleotide sequence of black currant reversion associated nepovirus RNA1. Virus Res. **79:** 145-152.

**Pang PS, Jankowsky E, Planet PJ, Pyle AM.** 2002. The hepatitis C viral NS3 protein is a processive DNA helicase with cofactor enhanced RNA unwinding. EMBO J. **21:** 1168-1176.

**Parsley TB, Towner JS, Blyn LB, Ehrenfeld E, Semler BL.** 1997. Poly (rC) binding protein 2 forms a ternary complex with the 5'-terminal sequences of poliovirus RNA and the viral 3CD proteinase. RNA. **3:** 1124-1134.

**Pathak HB, Ghosh SK, Roberts AW, Sharma SD, Yoder JD, Arnold JJ, Gohara DW, Barton DJ, Paul AV, Cameron CE.** 2002. Structure-function relationships of the RNA-dependent RNA polymerase from poliovirus (3Dpol). A surface of the primary oligomerization domain functions in capsid precursor processing and VPg uridylylation. J. Biol. Chem. **277:** 31551-31562.

**Paul AV, Rieder E, Kim DW, Van Boom JH, Wimmer E.** 2000. Identification of an RNA hairpin in poliovirus RNA that serves as the primary template in the in vitro uridylylation of VPg. J. Virol. **74:** 10359-10370.

**Paul AV, Van Boom JH, Filippov D, Wimmer E.** 1998. Protein-primed RNA synthesis by purified poliovirus RNA polymerase. Nature **393:** 280-284.

**Pelham HR.** 1990. The retention signal for soluble proteins of the endoplasmic reticulum. Trends Biochem. Sci. **15:** 483-486.

**Peters SA, Mesnard JM, Kooter IM, Verver J, Wellink J, Van Kammen A.** 1995. The cowpea mosaic virus RNA 1-encoded 112 kDa protein may function as a VPg precursor *in vivo*. J. Gen. Virol. **76:** 1807-1813.

**Peters SA, Verver J, Nollen EA, Van Lent JW, Wellink J, Van Kammen A.** 1994. The NTP-binding motif in cowpea mosaic virus B polyprotein is essential for viral replication. J. Gen. Virol. **75 :** 3167-3176.

**Peters SA, Voorhorst WG, Wellink J, Van Kammen A.** 1992. Processing of VPg-containing polyproteins encoded by the B-RNA from cowpea mosaic virus. Virology **191:** 90-97.

**Peters SA, Voorhorst WG, Wery J, Wellink J, Van Kammen A.** 1992. A regulatory role for the 32K protein in proteolytic processing of cowpea mosaic virus polyproteins. Virology **191:** 81-89.

**Pfister T, Jones KW, Wimmer E.** 2000. A cysteine-rich motif in poliovirus protein 2C(ATPase) is involved in RNA replication and binds zinc in vitro. J. Virol. **74:** 334-343.

**Pfister T, Wimmer E.** 1999. Characterization of the nucleoside triphosphatase activity of poliovirus protein 2C reveals a mechanism by which guanidine inhibits poliovirus replication. J. Biol. Chem. **274:** 6992-7001.

**Plotch SJ, Palant O.** 1995. Poliovirus protein 3AB forms a complex with and stimulates the activity of the viral RNA polymerase, 3Dpol. J. Virol. **69**: 7169-7179.

**Porter AG.** 1993. Picornavirus nonstructural proteins: emerging roles in virus replication and inhibition of host cell functions. J. Virol. **67:** 6917-6921.

**Pouwels J, Carette J, Van Lent J, Wellink J.** 2002. Cowpea mosaic virus: effects on host cell processes. MOLECULAR PLANT PATHOLOGY **3:** 411-418.

**Prod'homme D, Le Panse S, Drugeon G, Jupin I.** 2001. Detection and subcellular localization of the turnip yellow mosaic virus 66K replication protein in infected cells. Virology **281:** 88-101.

**Pryme IF.** 1986. Compartmentation of the rough endoplasmic reticulum. Mol. Cell. Biochem. **71:** 3-18.

**Quadt R, Kao CC, Browning KS, Hershberger RP, Ahlquist P.** 1993. Characterization of a host protein associated with brome mosaic virus RNA-dependent RNA polymerase. Proc. Natl. Acad. Sci. USA **90:** 1498-1502.

**Rapoport TA.** 1990. Protein transport across the ER membrane. Trends Biochem. Sci. **15:** 355-358.

**Reichel C, Beachy RN.** 1998. Tobacco mosaic virus infection induces severe morphological changes of the endoplasmic reticulum. Proc. Natl. Acad. Sci. **95:** 11169-11174.

**Restrepo-Hartwig MA, Carrington JC.** 1992. Regulation of nuclear transport of a plant potyvirus protein by autoproteolysis. J. Virol. **66:** 5662-5666.

**Restrepo-Hartwig MA, Carrington JC.** 1994. The tobacco etch potyvirus 6-kilodalton protein is membrane-associated and involved in viral replication. J. Virol. **68:** 2388-2397.

**Rice CM.** 1996. Flaviviridae: the viruses and their replication, p. 931-959. In B. N. Fields, D. M. Knipe, and P. M. Howley (ed.), Fields virology, 3rd ed Lippincott-Raven Publishers, Philadelphia, Pa .

**Rieder E, Paul AV, Kim DW, Van Boom JH, Wimmer E.** 2000. Genetic and biochemical studies of poliovirus cis-acting replication element cre in relation to VPg uridylylation. J. Virol. **74:** 10371-10380.

**Ritzenthaler CC, Laporte F, Gaire P, Dunoyer C, Schmitt S. Duval A, Piéquet A, Loudes M, Rohfritsch O, Stussi-Garaud C, Pfeiffer P.** 2002. Grapevine fanleaf virus replication occurs on

endoplasmic-derived membranes. J. Virol. **76:** 8808-8819.

**Ritzenthaler C, Pinck M, Pinck L.** 1995. Grapevine fanleaf nepovirus P38 putative movement protein is not transiently expressed and is a stable final maturation product in vivo. J. Gen. Virol. **76:** 907-915.

**Ritzenthaler C, Viry M, Pinck M, Margis R, Fuchs M, Pinck L.** 1991. Complete nucleotide sequence and genetic organization of grapevine fanleaf nepovirus RNA1. J. Gen. Virol. **72:** 2357-2365.

**Rodriguez PL, Carrasco L.** 1993. Poliovirus protein 2C has ATPase and GTPase activities. J. Biol. Chem. **268:** 8105-8110.

**Rosenberg S.** 2001. Recent advances in the molecular biology of hepatitis C virus. J. Mol. Biol. **313:** 451-464.

**Rott ME, Gilchrist A, Lee L, Rochon DM.** 1995. Nucleotide sequence of the tomato ringspot virus RNA1. J. Gen. Virol. **76:** 465-473.

**Rott ME, Tremaine JH, Rochon DM.** 1991a. Comparison of the 5' and 3' termini of tomato ringspot virus RNA1 and RNA2: evidence for RNA recombination. Virology **185:** 468-472.

**Rott ME, Tremaine JH, Rochon DM.** 1991b. Nucleotide sequence of tomato ringspot virus RNA-2. J. Gen. Virol. **72:** 1505-1514.

**Ryan MD, Flint M.** 1997. Virus-encoded proteinases of the picornavirus super-group. J. Gen. Virol. **78:** 699-723.

**Ryan MD, Monaghan S, Flint M.** 1998. Virus-encoded proteinases of the Flaviviridae. J Gen Virol. **79:** 947-959.

**Rust RC, Landmann L, Gosert R, Tang BL, Hong W, Hauri HP, Egger D, Bienz K.** 2001. COPII proteins are involved in production of the vesicles that form the poliovirus replication complex. J. Virol. **75:** 9808-9818.

**Sachs AB, Sarnow P, Hentze MW.** 1997. Starting at the beginning, middle, and end: translation initiation in eukaryotes. Cell **89:** 831-838.

**Sanfaçon H.** 1995. Nepoviruses p.129-141. *In* R.P. Singh, U.S. Singh and K. Kohmoto (ed.), Pathogenesis and host specificity in plant diseases, Vol. III. Viruses and Viroids. Pergamon Press, Oxford.

**Sanfaçon H, Wieczorek A, and Hans F.** 1995. Expression of the tomato ringspot nepovirus movement and coat proteins in protoplasts. J. Gen. Virol. **76:** 2299-2303.

**Sankaram MB, and Marsh D.** 1993. p. 127-162. *In* A. Watts (ed.), Protein-Lipid Interactions. Elsevier Science Publishers B.V., Amsterdam.

**Sasaki J, Nakashima N.** 2000. Methionine-independent initiation of translation in the capsid protein of an insect RNA virus. Proc. Natl. Acad. Sci. USA **97:** 1512-5.

**Schaad MC, Haldeman-Cahill R, Cronin S, Carrington JC.** 1996. Analysis of the VPg-proteinase (NIa) encoded by tobacco etch potyvirus: effects of mutations on subcellular transport, proteolytic processing, and genome amplification. J. Virol. **70:** 7039-48.

**Schaad MC, Jensen PE, Carrington JC.** 1997. Formation of plant RNA virus replication complexes on membranes: role of an endoplasmic reticulum-targeted viral protein. EMBO J. **16:** 4049-4059.

**Schlegel A, Giddings THJr, Ladinsky MS, Kirkegaard K.** 1996. Cellular origin and ultrastructure of membranes induced during poliovirus infection. J. Virol. **70:** 6576-6588.

**Schmidt-Mende J, Bieck E, Hugle T, Penin F, Rice CM, Blum HE, Moradpour D.** 2001. Determinants for membrane association of the hepatitis C virus RNA-dependent RNA polymerase. J. Biol. Chem. **276:** 44052-63.

**Schroder K, Martoglio B, Hofmann M, Holscher C, Hartmann E, Prehn S, Rapoport TA, Dobberstein B.** 1999. Control of glycosylation of MHC class II-associated invariant chain by translocon-associated RAMP4. EMBO J. **18:** 4804-15.

**Schwartz M, Chen J, Janda M, Sullivan M, den Boon J, Ahlquist P.** 2002. A positive-strand RNA virus replication complex parallels form and function of retrovirus capsids. Mol. Cell **9:** 505-514.

**Segrest JP, De Loof H, Dohlman JG, Brouillette CG, Anantharamaiah GM.** 1990. Amphipathic helix motif: classes and properties. Proteins. **8:** 103-117.

**Staehelin LA.** 1997. The plant ER: a dynamic organelle composed of a large number of discrete functional domains. Plant J. **11:** 1151-1165.

**Suhy DA, Giddings THJr, Kirkegaard K.** 2000. Remodeling the endoplasmic reticulum by polivirus infection and by individual viral proteins: an autophagy-like origin for virus-induced vesicles. J. Virol. **74:** 8953-8965.

**Sullivan M, Ahlquist P.** 1997. Cis-acting signals in bromovirus RNA replication and gene expression: networking with viral proteins and host factors. Semin. Virol. **8:** 221-230.

**Sullivan ML, Ahlquist P.** 1999. A brome mosaic virus intergenic RNA3 replication signal functions with viral replication protein 1a to dramatically stabilize RNA in vivo. J. Virol. **73:** 2622-2632.

**Sun FC, Xiang Y, Sanfaçon H.** 2001. Homology-dependent resistance to tomato ringspot nepovirus in plants transformed with the VPg-protease coding region. Can. J. Plant Pathol. **23:** 292-299.

**Teasdale RD, Jackson MR.** 1996. Signal-mediated sorting of membrane proteins between the endoplasmic reticulum and the Golgi apparatus. Annu. Rev. Cell Dev. Biol. **12:** 27-54.

**Tenllado F, Bol JF.** 2000. Genetic dissection of the multiple functions of alfalfa mosaic virus coat protein in viral RNA replication, encapsidation, and movement. Virology **268:** 29-40.

**Teterina NL, Egger D, Bienz K, Brown DM, Semler BL, Ehrenfeld E.** 2001. Requirements for assembly of poliovirus replication complexes and negative-strand RNA synthesis. J. Virol. **75:** 3841-3850.

**Teterina NL, Gorbalenya AE, Egger D, Bienz K, Ehrenfeld E.** 1997. Poliovirus 2C protein determinants of membrane binding and rearrangements in mammalian cells. J. Virol. **71:** 8962-8972.

**Towner JS, Ho TV, Semler BL.** 1996. Determinants of membrane association for poliovirus protein 3AB. J. Biol. Chem. **271:** 26810-26818.

**Towner JS, Mazanet MM, Semler BL.** 1998. Rescue of defective poliovirus RNA replication by 3AB-containing precursor polyproteins. J. Virol. **72:** 7191-7200.

**Van Bokhoven H, Le Gall O, Kasteel D, Verver J, Wellink J, Van Kammen AB.** 1993. Cis- and trans-acting elements in cowpea mosaic virus RNA replication. Virology **195:** 377-386.

**Van Bokhoven H, Verver J, Wellink J, Van Kammen A.** 1993. Protoplasts transiently expressing the 200K coding sequence of cowpea mosaic virus B-RNA support replication of M-RNA. J. Gen. Virol. **74:** 2233-2241.

**Van Der Heijden MW, Carette JE, Reinhoud PJ, Haegi A, Bol JF.** 2001. Alfalfa mosaic virus replicase proteins P1 and P2 interact and colocalize at the vacuolar membrane. J. .Virol. **75:** 1879-1887.

**Vartapetian AB, Koonin EV, Agol VI, Bogdanov AA.** 1984. Encephalomyocarditis virus RNA synthesis in vitro is protein-primed. EMBO J. **3:** 2593-2598.

**Viry M, Serghini MA, Hans F, Ritzenthaler C, Pinck M, Pinck L.** 1993. Biologically active transcripts from cloned cDNA of genomic grapevine fanleaf nepovirus RNAs. J. Gen. Virol. **74:** 169-174.

**Von Heijne G.** 1990. Protein targeting signals. Cur. Opin. Cell Biol. **2:** 604-608.

**Von Heijne G.** 1992. Cleavage-site motifs in protein targeting sequences. Genet. Eng. **14:** 1-11.

**Walker JE, Saraste M, Runswick MJ, Gay NJ.** 1982. Distantly related sequences in the alpha- and beta-subunits of ATP synthase, myosin, kinases and other ATP-requiring enzymes and a common nucleotide binding fold. EMBO J. **1:** 945-51.

**Wang A, Carrier K, Chisholm J, Wieczorek A, Huguenot C, and Sanfaçon H.** 1999. Proteolytic processing of tomato ringspot nepovirus 3C-like protease precursors: Definition of the domains for the VPg, protease and putative RNA-dependent RNA-polymerase. J. Gen. Virol. **80:** 799-809.

**Wang A, Sanfaçon H.** 2000a. Proteolytic processing at a novel cleavage site in the N-terminal region of the tomato ringspot nepovirus RNA-1 encoded polyprotein in vitro. J. Gen. Virol. **82:** 1785-1790.

**Wang A, Sanfaçon H.** 2000b. Diversity in the coding regions for the coat protein, VPg, protease, and putative RNA-dependent RNA polymerase among tomato ringspot nepovirus isolates. Can. J. Plant Pathol. **22:** 145-149.

**Wang X, Bogdanov M, Dowhan W.** 2002. Topology of polytopic membrane protein subdomains is dictated by membrane phospholipid composition. EMBO J 21: 5673-5681.

**Wang Z, Kiledjian M.** 2000. The poly(A)-binding protein and an mRNA stability protein jointly regulate an endoribonuclease activity. Mol. Cell. Biol. **20:** 6334-6341.

**Wellink J, Le Gall O, Sanfaçon H, Ikegami M, and Jones AT.** 2000. Family Comoviridae in "Virus Taxonomy: The classification and nomenclature of viruses. The seventh report of the international committee on Taxonomy of viruses" (Van Regenmortel, M.H.V., Fauquet, C.M., Bishop, D.H.L., Carsten, E.B., Estes, M.K. Lemon, S.M.., Maniloff, J., Mayo, M.A., McGeoh, D.J., Pringle, C.R., Wickner, R.B., Eds., Acadmic Press, San Diego.) 691-701.

**Wellink J, Van Bokhoven H, Le Gall O, Verver J, Van Kammen A.** 1994. Replication and translation of cowpea mosaic virus RNAs are tightly linked. Arch Virol. **9:** 381-392.

**Wieczorek A, Sanfaçon H.** 1993. Characterization and subcellular localization of tomato ringspot nepovirus putative movement protein. Virology **194:** 734-742.

**Wieczorek A, Sanfaçon H.** 1995. An improved method for the generation and transfection of protoplasts from *Cucumis sativus* cotyledons. Plant Cell Rep. **114:** 603-610.

**Wienecke K, Glas R, Robinson DG.** 1982. Organelles involved in the synthesis and transport of hydroxyproline-containing glycoproteins in carrot root disks. Planta **155:** 58-63.

**Wolk B, Sansonno D, Krausslich HG, Dammacco F, Rice CM, Blum HE, Moradpour D.** 2000. Subcellular localization, stability, and trans-cleavage competence of the hepatitis C virus NS3-NS4A complex expressed in tetracycline-regulated cell lines. J. Virol. **74:** 2293-304.

**Wu SX, Ahlquist P, and Kaesberg P.** 1992. Active complete *in vitro* replication of nodavirus

RNA requires glycerophospholipid. Proc. Natl. Acad. USA **89:** 11136-11140.

**Xiang W, Cuconati A, Paul AV, Cao X, Wimmer E.** 1995. Molecular dissection of the multifunctional poliovirus RNA-binding protein 3AB. RNA **1:** 892-904.

**Xiang W, Paul AV, Wimmer E.** 1997. RNA signals in entero- and rhinovirus genome replication. Semin. Virol. **8:** 256-273.

**Yang M, Ellenberg J, Bonifacino JS, Weissman AM.** 1997. The transmembrane domain of a carboxyl-terminal anchored protein determines localization to the endoplasmic reticulum. J. Biol. Chem. **272:** 1970-1975.

**Ypma-Wong MF, Filman DJ, Hogle JM, Semler BL.** 1988. Structural domains of the poliovirus polyprotein are major determinants for proteolytic cleavage at Gln-Gly pairs. J. Biol. Chem. **263:** 17846-17856.

**Zalloua PA, Buzayan JM, Bruening G.** 1996. Chemical cleavage of 5'-linked protein from tobacco ringspot virus genomic RNAs and characterization of the protein-RNA linkage. Virology **219:** 1-8.

**Zhang GF, Staehelin LA.** 1992. Functional compartmentation of the Golgi apparatus of plant cells. Plant Physiol. **99:** 1070-1083.

**Ziegler E, Borman AM, Deliat FG, Liebig HD, Jugovic D, Kean KM, Skern T, Kuechler E.** 1995. Picornavirus 2A proteinase-mediated stimulation of internal initiation of translation is dependent on enzymatic activity and the cleavage products of cellular proteins. Virology **213:** 549-557

**Zimmer G, Conzelmann KK, Herrler G.** 2002. Cleavage at the furin consensus sequence RAR/KR(109) and presence of the intervening peptide of the respiratory syncytial virus fusion protein are dispensable for virus replication in cell culture. J. Virol. **76:** 9218-9224.